Formation of some transition metal carbides

By

ANDREAS CHRYSANTHOU

A Thesis Submitted for the Degree of Doctor of Philosophy

of the University of London and for the

Diploma of Imperial College

Department of Metallurgy & Materials Science
Imperial College of Science & Technology
Prince Consort Road
LONDON
SW7 2BP

June 1986

ABSTRACT

A study of the production of tungsten, molybdenum, niobium and calcium carbides was carried out using graphite, Collie coal and carbon monoxide as carburising agents. In particular, the direct reduction/carburisation of oxides was investigated.

WC was produced directly from WO_2 and CO at low temperatures without the formation of tungsten metal. At higher temperatures the reaction mechanism changed, with complete metallisation taking place prior to carbide formation. Under these conditions, W_2C was formed at temperatures as low as 800°C even though it is not a thermodynamically stable phase below 1250°C. It was shown that the formation of this metastable phase was related to the difficulty of nucleation of WC on a tungsten surface. Once nucleation of WC on W_2C had taken place, the latter was consumed and the former proceeded to grow on tungsten metal. Ordered and disordered modifications of W_2C were observed and their appearance was explained in terms of the stoichiometry of the phase.

During reduction with graphite, Mo_2C was produced directly from MoO_2. However, when Collie coal, a more reactive form of carbon, was used as the reducing agent, molybdenum was formed before carburisation took place. This change in mechanism was attributed to the much greater reactivity of the coal. Metastable carbides of 'MoC' were also observed and their formation is discussed in terms of the necessary conditions for their production.

Direct formation of NbC from Nb_2O_5 via NbO_2 was achieved with Collie coal. With the less reactive graphite no reaction occurred.

During the reaction of niobium with CO, niobium was observed to both carburise and oxidise simultaneously. The reasons for this complex reaction path and the reaction mechanism is explained.

The formation of CaC_2 from CaO was studied under controlled atmospheres. The reaction ceased after approximately 70% conversion to CaC_2. At this stage a liquid solution formed between CaC_2 and CaO is proposed to behave ideally. As a result, the activity ratio of CaC_2 to CaO increased to about 2 to 3 and the CO pressure decreased in order to maintain thermodynamic equilibrium, making further reaction impossible. The available thermodynamic data for the reaction were found to be in error. A more accurate equation for the free energy of the reaction has been proposed.

C O N T E N T S

LIST OF FIGURES AND ILLUSTRATIONS

PAGE

MOLYBDENUM CARBIDE

NIOBIUM CARBIDE

CALCIUM CARBIDE

PAGE

LIST OF PLATES

INTRODUCTION

Carbide formation is fairly common among transition metals. Most of these carbides have extremely high melting points and therefore are frequently referred to as "refractory carbides".

Their unusual properties make transition metal carbides commercially important. Some of these properties are listed below:

1. One of their most important properties is their great hardness. Many transition metal carbides have microhardness values between 2000 and 3000 Kg/mm^2 (values which lie between those of Al_2O_3 and diamond). Such high hardness values have resulted in their extensive use as cutting tools and for wear-resistant surfaces.
2. They have extremely high melting points - several carbides melt above 3000°C.
3. They are chemically stable at room temperature and are attacked slowly even by very concentrated acid solutions, but they readily oxidise at high temperatures to form oxides.
4. These compounds are extremely strong, particularly at high temperatures, and possess high Young's modulus values, 40-90 x 10^6 psi, compared to 20-40 x 10^6 psi for most transition metal elements. They are brittle at room temperature, but they undergo a brittle-to-ductile transition at high temperatures.
5. Carbides of this group are typically metallic in their electrical, magnetic and optical properties and most of these properties differ only slightly from those of the parent metals.

The principal commercial application for carbides is as the main

constituent in cemented carbides in which carbides are bonded together in a metal matrix such as cobalt and nickel. Their great hardness and wear resistance, good thermal shock resistance and thermal conductivity, good oxidation resistance and the compatibility of the carbide particles with the binder gives cemented carbides a unique set of properties necessary for use as cutting tools. They are also used extensively as spikes for snow tyres, extrusion and pressing dies, drilling tools in mining and as wear resistant surfaces in machines.

They have excellent alloying properties particularly with steel in which they can dissolve to a considerable effect. Therefore, they are alloyed with steel in order to improve their strength and hardness. In addition, tungsten, vanadium and niobium carbides are responsible for grain refinement which increases the strength, toughness and wear resistance of steel.

In high temperature applications carbides are useful in rocket nozzles and jet engine components. They are also extensively used as a ball-mill grinding medium.

Many transition metal carbides have thermal and electrical conductivities of the same order as those of the pure metals, but at the same time they are hard, refractory and resistant to chemical attack. This makes them important in gas turbine manufacture.

In industry, transition metal carbides are generally produced by a two-stage process. The pure oxide is initially reduced to give the metal. The reduction processes which are used to produce molybdenum and tungsten are listed in Table 1.

TABLE 1 - Reduction Processes

Reduction Process/ Furnace Type	Compound	Reducing Agent	Temperature (°C)
Batch Operations			
1. Carbon reduction	Ammonium Paratungstate (APT)	Carbon or Hydrocarbons	1300 - 1400
2. Hydrogen reduction	Oxide Acid	H_2	700 - 900
Continuous Operations			
3. Walking beam or belt type	APT Oxide Acid	H_2	700 - 1000
4. Multitube pusher type	Oxides	H_2	700 - 1000
5. Rotary kiln	APT Oxides	H_2	700 - 1200
6. Plasma	Chlorides APT Oxide	H_2	5000
7. Fluidised bed	Oxide	H_2	700

The processes numbered 3, 4 and 5 are preferred in modern plants.

These are illustrated in Figure 1. They have been designed to give high throughput rates with as low a hydrogen consumption as possible. For submicron powder, fine grain sized oxides are used, whereas for greater powder sizes coarser oxides are used. The particle size can be controlled by varying the layer thickness, the temperature and the hydrogen flow and its water content.

Rotary furnaces are currently experiencing a renaissance in Europe. With their agitated powder charge they should create good reaction conditions between oxide and hydrogen and also good heat transfer resulting in high throughput and low hydrogen and heat consumption. As the operation is almost fully automatic, labour costs are minimised. However, this type of furnace is less flexible due to its lack of defined charge depth and produces more or less agglomerated powders with powder characteristics different from those reduced in a static bed.

Hydrogen reduction in a plasma is still at a small plant stage. Extremely fine powders are produced which tend to be pyrophoric and therefore have to be deactivated.

The gas phase reaction between chloride and hydrogen requires a further heat-treatment to remove traces of chloride.

Electrolytic processes are also used, as in the case of tantalum. A cast iron pot is employed to contain the fused electrolyte which is a mixture of potassium tantalum fluoride and tantalum pentoxide. The pot also acts as a cathode and a graphite rod as the anode. The process is carried out at 700°C. The metal powder collects at the cathode and after cooling it is purified by washing with water,

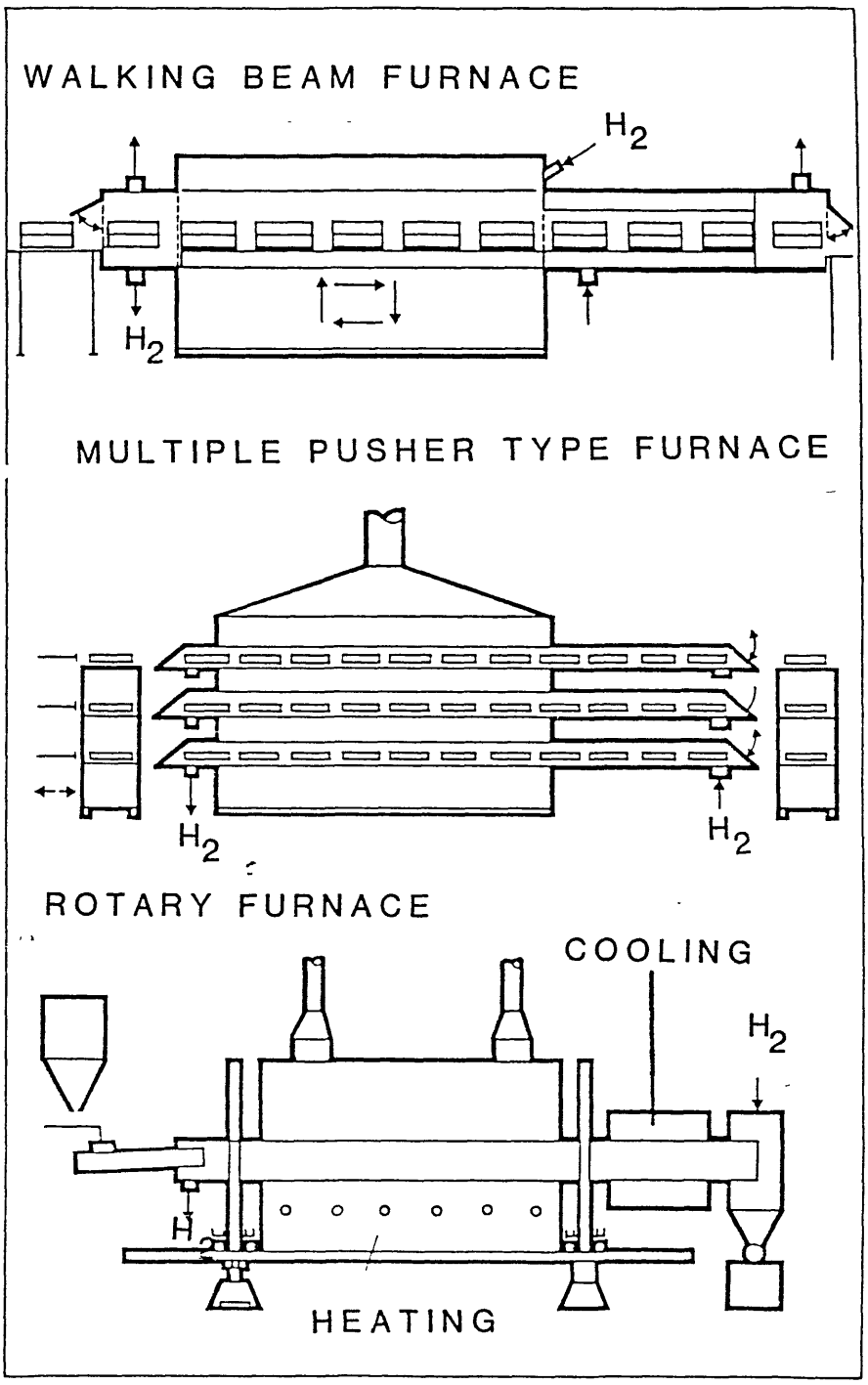
WALKING BEAM FURNACE
H_2
H_2
MULTIPLE PUSHER TYPE FURNACE
H_2
H_2
ROTARY FURNACE
COOLING
H_2
H_2
HEATING

FIGURE 1

followed by alternate treatments with dilute sulphuric acid and dilute potassium hydroxide.

The carbides are then produced by solid state reaction between the pure metal and carbon black. In the case of molybdenum and tungsten carbide powders, resistance heated furnaces working at around 1550°C are used. For coarser powders induction-heated furnaces operating at temperatures ranging between 1800°C to 2000°C are preferred.

Calcium carbide is commercially important because it is the basis of the production of acetylene by its reaction with water and is also commonly used as a desulphurising agent in steelmaking. In addition, it can be used to reduce very stable metal oxides such as MgO.

Commercial calcium carbide is manufactured from lime and coke in an electric furnace at temperatures of 1800°C to 2100°C. In the upper part of the furnace the mix is pre-heated by the rising gas. The reaction between lime and coke takes place at the hearth of the furnace at about 1920°C. The bulk of the carbide is formed directly from lime. At these temperatures the vapour pressure of calcium in equilibrium with CaC_2 is high and some vapour is evolved which reacts with carbon in the mix. The product is super-heated to about 2100°C so that it can flow out of the furnace as a melt. It contains approximately 80% CaC_2 and 20% CaO.

Since carbide production is costly and time and energy consuming, this study was initially undertaken in order to examine alternative routes, such as the direct formation of the carbide from the oxide at lower temperatures than those presently used in industry.

EXPERIMENTAL APPARATUS AND TECHNIQUE

An apparatus was constructed consisting of a platinum resistance furnace with a silica reaction tube 32 mm i.d. The furnace consisted of an alumina tube 48 mm i.d. x 470 mm long x 5 mm thick wound with platinum wire. Two layers of alumina bricks served as insulation. A second alumina tube 35 mm i.d. x 920 mm long x 4 mm thick was connected to a water cooling system and inserted inside the furnace tube. Using this assembly, a hot zone of 30 mm in length was achieved.

Samples were prepared by weighing the appropriate quantities of oxide and graphite which were mixed and roll-milled for periods greater than 12 hours to allow through mixing. Pellets 6 mm diameter were made by pressing the mixtures in an iron die. In all experiments, twice the stoichiometric quantity of carbon necessary to react with the oxide to form the carbide and CO was used.

The sample was placed on a platinum pan of known weight and weighed. It was then introduced into the reaction tube by suspending from the extension of a linear variable differential transformer (L.V.D.T.). Having flushed the tube with argon or the reacting gas at 500 cm^3/min, the reaction tube was lowered into the furnace for reaction to commence.

Weight changes were determined with time using a L.V.D.T. with an output of 0.5 mV per mg. The d.c. output was fed to a chart recorder which had been calibrated previously against the L.V.D.T. output, so that the weight change could be monitored continuously.

After each experiment the sample was weighed using an analytical

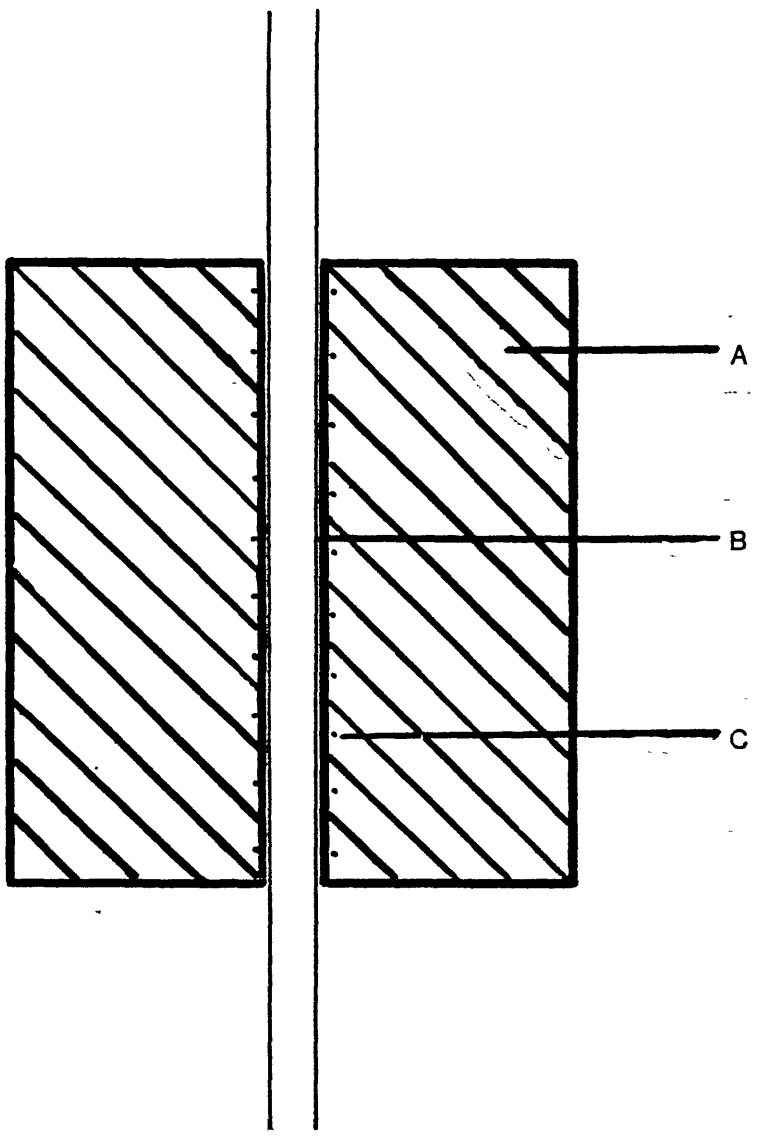

FIGURE 1A

Key to Figure 1A

A Alumina Insulation
B Alumina Tubes
C Platinum Windings

Key to Figure 1B

A Armature of the L.V.D.T.
B Zero Adjustment
C Alumina Adapter
D Platinum Wire and Hook
E Perspex Holder
F L.V.D.T. Support
G Rubber Pad
H L.V.D.T. Box
I Water Inlet
J Rubber 'O' Ring
K Split Brass Sleeve
L Electrical Leads
N Argon Gas Inlet
O Water Outlet
P Mild Steel Plate
R Quartz Reaction Tube
S Seal
T Thermocouple

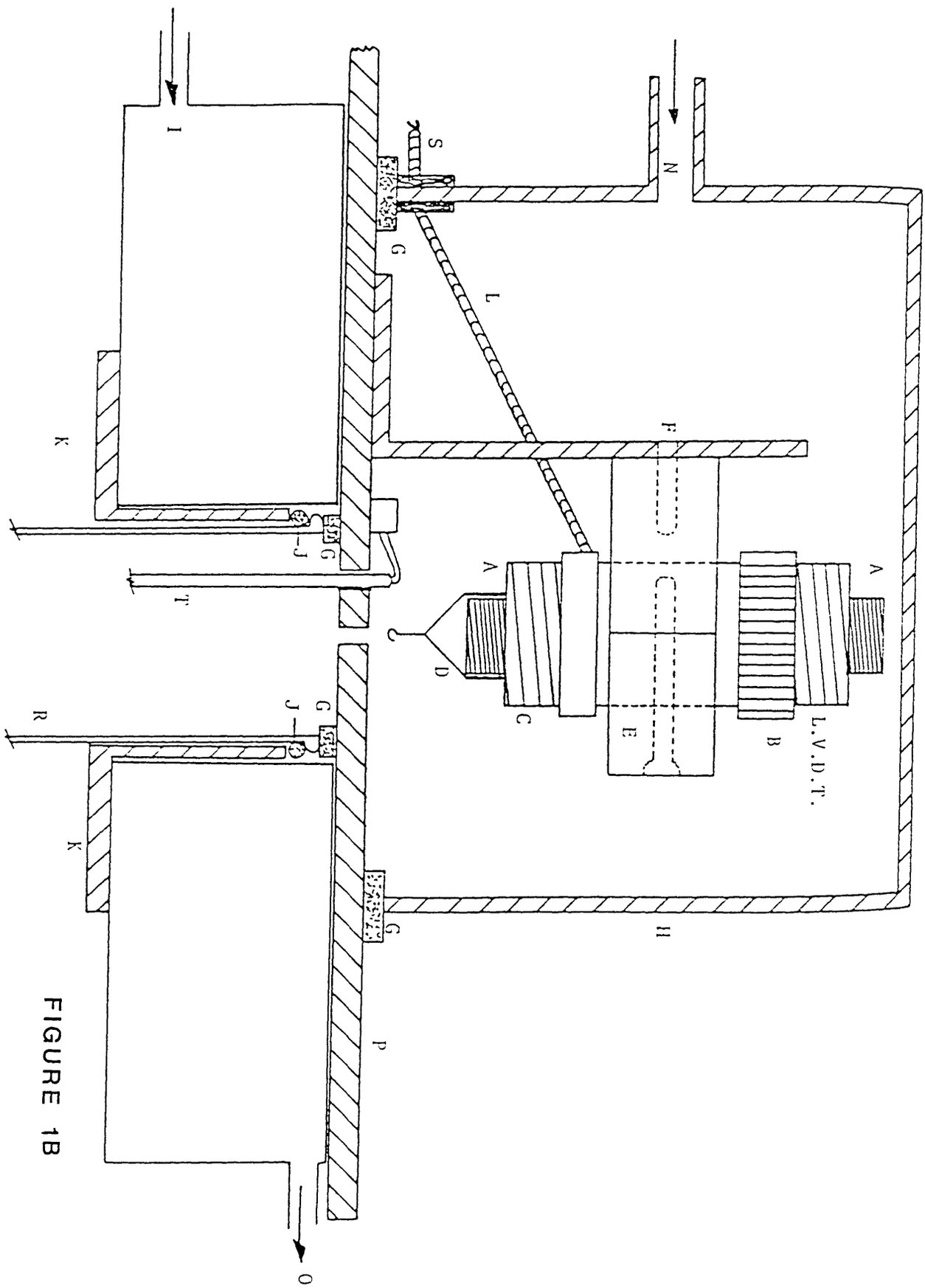

FIGURE 1B

balance and the change in weight compared with the experimental value to check the accuracy of the weight change. At all times, the agreement between these two values was within 0.2%.

Samples were analysed by an X-ray diffraction technique using a Guinier focussing camera with monochromatic Co $k\alpha_1$ radiation to determine the phases which had formed during the reaction period. Wire samples were analysed by means of the Debye-Scherrer method.

Samples for optical and electron microscopy were mounted in "Metset" mounting resin. They were ground with silicon carbide paper to 800 grade and polished with 6 μm, 3 μm, 1 μm and 1/4 μm "Hyprez" diamond paste. The optical microscope used was a Reichert MeF II Inverted Photographic Microscope.

EXPERIMENTAL TECHNIQUE AND APPARATUS FOR REDUCTION UNDER CONTROLLED ATMOSPHERES

A diagram of the apparatus used for studying the carbothermic reduction of CaO is shown in Figure 2. The main feature of the apparatus was the use of a Cartesian manostat which was used to control the pressure in the reaction tube.

An arrangement of saffil insulators supported by an alumina tube was placed inside a silica tube. A graphite crucible which also acted as an electrical susceptor rested inside the insulators and was heated using radio frequency coil. The temperature was measured using a Pt/Pt-30%Rh thermocouple in contact with the bottom of the crucible and was controlled by means of a potentiometer. Having established the

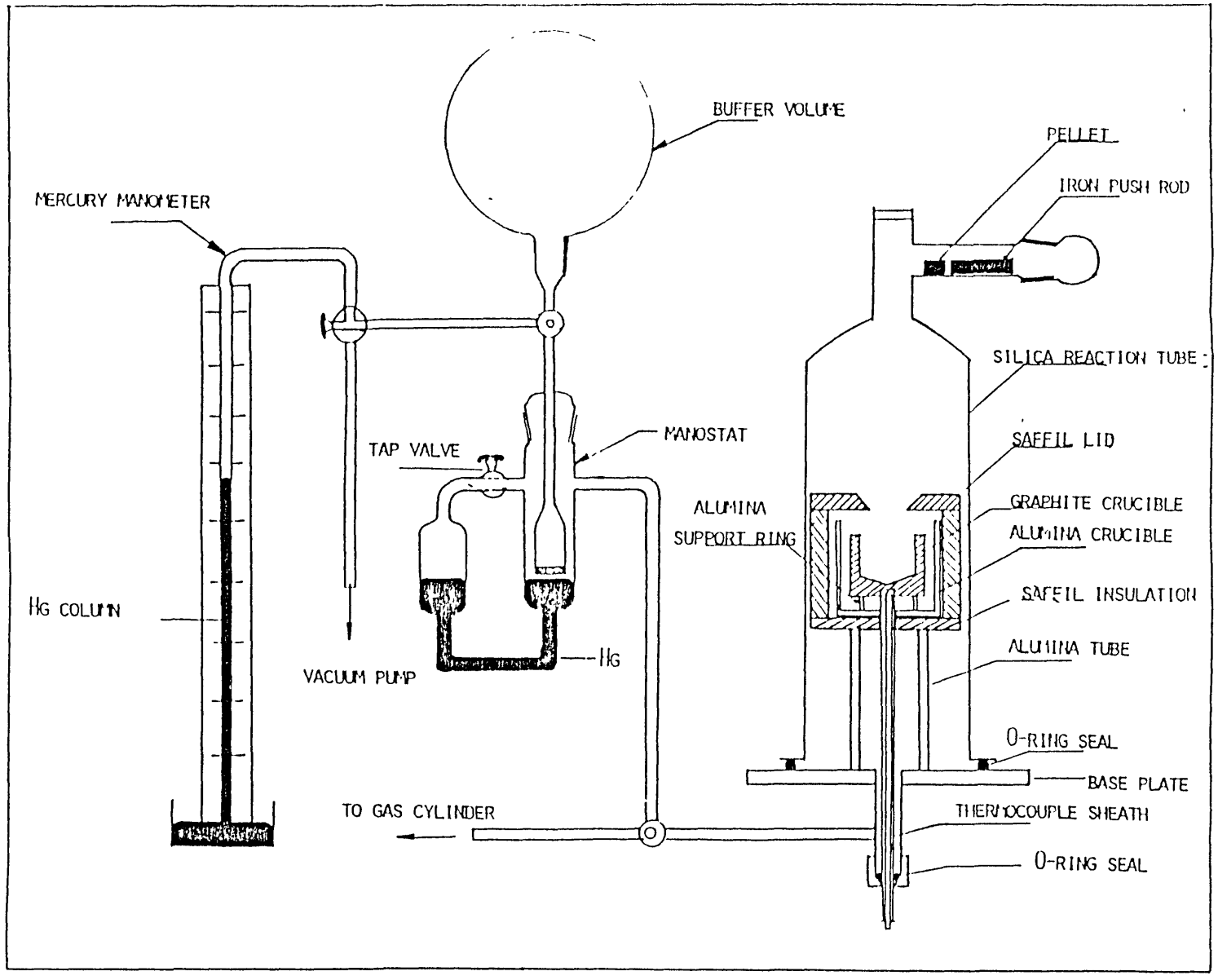
BUFFER VOLUME
PELLET
IRON PUSH ROD
MERCURY MANOMETER
SILICA REACTION TUBE
MANOSTAT
TAP VALVE
SAFFIL LID
ALUMINA
SUPPORT RING
GRAPHITE CRUCIBLE
ALUMINA CRUCIBLE
Hg COLUMN
SAFFIL INSULATION
ALUMINA TUBE
VACUUM PUMP
Hg
O-RING SEAL
BASE PLATE
TO GAS CYLINDER
THERMOCOUPLE SHEATH
O-RING SEAL

FIGURE 2

required temperature, the system was evacuated and then some gas was introduced to the desired pressure which was measured using a mercury column. The gas on one side of the Cartesian manostat was then isolated from the gas on the other side. Thus, in order to maintain the pressure balance between the two sections of the manostat, any gas which was generated during reaction was allowed to leave the system. Using a magnet and a rod the sample was dropped into the graphite crucible for the reaction to commence. The progress of the reaction was followed by measuring the volume of the gas which was evolved at specific time intervals. The weight change calculated by measuring the volume of gas evolved was in good agreement with the actual weight change measured using an analytical balance at the end of the experiment.

TUNGSTEN CARBIDE

THE TUNGSTEN CARBIDE SYSTEM

Using melting point determinations and optical microscopic observations, Sykes[1] established the tungsten-carbon phase diagram. He showed that two carbides W_2C and WC existed, the former melted congruently at 2750°C whilst the latter decomposed peritectically at 2600°C. In 1927, Skanpy[2] had observed that W_2C exhibited a polymorphic change at high temperatures to form β-W_2C. This phase change was not substantiated by Sykes but it was confirmed in subsequent work by Goldschmidt et al[3]. Observations made by Orton[4] on the carburisation of tungsten with methane-hydrogen indicated a eutectoid reaction at 1215°C in which W_2C decomposed to W and WC. Later work by Sara[5] using differential thermal analysis techniques produced new results for the high temperature region of the phase diagram. A eutectic between W and W_2C was observed at 2710°C and the high temperature phase β-W_2C, reported by Skanpy was confirmed at 2760°C. At the eutectoid temperature 2525°C between W_2C and WC, evidence was presented for a carbon excess above the stoichiometric formula in the W_2C phase. A cubic phase was observed and designated β-WC, which formed by peritectic reaction at 2785°C. This phase was seen to be stable at temperatures above 2525°C. At 2755°C, α-WC was seen to decompose into β-WC and C.

Perhaps, the most important work on the phase relationships is that due to Rudy et al[6] whose phase diagram is shown in Figure 1. Rudy and Windisch[7] used differential thermal analysis to study the stability of W_2C. Samples of different compositions were equilibrated

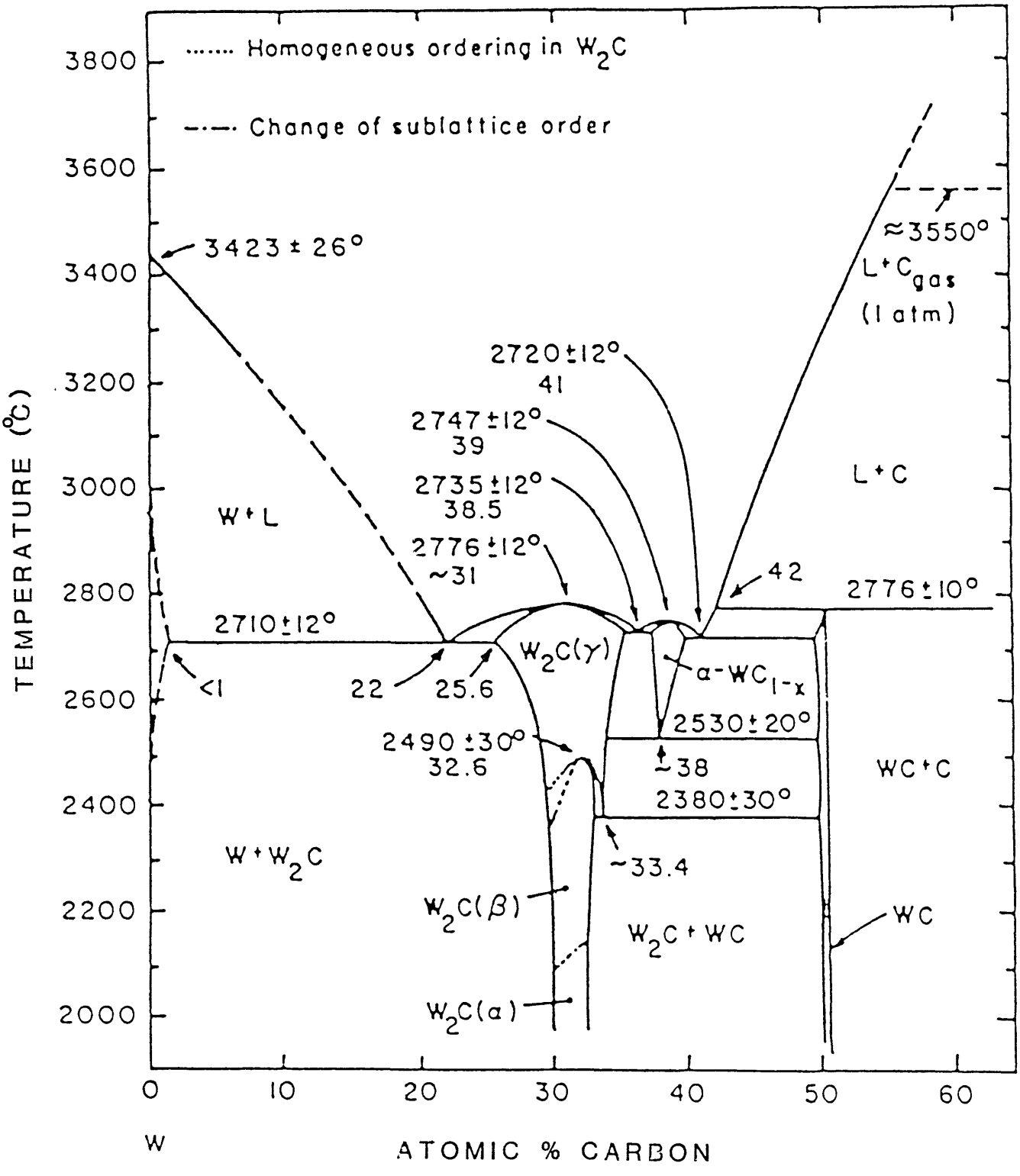

THE W-C SYSTEM

FIGURE 1

for 10 minutes at various temperatures and then quenched in a tin bath at about 300°C. The specimens were then analysed by X-ray diffraction. They reported that W_2C exists in three crystallographic forms:

(i) A disordered hexagonal modification designated as γ-W_2C which is stable between 2450°C and the melting point.

(ii) An orthorhombic modification, β-W_2C with a stability range between 2100°C and 2400°C and lattice parameters a = 4.728 Å, b = 6.009 Å and c = 5.193 Å. The X-ray diffraction pattern of this modification revealed a splitting of certain lines.

(iii) An ordered hexagonal modification, α-W_2C existing between the eutectoid temperature (1250°C) and 2100°C with lattice parameters a = 3.000 Å and c = 4.730 Å.

The high temperature modification of WC, β-WC has a face-centred cubic structure which is stable above 2525°C. The low temperature form, α-WC has a simple hexagonal structure with lattice parameters a = 2.9063 Å and c = 2.8368 Å.

There is disagreement as to the temperature at which the eutectoid decomposition of W_2C and WC occurs. Orton[4] observed a temperature of 1215°C. Using differential thermal analysis Rudy and Windisch[7] measured a temperature of 1250°C. Worrell[8] calculated eutectoid temperature of 1327°C by combining thermodynamic values from other sources.

Gleiser and Chipman[9] determined the standard free energy of formation of WC between 945°C and 995°C to be -8340 ± 300 cal/mol from equilibrium experiments for the reaction

$$WC + CO_2 = W + 2CO$$

Gupta and Seigle[10] measured the carbon activity in the two phase regions W-WC and W-W_2C with the following results:

$$\Delta G^\circ (WC) = - 10,000 + 1.19T \text{ cal/mol } (887^\circ - 1300^\circ C)$$

$$\Delta G^\circ (W_2C) = - 7,300 + 0.56T \text{ cal/mol } (1300^\circ - 1387^\circ C).$$

These values are in reasonable agreement with those of Gleiser and Chipman[9] and Worrell[8] whose values are:-

$$\Delta G^\circ (WC) = - 9600 + 1.0T \text{ cal/mol}$$

$$\Delta G^\circ (W_2C) = - 6400 + 1.0T \text{ cal/mol}$$

PREPARATION OF TUNGSTEN CARBIDE

The direct reduction of WO_3 with carbon or calcium carbide to form tungsten carbides was initially studied by Moissan[11] who identified W_2C. Schwarzkopf and Kieffer[12] found that the gas atmosphere in the furnace during carburisation of WO_3 was important. With CO present in the furnace, they found that only 80-90% of the theoretical carbon was required.

Miyabe, Hara, Sho and Kawakata[13] recently described a continuous direct carburisation process for WC production from WO_3 using a rotary kiln. WO_3 was mixed with sufficient carbon to form WC and heated in

nitrogen at 1000°C followed by a hydrogen treatment at 1400°C.

Hilpert and Ornstern[14] carburised samples at temperatures between 600° and 1000°C using CO and CH_4/H_2. Using CO, it was shown that the carburisation rate at low temperatures was slow and it was only at 1000°C that maximum carbon uptake was achieved. It seems the higher carbon contents are associated with the presence of free carbon. It was suggested that carbon deposition only occurred after the carburisation reaction was complete. Newkirk and Aliferis[15] studied the carburisation of tungsten and a range of oxides with CH_4/H_2 in the temperature range 850°-1000°C. At 1000°C, WC was produced from all starting materials. It was stated that the reaction proceeded by rapid reduction to tungsten followed by carburisation.

Using thermogravimetry, Davidson, Alexander and Wadsworth[16] studied the kinetics of tungsten carburisation in CH_4/H_2 mixtures. Carbon deposition was avoided by keeping the methane composition below the $C/CH_4/H_2$ equilibrium concentration. The initial reduction rate was observed to be linear and coincided with the formation of W_2C. The subsequent rate was shown to be much slower and was observed to be parabolic and coincided with WC formation. In several studies, the formation of W_2C below the eutectoid temperature has been reported even at temperatures as low as 900°C. During the reduction of WO_3 most workers agree that intermediate oxides are formed initially. Some workers have also reported that carbide formation begins only after the elimination of all oxygen.

The production of WC from ore containing WO_3 by reduction with carbon at 1400°C has been described by Chretien, Freudlich and

Josien[17]. The reaction product contained W_2C, but WC was separated by leaching with 1:4 HNO_3-HF mixtures. A maximum yield of 88% was claimed.

According to Tih and Wang[18] for the complete carbothermic reduction of WO_3 to the metal, a temperature higher than 1050°C is necessary.

Basu and Sale[19] studied the gas phase carburisation/reduction by CO of WO_3, $W_{18}O_{49}$ and WO_2 by means of thermogravimetry and X-ray diffraction analysis. Curves of % weight loss against time and X-ray diffraction showed that below 900°C WC was formed directly from WO_2. At 1000° and 1100°C a greater than theoretical weight loss was obtained during the early stages of the reaction indicating that tungsten was being produced. This was subsequently carburised to give tungsten carbide with an overall weight change equal to the theoretically predicted value. According to the authors the glass spring balance which was employed for these experiments did not allow rapid retrieval of the samples at the higher temperatures, so this observation could not be checked by X-ray diffraction.

Hara and Miyake[20] studied the formation of the tungsten carbides from tungsten by reacting tungsten powder with carbon black for 20 minutes between 1000°C and 1900°C. Samples were then analysed by X-ray diffraction. In addition, a carbon analysis was carried out using the combustion method. The results of this study are shown below in Table 1 and Figure 2.

TABLE 1

Temperature (°C)	Total Wt% Carbon	Free Wt% Carbon	Combined Carbon
1000	6.21	6.13	0.08
1200	6.04	4.78	1.26
1300	6.22	2.98	3.38
1400	6.24	1.10	5.14
1450	6.29	0.47	5.82
1500	6.24	0.31	5.93
1550	6.25	0.15	6.10
1600	6.25	0.13	6.12
1650	6.26	0.13	6.13
1900	6.33	0.21	6.12

It is interesting to note that W_2C was observed to form at 1000°C where it is unstable and that below 1200°C it takes more than 20 minutes for WC to begin to form. Figure 2 shows that the W_2C line intensity reaches a maximum at about 1220°C.

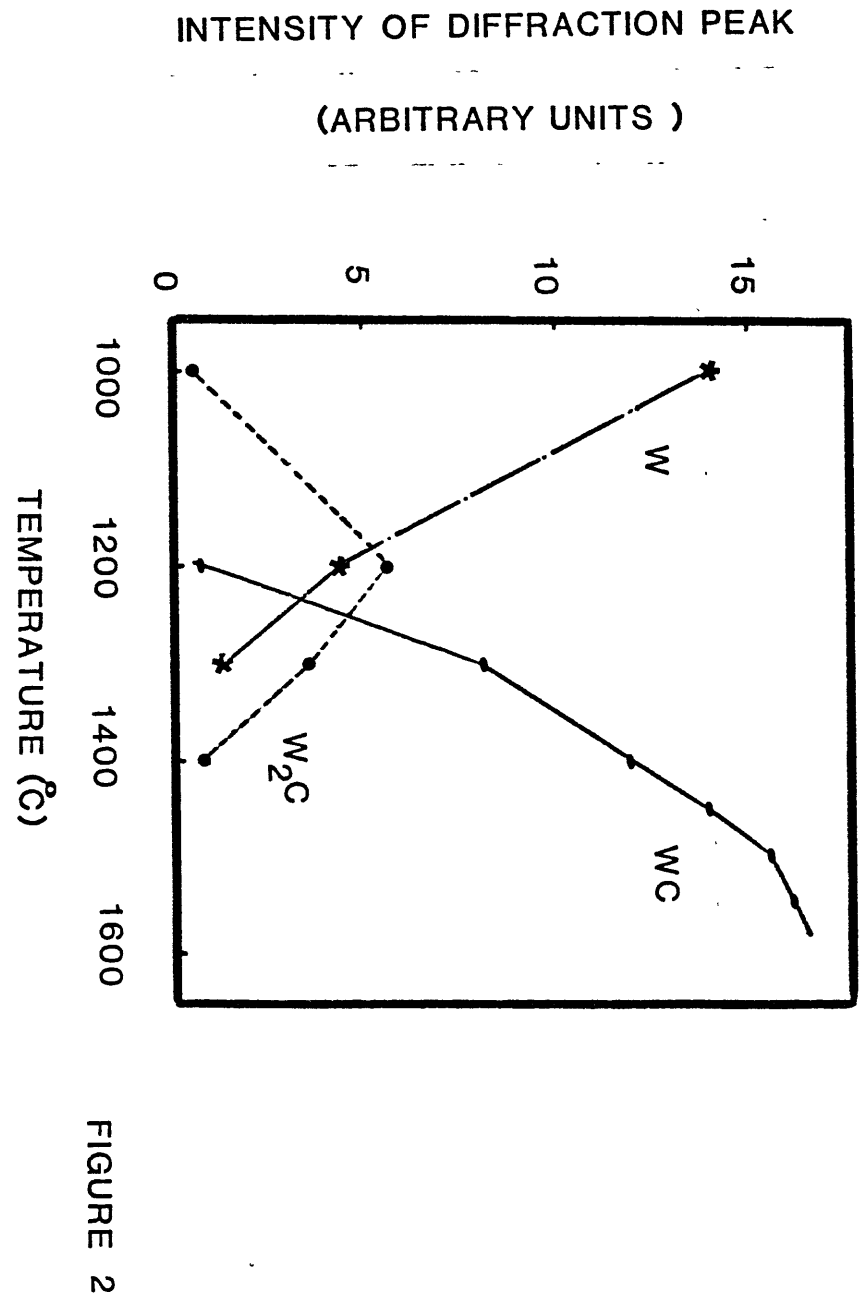
INTENSITY OF DIFFRACTION PEAK
(ARBITRARY UNITS)
0
5
10
15
1000
1200
1400
1600
TEMPERATURE (°C)
W
W2C
WC

FIGURE 2

RESULTS

Reduction Of WO_3 With Graphite

The reduction/carburisation of tungsten trioxide with graphite was observed to occur at temperatures above 970°C. A plot of % weight loss against time is shown in Figure 3. By stopping the reduction at appropriate times the reduction sequence was found to be

$$WO_3 \rightarrow W_{20}O_{58} \rightarrow W_{18}O_{49} \rightarrow WO_2 \rightarrow W \rightarrow W_2C \rightarrow WC$$

Carbide formation started when all oxygen was removed. This substantiates the work of Hegedus and Gado[21].

After 65 minutes at 1170°C, the products were tungsten, α-W_2C and α-WC, with tungsten and α-W_2C being the major phases present.

At 1120°C the same products were observed, but after 65 minutes less α-WC was observed than at the higher temperature.

At 1050°C, the same three phases were present except that the W_2C structure was distorted to give an orthorhombic modification usually associated with the ordering of interstitial atoms.

The reduction at 990°C was very slow. It took about two hours before any W_2C was produced. After 18 hours the same products as before were formed, with the three phases appearing to be evenly distributed. The W_2C structure was again distorted.

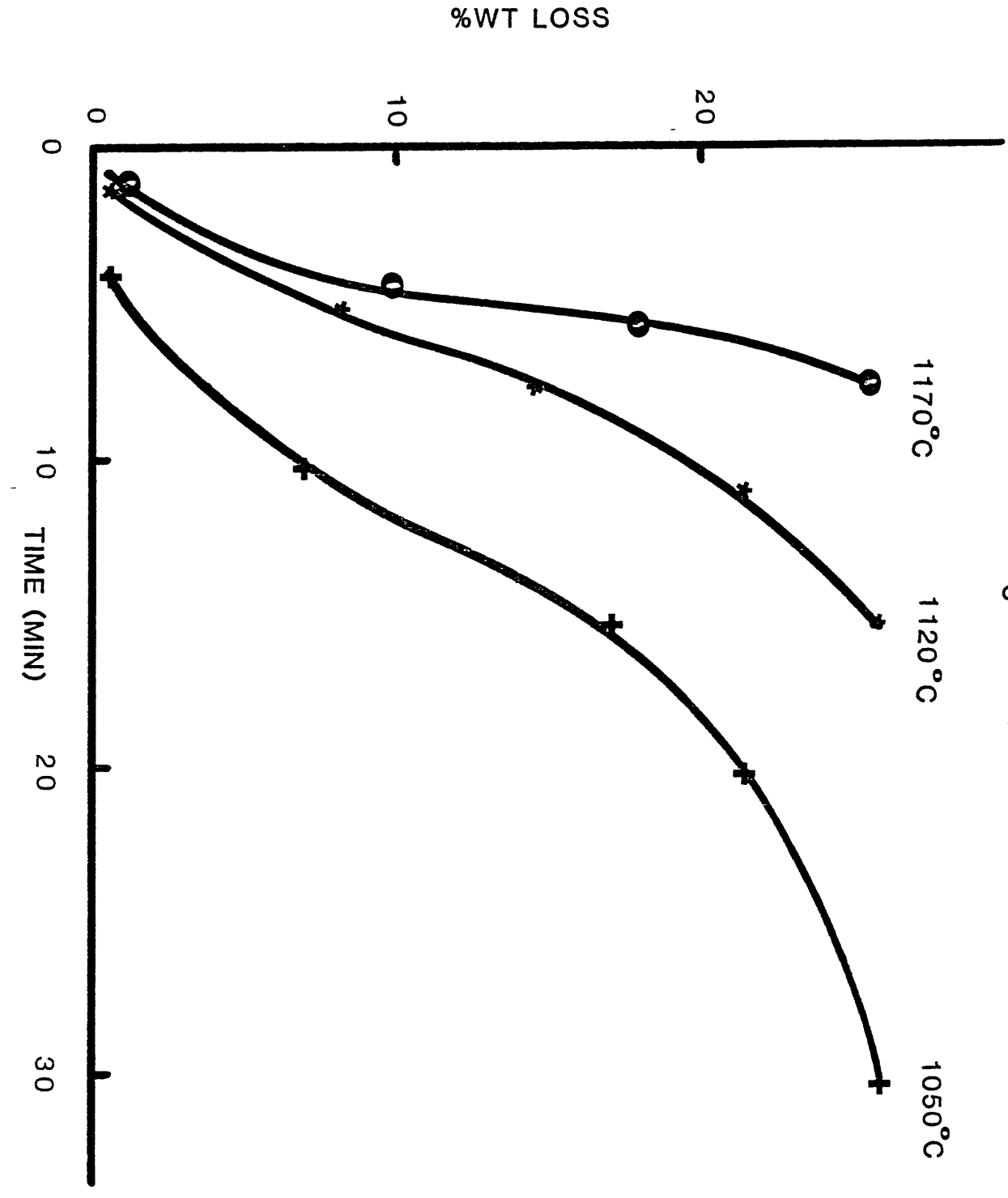

REDUCTION OF WO_3 WITH CARBON AT DIFFERENT TEMPERATURES

Reduction of WO_3 With Collie Coal

The % weight loss against time for the reaction between WO_3 and Collie Coal is shown in Figure 4. As expected, faster rates were observed with Collie coal than with graphite.

After 65 minutes at 1170°C, the products were the same as those with graphite, but α-WC was the major phase.

The products at 1050°C and 1120°C were the same as those with graphite. Although carburisation was at a more advanced stage after an equivalent period of time, W and W_2C were still the major phases present.

At 990°C carbide formation started after one hour, compared to two hours when graphite was used. The W_2C structure was again distorted at temperatures below 1050°C.

Reduction of WO_3 With Graphite Using 5% Hydrated $FeCl_3$ As a Catalyst

This reaction was investigated at 1050°C, 1120°C and 1170°C. The recorded weight loss was about 50% greater than the expected one. $FeCl_3$, which is unstable and volatile at these temperatures, decomposes according to the reaction

$$2FeCl_{3(g)} \rightarrow 2FeCl_{2(g)} + Cl_{2(g)}$$

Tungsten and its oxides can react with chlorine to form either chlorides or oxychlorides, all of which are extremely volatile. This accounted for the extra weight loss which was recorded. For this reason, the weight loss with time is not shown as this would be

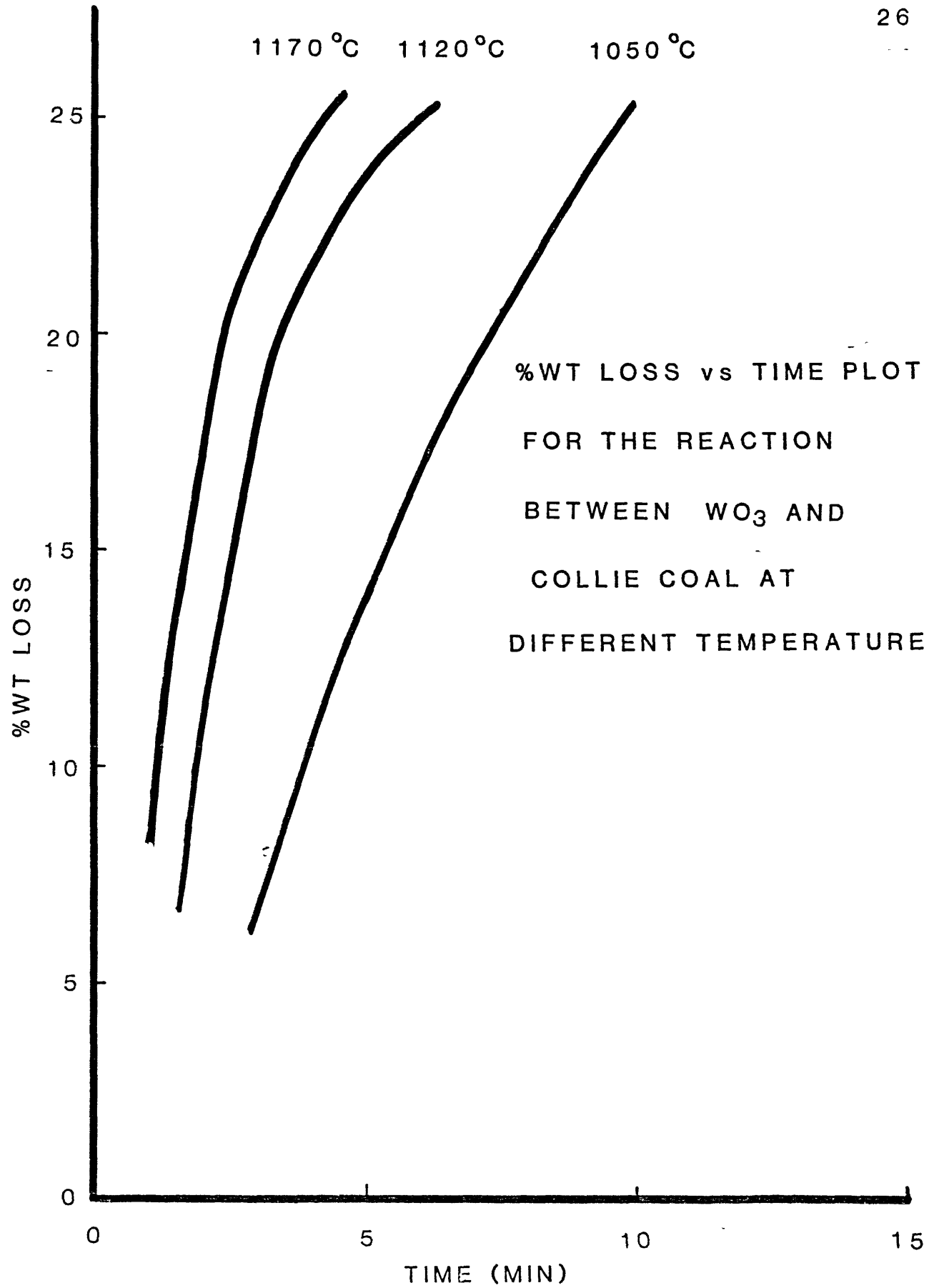
1170 °C
1120 °C
1050 °C
25
20
15
10
5
0
%WT LOSS
0
5
10
15
TIME (MIN)
%WT LOSS vs TIME PLOT
FOR THE REACTION
BETWEEN WO_3 AND
COLLIE COAL AT
DIFFERENT TEMPERATURES

FIGURE 4

meaningless.

Reduction Of WO_3 With CO

A plot of the weight loss against time for the reaction of WO_3 with CO at 1120°C, 1050°C and 800°C is shown in Figure 5. It is evident from this figure that the initial weight losses at 1050°C and 1120°C were followed by weight gains. The theoretical weight loss required to produce WC from WO_3 is about 15.5%. The greater than theoretical weight loss observed during the initial stages of the reaction at 1050°C and 1120°C indicated that the reaction sequence was W oxides → W → W carbides. The results of the X-ray diffraction analysis were in agreement with this observation.

At 800°C, the sample behaved differently, as shown in the figure. This indicated that a different reaction path was followed. This observation was checked by X-ray diffraction analysis of samples which had not been completely carburised. The reaction sequence followed was $WO_3 \rightarrow WO_2 \rightarrow WC$ without the formation of metallic tungsten. This observation is in agreement with the work of Basu and Sale[19].

Figure 6 shows a plot of ΔG° vs temperature for the reactions:

$$WO_2 + 2CO \rightarrow W + 2CO_2 \quad (1)$$

$$WO_2 + 4CO \rightarrow WC + 3CO_2 \quad (2)$$

This predicts that at temperatures below 910°C reaction (2) will occur and at temperatures above 910°C reaction (1) will.

RATE OF REDUCTION OF WO_3 WITH CO

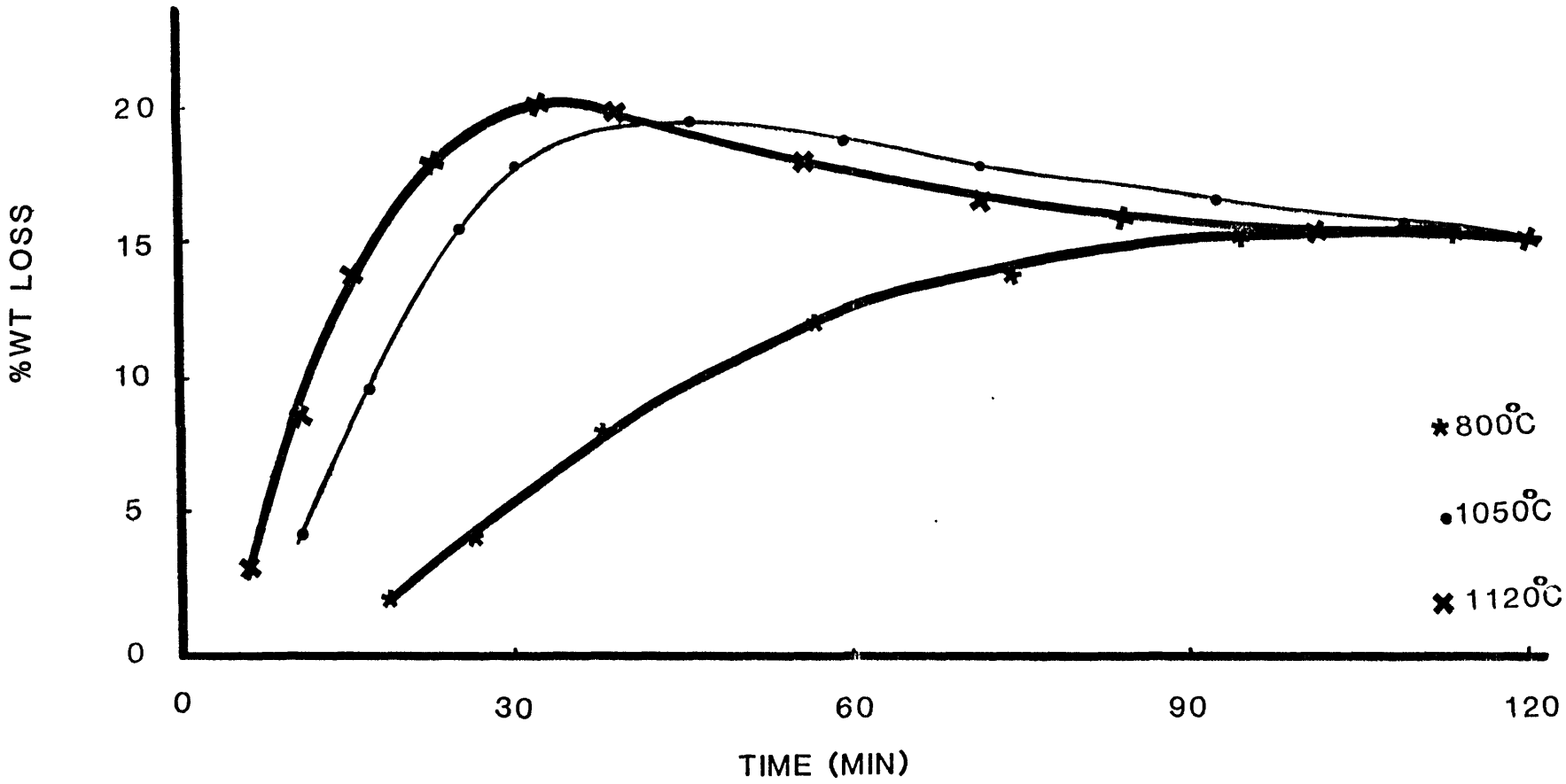

FIGURE 5

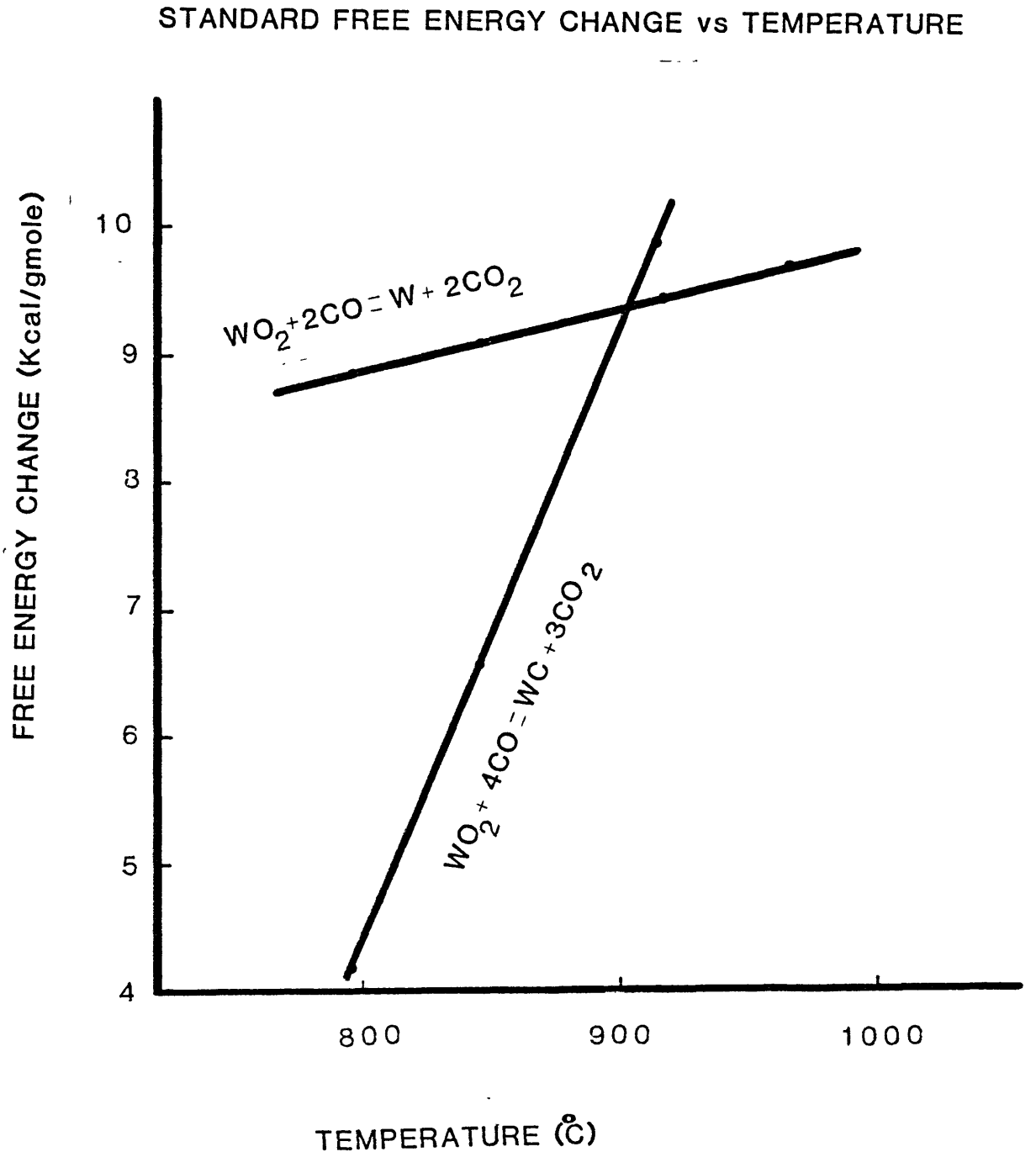
STANDARD FREE ENERGY CHANGE vs TEMPERATURE
FREE ENERGY CHANGE (Kcal/gmole)
10
9
8
7
6
5
4
$WO_2+2CO=W+2CO_2$
$WO_2+4CO=WC+3CO_2$
800
900
1000
TEMPERATURE (°C)

FIGURE 6

REACTIONS IN CO/CO_2 ATMOSPHERES

At first it was thought that the appearance of W_2C during the carburisation of tungsten slowed down the reaction and that if conditions were introduced whereby WC could be formed directly from the metal, then the kinetics would be speeded up. In order to investigate this, experiments were carried out using controlled CO/CO_2 atmospheres. The data given by Kubaschewski, Evans and Alcock[22] were used to calculate the pCO_2/pCO ratios for the following reactions at 1050°C.

1. $2W + 2CO \rightarrow W_2C + CO_2$

$\Delta G° = -47,200 + 40.7T$ cal/mol

$K = 0.08$

$pCO_2/pCO = 0.074$ corresponding to $pCO_2 = 6.92\%$ and $pCO = 93.08\%$

2. $W_2C + 2CO \rightarrow 2WC + CO_2$

$\Delta G° = -53.600 + 44.7T$

$K = 0.122$

$pCO_2/pCO = 0.110$; $pCO_2 = 9.88\%$; $pCO = 90.12\%$

3. $W + 2CO \rightarrow WC + CO_2$

$\Delta G^\circ = -50,400 + 42.7T$

$K = 0.099$

$pCO_2/pCO = 0.090$; $pCO_2 = 8.29\%$; $pCO = 91.71\%$

4. $W + 2CO_2 \rightarrow WO_2 + 2CO$

$\Delta G^\circ = -3,500 - 4.9T$

$K = 0.022$

$pCO_2/pCO = 0.150$; $pCO_2 = 11.68\%$; $pCO = 88.32\%$

According to these values, it was expected that in atmospheres containing less than 6.92% CO_2, reaction 1 will take place, followed by reaction 2. However, during heat treatments in atmospheres varying between 2% to 10% CO_2, no weight changes took place, even after a few days. This observation suggested that either:-

1. The nucleation of WC on tungsten was difficult and W_2C, which was previously reported to be unstable below 1250°C, forms as a metastable phase because it is easier to nucleate.

or

2. The thermodynamic data were wrong.

In order to investigate this, it was decided to carry out heat-treatments of partially carburised samples in controlled CO/CO_2 atmospheres. Tungsten samples were partially carburised for long

enough periods until about 2.3 weight % was gained and were then heat-treated at 1050°C for 16 hours in CO/CO_2 atmospheres of composition varying between 2% to 10% CO_2.

In atmospheres containing 98% CO - 2% CO_2 and 96% CO - 4% CO_2, weight gains were recorded. WC was observed to grow while W_2C was being depleted. Since WC growth took place, this result meant that the nucleation of WC on W was indeed difficult. In atmospheres containing 94% CO - 6% CO_2 and 90% CO - 10% CO_2, weight losses were recorded with W_2C and WC depletion taking place, coupled with tungsten growth. As a result of these heat-treatments it became apparent that metastable W_2C cannot form at carbon activities below unity. Further confirmation of this was obtained when W_2C was observed to decompose when heat treated in argon atmospheres at 1050°C. The diffraction lines for the orthorhombic W_2C structure became sharper and had shifted, with the unit cell parameters becoming smaller as the conditions became more oxidising (as the CO_2 content was increased). This implied that the W_2C composition was becoming less rich in carbon as the W_2C was being depleted. As the W_2C disappeared, a hexagonal modification appeared such that the unit cell parameters became smaller, indicating that the W_2C stoichiometry followed the carbon activity at the W_2C-WC boundary. In experiments with 6% CO_2 and 10% CO_2 the unit cell dimensions were very small, much smaller than those reported for the hexagonal modification by previous workers. This confirmed the tendency of the stoichiometry of W_2C to be determined by the activity of carbon in the system.

When WC powder of 99.95% purity was heat-treated in an atmosphere

of 94% CO - 6% CO_2, WC did not oxidise. Since WC had previously been oxidised under the same conditions, but in the presence of W_2C, it seemed that the nucleation of W on WC was difficult as was the nucleation of WC on W.

Carburisation of Tungsten With CO

Tungsten powder of an average particle size of 2 μm was carburised with CO. The weight gain with time is shown in Figures 7, 8 and 9.

From the X-ray diffraction patterns it was observed that during the initial stages of reaction, W_2C was formed. However, during the final stages of carburisation only W and WC were found to be present. As this was puzzling, the carburisation procedure was studied by stopping the reaction at appropriate times and analysing the samples. The initial W_2C growth continued until nucleation of WC took place. WC then grew, first at the expense of W_2C and then W.

By plotting (% weight gain)^2 against time (Figures 10 and 11), breaks were detected in the rate curves. Linear lines were drawn through the initial and later stages of carburisation. These lines indicated the times when nucleation of WC began. These were in good agreement with the experimental findings and in reasonable agreement with the work of Hara and Miyake[13]. At the higher temperatures a thicker W_2C layer was formed and the nucleation of WC occurred in less time.

From these results it was calculated that at 1120°C, a W_2C layer of 0.15 μm was formed before it was converted to WC.

%WEIGHT GAIN vs TIME PLOT FOR THE CARBURISATION OF W WITH CO AT 800°C

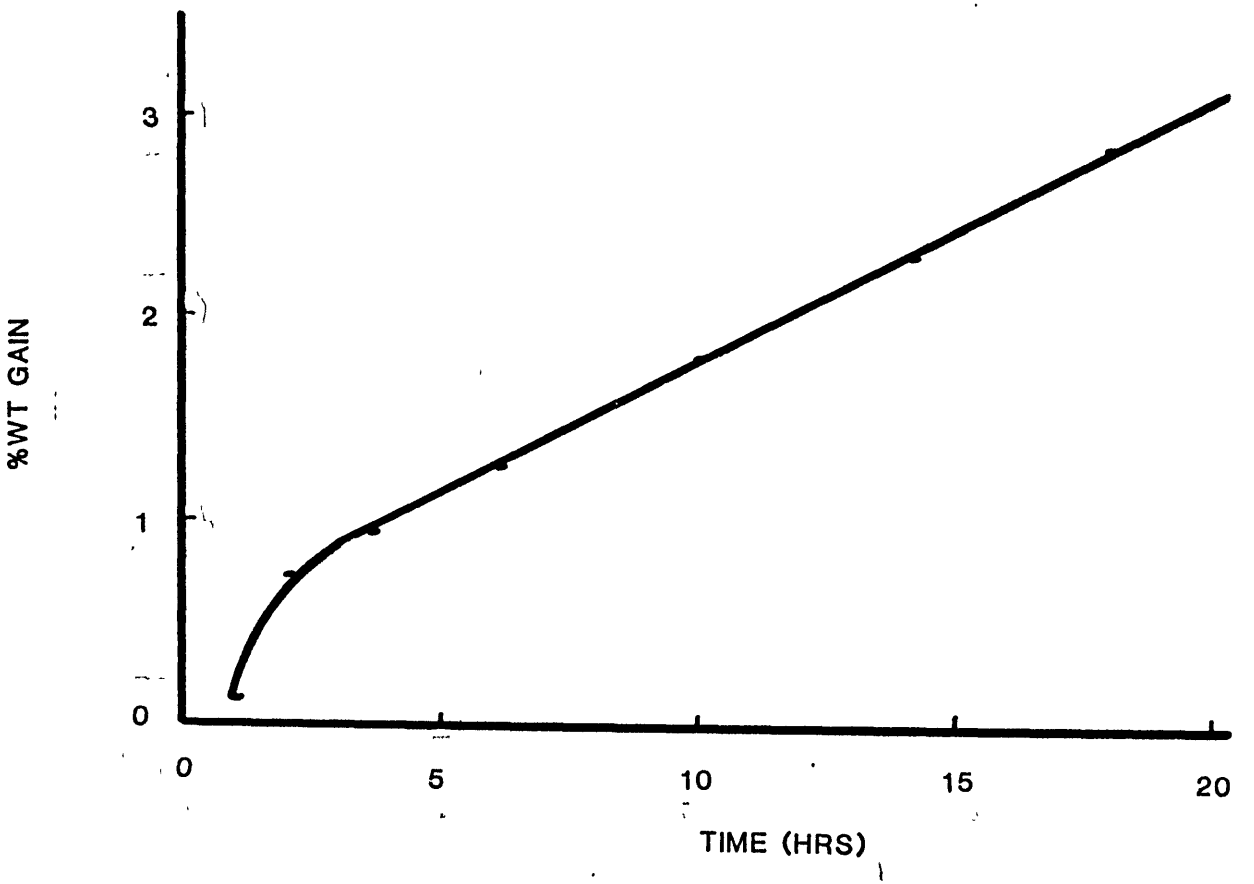

FIGURE 7

FIGURE 8

%WEIGHT GAIN vs TIME PLOT FOR THE CARBURISATION OF W WITH CO AT 1050°C

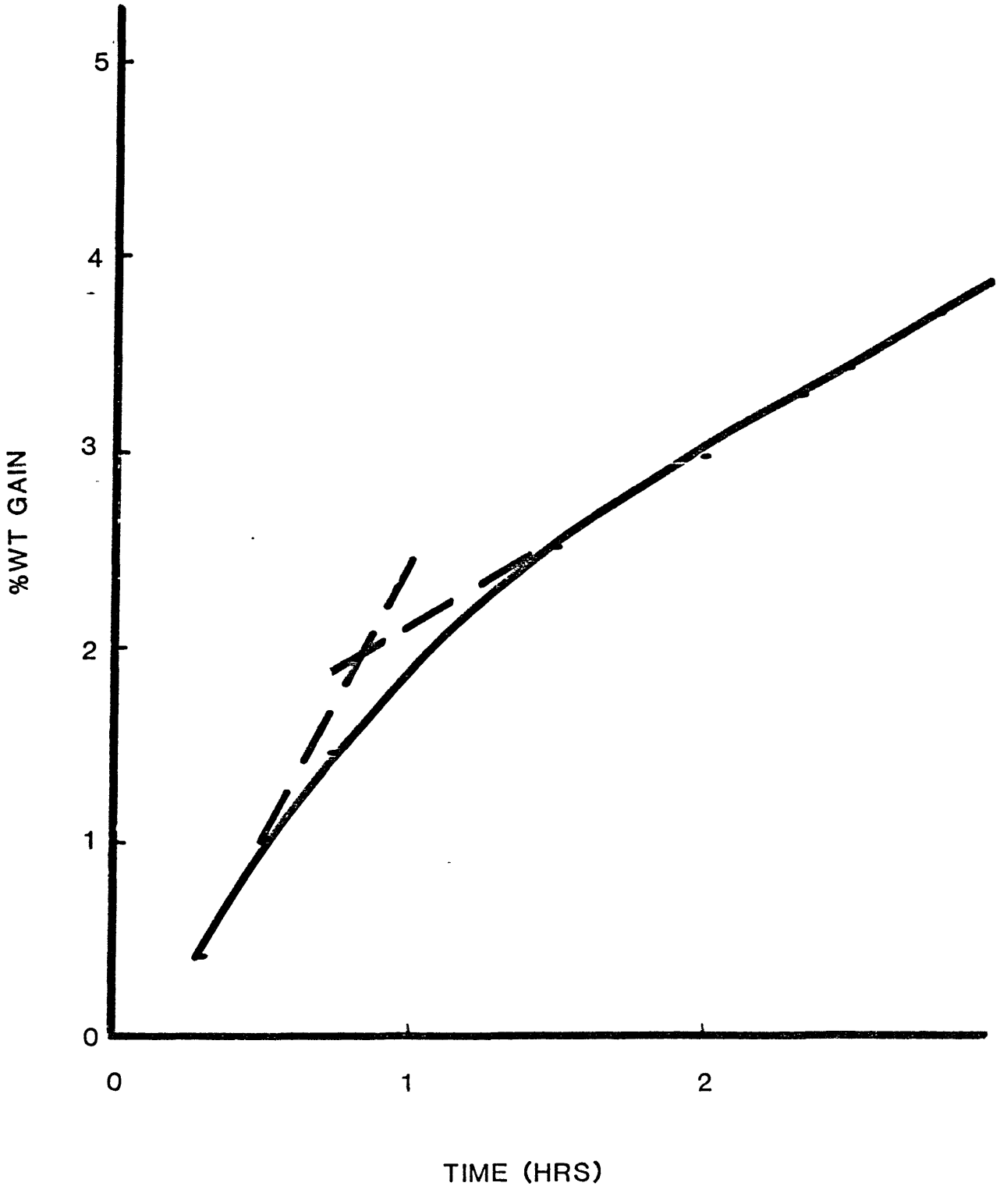

FIGURE 9

%WEIGHT GAIN vs TIME PLOT FOR THE CARBURISATION OF W WITH CO AT 1120°C

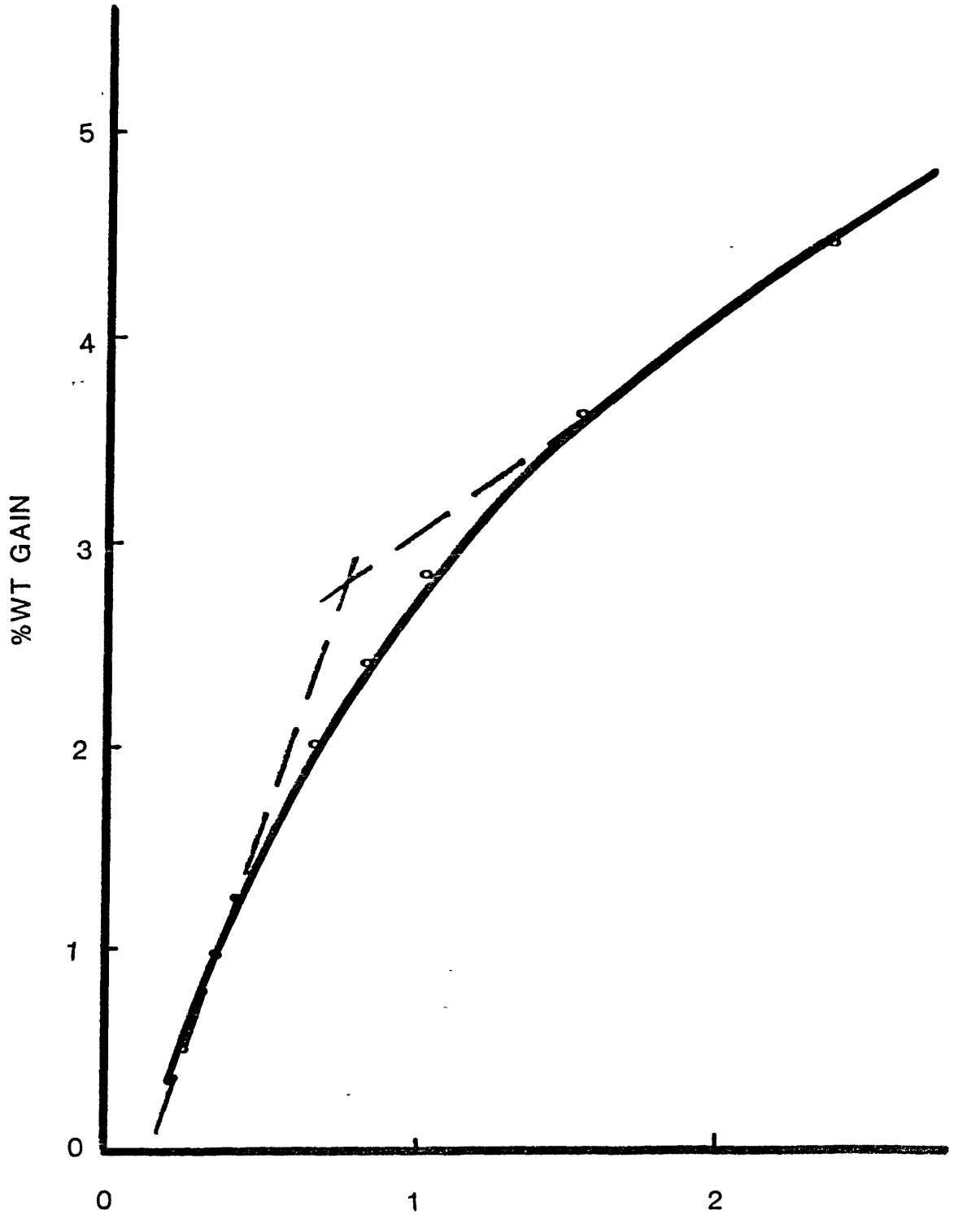

PARABOLIC RATE RELATIONSHIP FOR THE CARBURISATION OF W WITH CO AT 1050°C

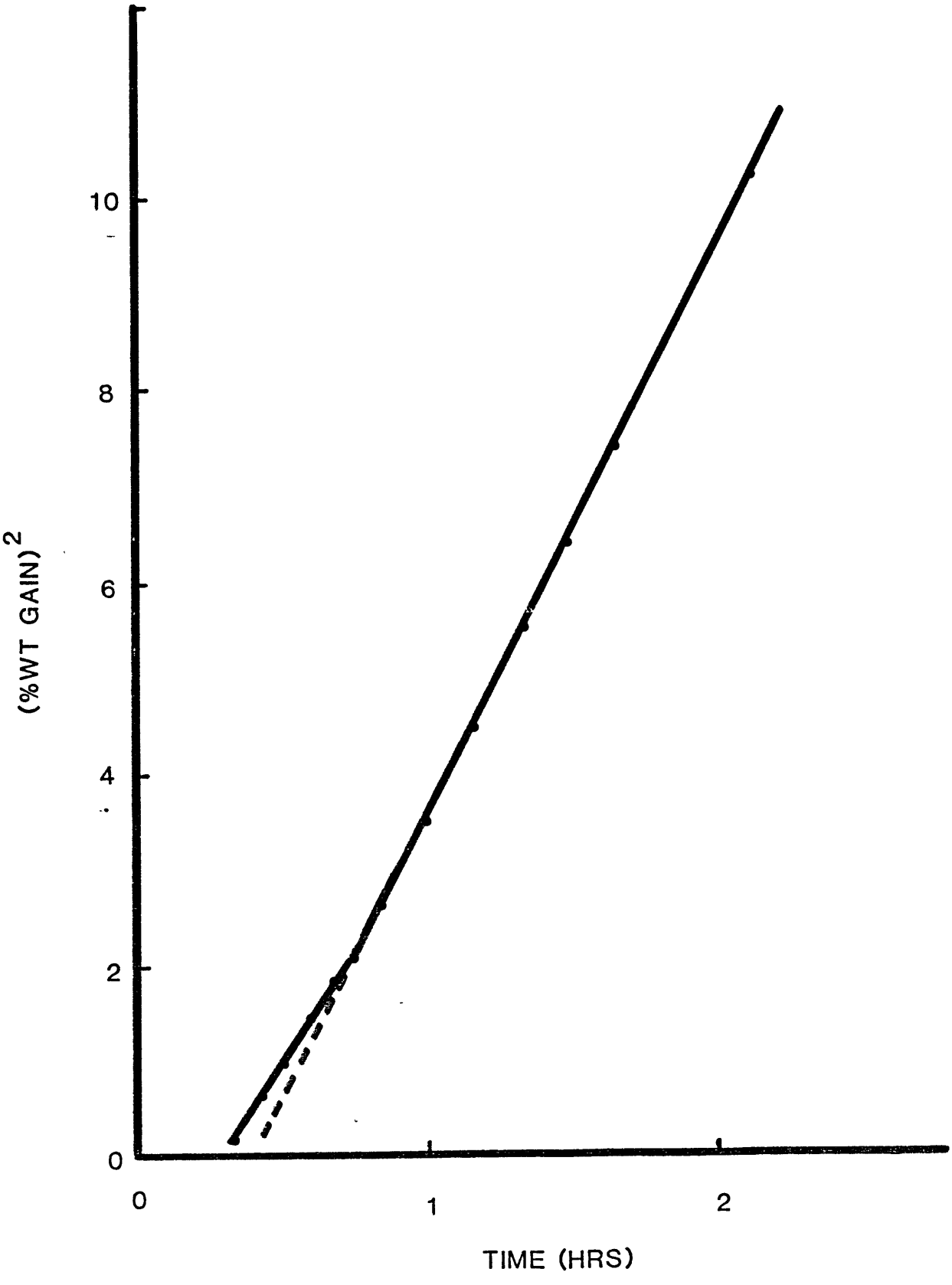

FIGURE 10

PARABOLIC RATE RELATIONSHIP FOR THE CARBURISATION OF W WITH CO AT 1120°C

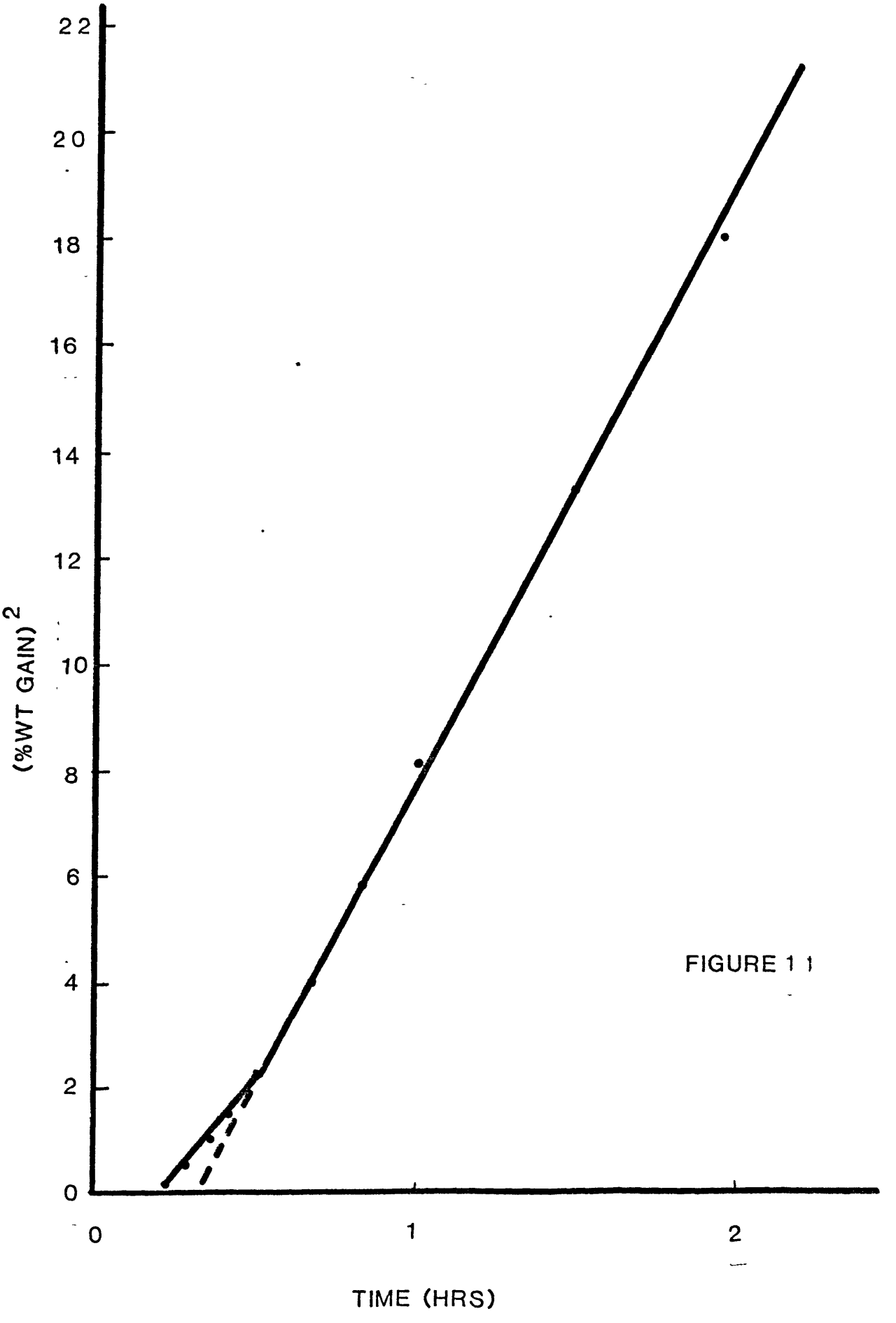

FIGURE 11

Carburisation of Tungsten Wires With CO

Tungsten wire of diameter 0.75 mm was reacted with CO at 1120°C. Reaction was extremely slow, due to the large specimen size and the low carbon diffusivity through the metal. After 240 hours a weight gain of 0.001 g was recorded, corresponding to a weight gain of 0.27%.

When the wire was analysed by means of X-ray diffraction, only W and WC were detected. This was in accordance with the results using tungsten powder, from which it was predicted that at 1120°C a W_2C layer of 0.15 μm would be formed. With the help of a light microscope the WC layer on tungsten wire was determined to be 6 μm. This meant that during the reaction time all the W_2C which was formed on the wire had been converted to WC which had continued to grow.

DISCUSSION

OBSERVATIONS OF THE PHASE RELATIONSHIPS IN THE TUNGSTEN-CARBIDE SYSTEM

Previous work has clearly indicated that W_2C is not stable below a temperature of about 1250 °C with respect to tungsten and WC. The results of the various carburisation treatments in the range 800 °C to 1120 °C were therefore most surprising because W_2C was observed in most specimens after reaction. At first, it was considered that the W_2C phase which formed was an oxycarbide in which partial replacement of carbon by oxygen stabilised the W_2X cph structure. A series of investigations of the W-WO_2-WC system failed completely to substantiate this hypothesis. On no occasion was W_2X observed, and in several experiments substantial reaction of WC and WO_2 occurred to produce tungsten and carbon monoxide. These experiments provided substantial proof that the cph phase which was observed in most carburisation experiments was not an oxycarbide.

In the light of this evidence, it became apparent that the cph phase formed was a metastable carbide. Support for this view comes from the results of several experiments. Experiments were carried out in the temperature range 1000° - 1200 °C with CO/CO_2 atmospheres with effective carbon activities from 0.036 to 1.0. The available thermodynamic data indicated that WC should be stable at carbon activities greater than 0.045 at 1050°C. Even with reaction times of up to 16 hours, no carburisation reaction was observed. These results

showed that nucleation of WC on tungsten was difficult and, in addition, no W_2C was formed. By contrast, in all experiments with gaseous carbon activities equal to or greater than unity, W_2C was observed to form very quickly and after reaction had proceeded for tens of minutes WC was observed in the reaction product. At first these results seemed very baffling. However, in view of the difficulties of nucleation of WC on tungsten and the fact that whereas W_2C is unstable with respect to W and WC, it is stable with respect to tungsten and carbon, it seems that metastable W_2C forms because of the much easier nucleation of this phase compared to WC. Furthermore, the experimental results indicate that nucleation of WC on W_2C is much easier than on tungsten surfaces.

Having established that the formation of metastable W_2C occurs and is possible, it is interesting to establish the composition of this metastable phase. Once again, the results were surprising because at temperatures below about 1100°C the X.R.D. patterns of the W_2C which formed indicated that the orthorhombic modification of this phase was formed. At 1120°C, the cph modification only was formed with carbon monoxide and carbon and the orthorhombic modification was only observed when a higher carbon activity, 50% carbon monoxide - 50% hydrogen, was used. In a number of binary interstitial alloy systems, it has been established that the orthorhombic modification of the close packed hexagonal structure is related to the ideal stoichiometry M_2X. The modification is brought about by the ordered arrangement of the interstitial atoms within the interstitial sites which occurs at the critical composition. At interstitial atom compositions less than this

critical value, the interstitial atoms are randomly distributed throughout all the possible sites and a close packed hexagonal structure is observed. The unit cell dimensions observed for the orthorhombic modification are in excellent agreement with the unit cell dimensions expected at this critical W_2C composition. The appearance of this orthorhombic phase was totally unexpected because in the stable binary system it is not observed to appear until a temperature of 2100°C is reached. In addition, the close-packed hexagonal W_2C_{1-x} phase which is observed to be in equilibrium with tungsten and WC at 1250°C contains only 31 atm% carbon.

Thus, not only is metastable W_2C observed in the temperature range 800-1120°C, but it occurs at a composition with an ordered structure which is itself metastable up to 2100°C. Once again it should be remembered that stable W_2C exists in equilibrium with tungsten or WC at a carbon activity less than unity. The fact that metastable equilibrium can be achieved with carbon activities greater than unity allows the formation of this phase at these very low temperatures. At 1050°C many observations have been made which indicate that the composition of W_2C obtained by carburising with carbon monoxide lies in the range 33.3 to 35 atom%. At 1120°C, the composition obtained varies from 31 to 32 atom% carbon with carbon monoxide and the ordered structures is only observed with carbon monoxide-hydrogen mixtures.

KINETICS OF CARBIDE FORMATION

In all experiments with both tungsten trioxide and tungsten metal as starting material, carbide formation was only observed when carbon

or gaseous atmospheres with a carbon activity greater than unity were used. The results fall essentially into two main categories:-

(i) the reduction-carburisation of tungsten trioxide at temperatures below about 900°C.

(ii) the reduction and carburisation of tungsten trioxide and the carburisation of tungsten metal at temperatures greater than 900°C up to 1150°C.

REDUCTION-CARBURISATION OF TUNGSTEN TRIOXIDE BELOW 900°C

The reduction-carburisation of tungsten trioxide at temperatures below 900°C proceeded very rapidly to produce WC. Experiments which were stopped at various stages of reaction indicated that reduction of the trioxide occurred initially to the dioxide and subsequently tungsten monocarbide was formed. No evidence was observed at any time of the presence of either tungsten metal or W_2C. The initial stages of reduction exhibit a linear rate of reaction with time and is associated with the reduction to WO_2. WC formation does not occur until almost complete conversion of WO_3 to WO_2. At the onset of carbide formation, the rate of reaction becomes parabolic. At 800°C complete conversion to WC is achieved in approximately 2 hours. On the basis of the reaction rate the size of the carbide is estimated to be 0.15 μm. The ease of nucleation of WC on WO_2 and the rapid reaction rate are surprising in view of the problem associated with higher temperatures.

REDUCTION-CARBURISATION OF WO_3 ABOVE 900°C

In contrast to the lower temperature, the reduction-carburisation above 900°C proceeds by reduction of the oxide to tungsten followed by carburisation of the tungsten metal. Once again, the initial rate of the process is linear with time and proceeds to virtually complete conversion to tungsten before carbides are formed. The reduction phase takes 40 minutes at 1050°C and 30 minutes at 1125°C. When carburisation commences, W_2C is formed initially and growth proceeds until approximately 1/3 of the tungsten is converted to carbide. At this stage WC nucleates on the surface of the W_2C after about 25 minutes at 1125°C and 30 minutes at 1050°C. WC continues to grow until all the W_2C is consumed, whereupon WC continues to grow on the remaining tungsten metal until reaction is complete. Complete carburisation occurs at 1125°C at 120 minutes after the beginning of reduction. It is interesting to note that the time for complete carburisation at 1125°C is exactly equivalent to that for reaction at 800°C.

In order to explore the carburisation reaction more fully, a series of experiments on the carburisation of tungsten metal were completed. A variety of gas compositions were explored to carburise the metal at 1050°C and 1125°C.

The metal used in these experiments was powder almost spherical in shape with an average particle size of 2 μm and a size distribution between 1 and 3 μm. Once again, W_2C was observed to form almost instantaneously and continued to grow until a layer of 0.15 μm was

formed at 1050°C and 1120°C and 0.01 μm at 800°C. At which point, WC nucleated and converted the W_2C and then grew on tungsten until the reaction was completed.

Several experiments were completed following the weight change with time and many experiments were carried out for fixed times and the weight change measured. It is possible using the results of these experiments to obtain some information on the kinetics of the reaction. For the growth of a reaction product around a spherical particle of metal A reacting with another phase X,

$$\nu A + X = A_\nu X$$

the time and dependence of the molar flow F_X of reactant through the product layer $A_\nu X$ for isothermal conditions is given by

$$(F_X)_{r,t} = - 4\pi r^2 D \left[\frac{dc}{dr}\right]_{r,t} \quad \text{mole sec}^{-1} \qquad (1)$$

where r is the radial distance from the centre of the sphere, D is the diffusivity of X, assumed independent of composition and $\frac{dc}{dr}$ is the concentration gradient of X in the product layer.

As the reaction proceeds the radial position r_i of the reaction interface between the product layer and the unreacted core moves towards the centre of the sphere. When the rate of diffusion is greater than the rate of movement of the interface, a pseudo-steady state $\frac{dc}{dt} = 0$ approximation may be made. It is also assumed that the rate of reaction is controlled solely by diffusion in the product layer under the fixed boundary conditions $C = C_e$ (equilibrium concentration) at $r = r_i$ and $C = C_o$ at $r = r_o$.

The third assumption is that the radius r_o of the sphere (core + shell) remains unchanged. With these boundary conditions the integration of the above equation gives for molar flow

$$F_X = (4\pi r_o r_i / r_o - r_i)\, D\, (C_o - C_e) \qquad (2)$$

For the stoichiometry of this reaction, the following equality of fluxes may be written

$$\nu F_X / 4\pi r_o^2 = - F_A / 4\pi r_o^2 \qquad (3)$$

Noting that the instantaneous rate of reaction is given by

$$F_A = d\,(\rho\, 4/3\, \pi\, r_i^3)\, /dt \qquad (4)$$

where ρ is the molar density of A in the unreacted core the following relationship is obtained from equation 3:

$$\frac{\nu F_X}{4\pi} = -\rho\, r_i^2\, \frac{dr_i}{dt} \qquad (5)$$

Combining this with equation 2 and integrating gives the equation for r_i as a function of time t

$$2\left[\frac{r_i}{r_o}\right]^3 - 3\left[\frac{r_i}{r_o}\right]^2 + 1 = 6\nu D / \rho r_o^2\, (C_o - C_e)\, t \qquad (6)$$

The fraction **F** of the reactant A consumed is given by

$$\frac{r_1}{r_o} = (1 - F)^{1/3}$$

Inserting in equation 6 gives for the time dependence of fraction reacted

$$3 - 2F - 3(1 - F)^{2/3} = \frac{6\nu D}{\rho r_o^2} (C_o - C_e)\, t \qquad (7)$$

For diffusion control such a relationship is expected to hold for the present investigation. In fact, such a plot of $3-2F - 3(1-F)^{2/3}$ against time proved to be linear with two major portions related to the growth of W_2C and WC. From the linear portions of the graphs, permeabilities of carbon through W_2C and WC were computed, when the permeability is $D (C_o - C_e)$.

As expected from the experimental observations, the permeability of carbon through WC was observed to be greater than that through W_2C at all temperatures investigated. This is anticipated because once WC nucleates it quickly converts W_2C. Extrapolation of the permeability values indiates that the permeabilities became equal at 1256°C. This value is in excellent agreement with the temperature of 1250°C accepted as the W_2C eutectoid temperature. Thus at temperatures above this value the permeability of carbon through W_2C becomes greater than that through WC. This observation is necessary because above the eutectoid temperature W_2C is stable with respect to W and WC and thus must always

RELATIONSHIP BETWEEN log PERMEABILITY vs TEMPERATURE FOR WC AND WC_2

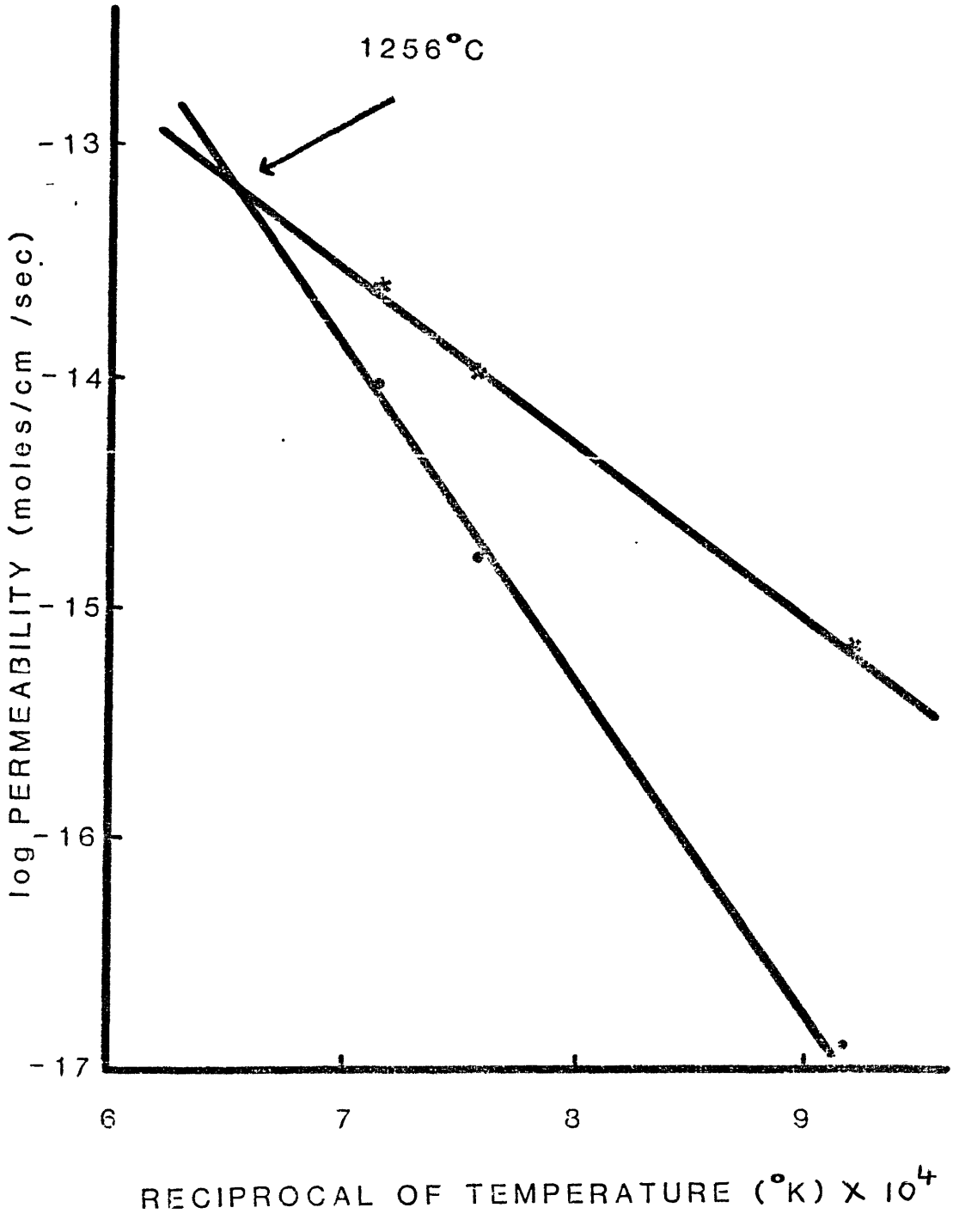

FIGURE 12

exist between these two phases. Thus, the kinetic results are in agreement with the concept of W_2C metastability below the eutectoid temperature. The presence of W_2C is related to the difficulty of nucleation of WC on a tungsten surface. It is also interesting to note that once WC forms, the stoichiometry of the W_2C becomes carbon deficient to equilibrate with the carbon activity exhibited by WC.

REFERENCES

1. Sykes W. Trans. Am. Soc. Steel Treat., 1930, 18, 968.
2. Skaupy F. Z. Electrochem. 1927, 33, 487.
3. Goldschmidt H. and Brand J. J. Less- Comm. Met. 1963, 5, 181.
4. Orton G. Trans. AIME 1964, 230, 600.
5. Sara R. J. Am. Cer. Soc. 1965, 48, 251.
6. Rudy E., Windisch St. and Hoffman J.R. AFML - TR 65-2 Part 1, Vol. 6, Air Force Materials Laboratory, Research and Technology Division, Air Force Systems Command Wright - Patterson A.F.B., Ohio 1966.
7. Rudy E. and Windisch St. J. Am. Cer. Soc. 1967, 50, 272.
8. Worrell W. J. Phys. Chem. 1964, 68, 954.
9. Gleiser M. and Chipman J. Trans. AIME 1962, 224, 1278.
10. Gupta D. and Siegle L. Metal Trans. A. 1975, 6A, 1939.
11. Moissan H. Compt. Rend. 1893, 116, 1225.
12. Schwarzkopf P. and Kieffer R. "Refractory Hard Metals" McMillan, 1953.
13. Miyake M., Hara A., Sho T. and Kawakata Y. Proc. Powd. Met. Conf. Stockholm, 1978.
14. Hilpert S. and Ornstein M. Ber. Dtsch. Chem. Ges. 1913, 1661.
15. Newkirk A. and Aliferis I. J. Am. Chem. Soc. 1957, 79, 4629.
16. Davidson C., Alexander G. and Wadsworth M. Met. Trans. B, 1978, 9B, 553.
17. Chretien A., Freundlich W. and Josien F.A. Compt. Rend. 1952, 234, 2608.

18. Hih and Wand "Tungsten" Plenum Press, New York, 1979.

19. Basu A.K. and Sale F.R. Met. Trans. 1978, 9B, 603.

20. Hara A. and Miyake M. Plans. Pulver 1970, 18, 91.

21. Hegedus A.J. and Gado P. Z. Anorg. Allgem. Chem. 1960, 305, 227.

22. Kubaschewski D., Evans E.L. and Alcock C.B. "Metallurgical Thermochemistry", Pergamon, Oxford, 1967.

MOLYBDENUM CARBIDE

THE Mo-C SYSTEM

Two compounds, Mo_2C and MoC, are accepted as existing in the molybdenum-carbon system and furthermore each of these compounds exhibits two crystallographic modifications. According to the most reliable results, the close packed hexagonal modification of Mo_2C is the only stable phase at room temperature.

Our understanding of the Mo-C system relied upon the phase diagrams constructed by Sykes et al[1] and Nowotny et al[2], until Rudy and co-workers[3] carried out an extensive study of the system using X-ray diffraction, metallographic and thermal analysis techniques. The phase diagram which resulted from this most recent work is shown in Figure 1. They demonstrated, for the first time, the existence of a high temperature phase change in Mo_2C and confirmed the earlier observation that MoC has two crystal forms. The low temperature α-Mo_2C modification has been reported[3] as orthorhombic with parameters a = 7.24 Å, b = 6.004 Å and c = 5.19 Å in agreement with the observations of Parthé[4] and Bowman[5], both of whom used neutron diffraction. The high temperature β-Mo_2C form is the disordered hexagonal close-packed structure with lattice parameters a = 3.012 Å and c = 4.736 Å[3,5]. It has been stated that the hexagonal structure is often obtained on quenching when the composition is carbon poor compared to $MoC_{0.5}$[6]. In view of this observation, it seems reasonable that only stoichiometric Mo_2C possesses an orthorhombic structure due to ordering of the carbon atoms in an essentially hexagonal array of molybdenum atoms. The higher carbon containing carbide is carbon-deficient and

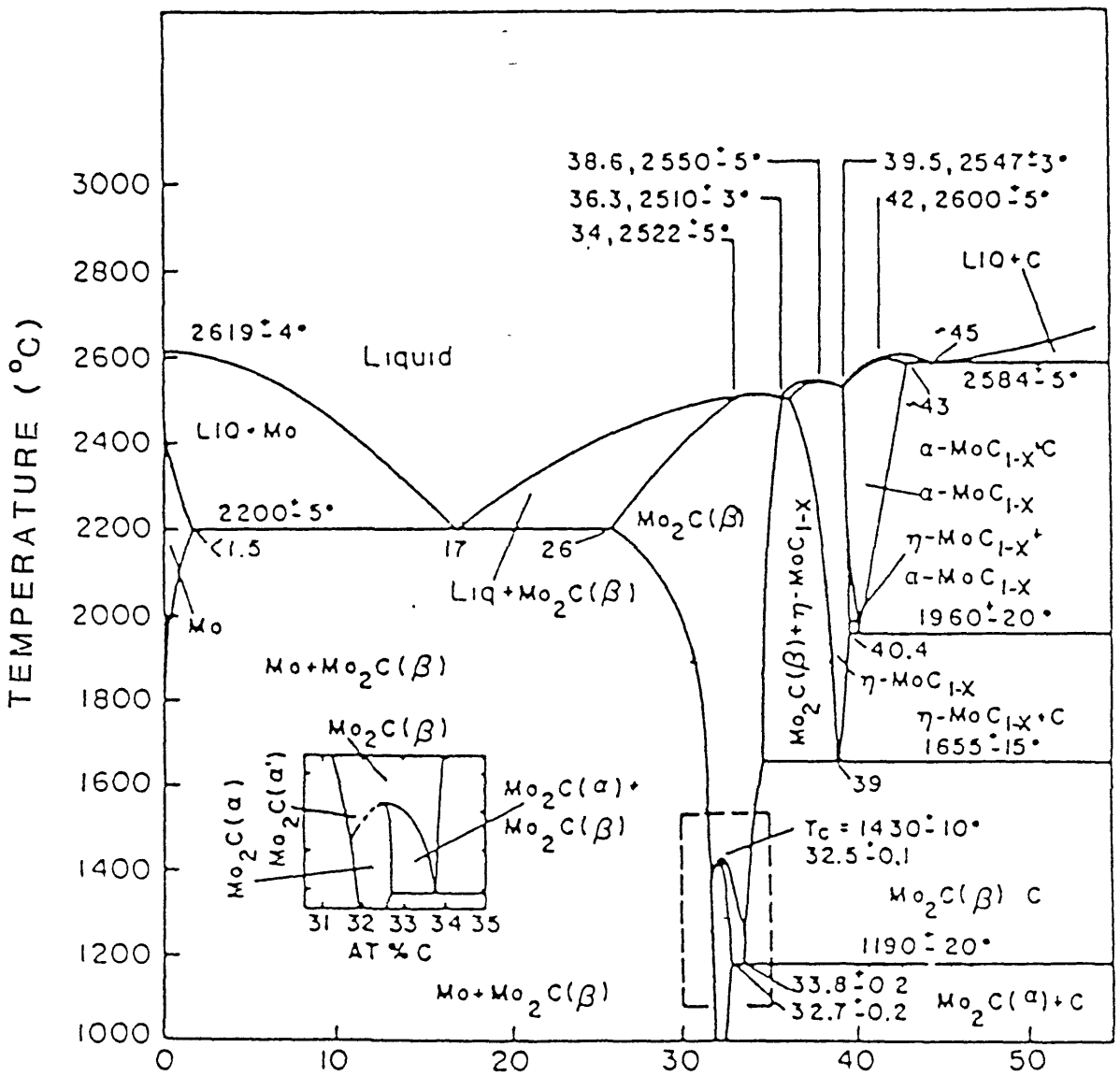

THE Mo-C SYSTEM

FIGURE 1

has been designated as MoC_{1-x}. η-MoC_{1-x}, the low temperature form, displays a hexagonal structure with an ABAB ... stacking arrangement of metal atoms and parameters a = 3.01 Å and c = 14.63 Å. At about 1960°C this phase is converted to α-MoC_{1-x} which is face-centred cubic with a = 4.281 Å. Other crystal forms have been reported which are thought to be metastable (see later).

The eutectic temperature between Mo and Mo_2C was established at 2205°C in agreement with the work of Nowotny et al[2] and Storms[7]. The eutectic composition was located at $MoC_{0.17\pm0.02}$ by metallographic inspection and at $MoC_{0.15}$ by Sykes et al[1].

Rudy et al[3] reported that Mo_2C in equilibrium with Mo shows the development of long range disorder as the temperature is raised (α-Mo_2C transforming to β-Mo_2C) with the order-disorder transition separated by a small temperature gap. On the other hand, Mo_2C in equilibrium with carbon transforms isothermally at 1190°C ± 20°C. Bowman[5], using high temperature neutron diffraction, observed an order-disorder transformation in high carbon Mo_2C in agreement with Rudy et al[3] and also reported a similar transition temperature of 1490°C ± 50°C when Mo_2C is in equilibrium with the metal. Considering that Bowman[5] also observed this transition to be much faster for hyperstoichiometric Mo_2C than for hypostoichiometric Mo_2C, the possibility exists that Rudy et al[3] did not heat-treat their samples long enough to be at equilibrium.

Both η-MoC_{1-x} and α-MoC_{1-x} are stable only at high temperatures. η-MoC_{1-x} can be easily retained during cooling, whereas a very rapid

quench is required to preserve α-MoC_{1-x}. A transition between the two modifications exists at around 1960°C ± 20°C[3]. According to the same authors, η-MoC_{1-x} decomposes into β-Mo_2C and carbon at about 1655°C ± 15°C. The value of 1450°C reported by Wallace et al[8] is probably inaccurate because they estimate the error in temperature measurement to be ± 100°C.

PREPARATION OF MOLYBDENUM CARBIDES

Methods of forming molybdenum carbides have been reported by various authors since the end of the last century. Moissan[9] obtained a product containing 5.48% - 5.68% carbon, nearly corresponding to the composition Mo_2C (theoretical 5.88%) by reducing MoO_3 with carbon or calcium carbide in an electric arc. The formation of MoC was later reported by Moissan and Hoffman[10]. Friederich and Sittig[11] prepared Mo_2C by heating pressed mixtures of molybdenum and carbon black in the appropriate ratio at 1200°C for an hour in a hydrogen atmosphere. The formation of MoC was also reported by the same authors[11] at 1500°C - 1600°C.

According to Hegedus and Neugebauer[12], when MoO_3 is reduced with carbon, MoO_2 is first produced. Production of the metal from MoO_2 begins at above 820°C and Mo_2C results only after the oxide has been eliminated. Huttig and Fattinger[13] reported that the reaction is promoted by the presence of hydrogen or hydrogen halides.

For the industrial production of Mo_2C, pure MoO_3 is used as the starting material. This is reduced to the metal with hydrogen at 900°C. The molybdenum powder is then mixed with sugar charcoal or carbon black and heated to 1500°C under a hydrogen atmosphere.

RESULTS

Reduction Of MoO_3 With Graphite

The reaction between molybdenum trioxide and graphite was studied at 690 °C, 820 °C and 890 °C.

At the lowest temperature, the reaction proceeded until a weight loss of about 10% was recorded and no further reaction occurred. X-ray diffraction analysis of the product revealed the presence of molybdenum dioxide, together with several weak extra diffraction lines, indicating the presence of Magneli-type oxide phases richer in oxygen than MoO_2. This identification was in accord with the weight loss, since a weight loss of 12.3% was required for conversion to MoO_2. By gradually increasing the temperature it was established that no further reaction would take place at temperatures below about 800°C.

The results of weight loss with time at 820°C and 890°C are shown in Figure 2. At both temperatures, incubation periods were observed associated with the fact that it took the sample a few minutes to heat up. At both temperatures, complete conversion to Mo_2C was observed. From the X-ray diffraction results it was established that the trioxide was reduced to the dioxide by way of intermediate Magneli-type phases and then Mo_2C was produced directly from the oxide without any observation of the production of molybdenum metal. This was contrary to the work of Hegedus and Neugebauer[12] who claimed a reaction sequence via the metal. As shown in Figure 2, and as expected, the reaction was temperature sensitive.

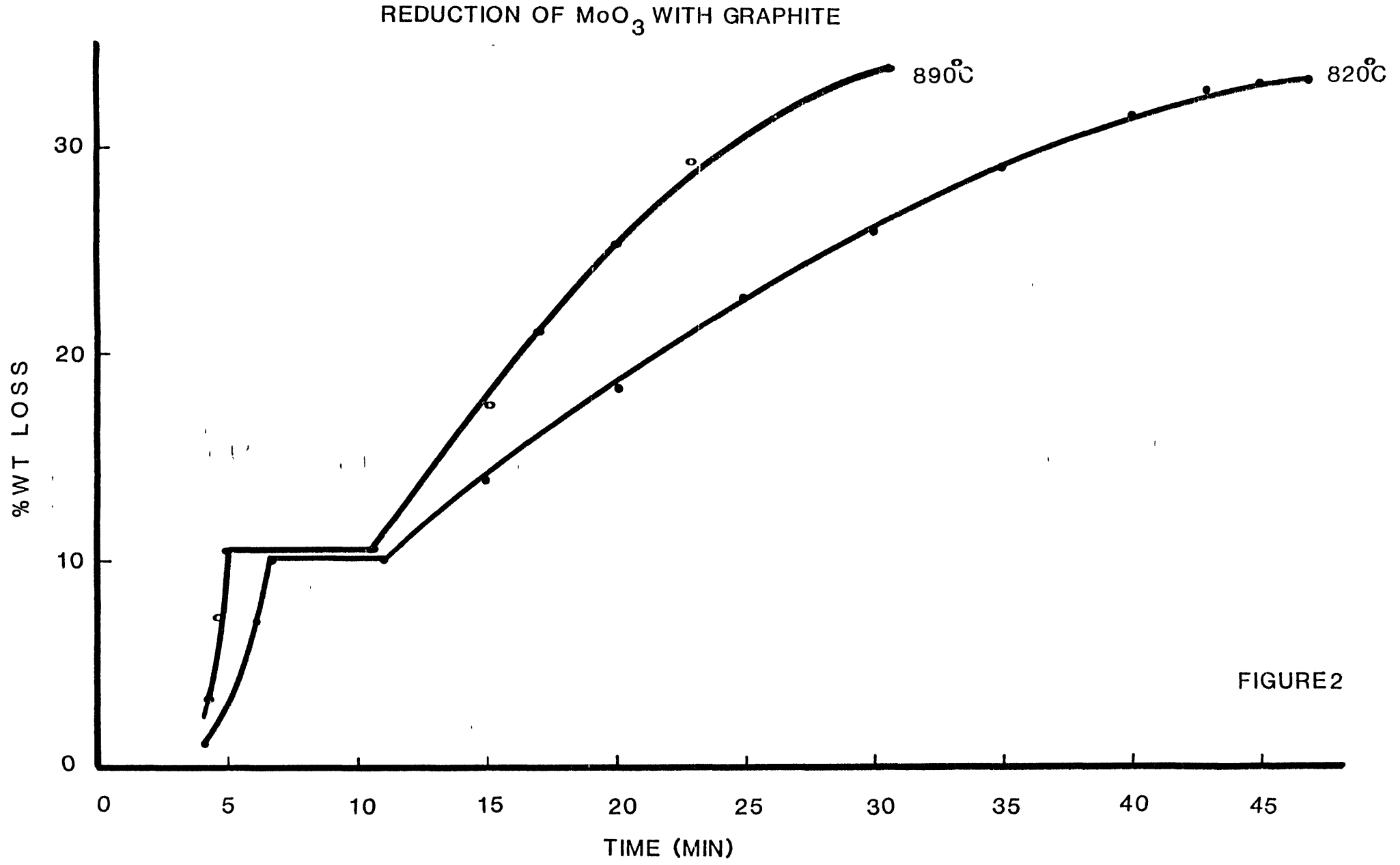
REDUCTION OF MoO_3 WITH GRAPHITE
890°C
820°C
% WT LOSS
0
10
20
30
0
5
10
15
20
25
30
35
40
45
TIME (MIN)

FIGURE 2

The product was β-Mo_2C with a close-packed hexagonal structure.

Reduction Of MoO_3 With Collie Coal

The rate of the reduction/carburisation of MoO_3 with Collie coal was observed to be extremely slow, taking up to 20 hours for complete carburisation to Mo_2C. The reason for the extreme tardiness of the reaction was related to a change in the reaction mechanism with the formation of molybdenum metal ($MoO_3 \rightarrow MoO_2 \rightarrow Mo \rightarrow Mo_2C$).

It was initially thought that molybdenum may have formed by reduction of MoO_2 by the volatile matter evolved from the coal. However, reduction using devolatilised coal was also extremely slow. The formation of the metal as an intermediary with coal is certainly due to the greater reactivity of coal compared to graphite.

Carburisation of Molybdenum With CO or CO-H_2 Mixtures

The formation of molybdenum monocarbide was observed only between 660°C to 900°C in the presence of carbon monoxide or carbon monoxide - hydrogen mixtures, indicating the necessity for high carburisation potentials. No monocarbide was formed in experiments carried out at temperatures above 900°C.

Plots of weight gain against time are shown for the carburisation of molybdenum in Figures 3 and 4. After about 10% weight gain (corresponding to about 60% conversion to MoC), carbon deposition was observed. The rate of carbide formation then virtually ceased and the monocarbide was never produced completely pure. In attempting to form pure MoC, submicron molybdenum powder was used to increase the rate of

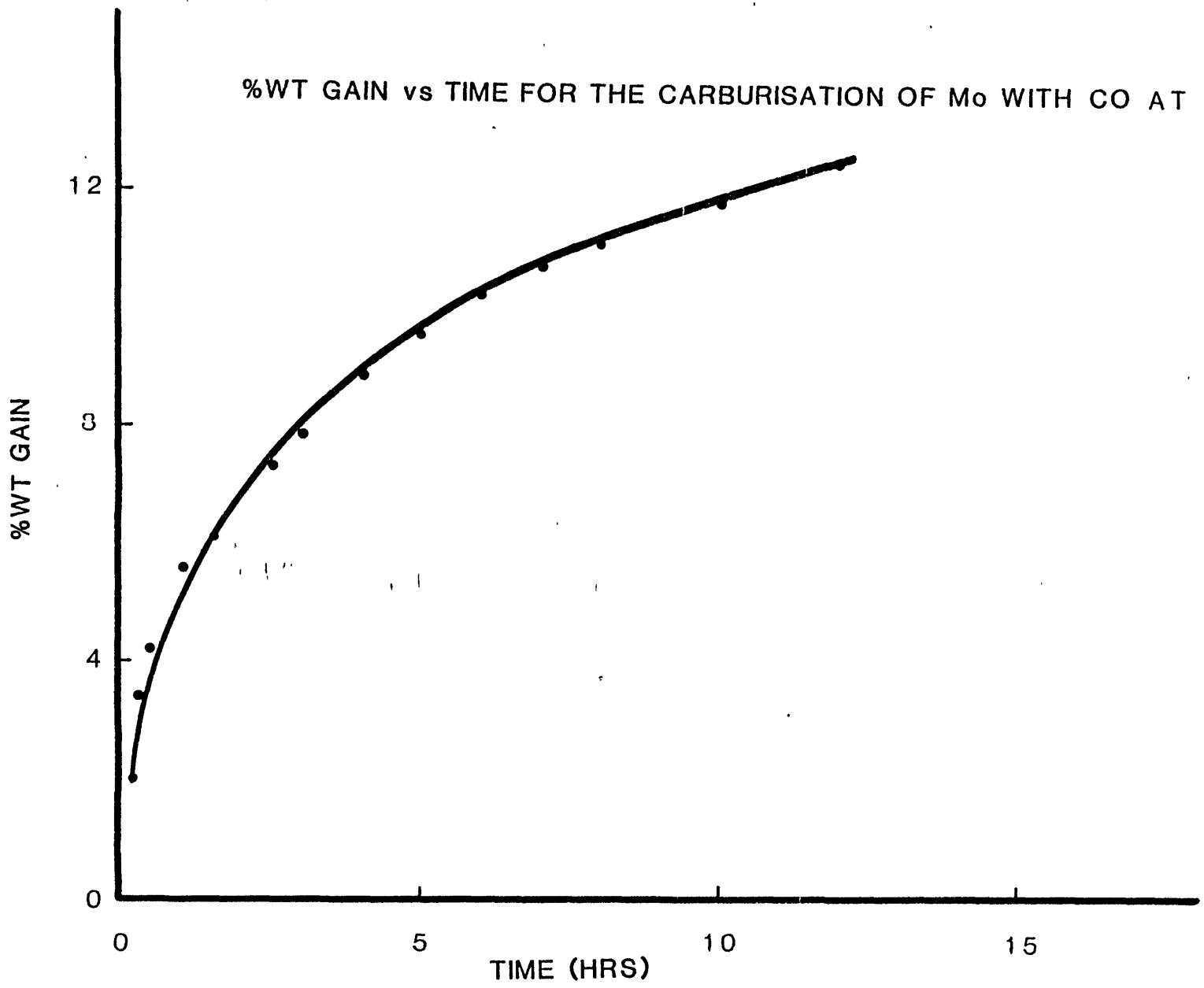
%WT GAIN vs TIME FOR THE CARBURISATION OF Mo WITH CO AT 900°C
%WT GAIN
12
8
4
0
0
5
10
15
TIME (HRS)

FIGURE 3

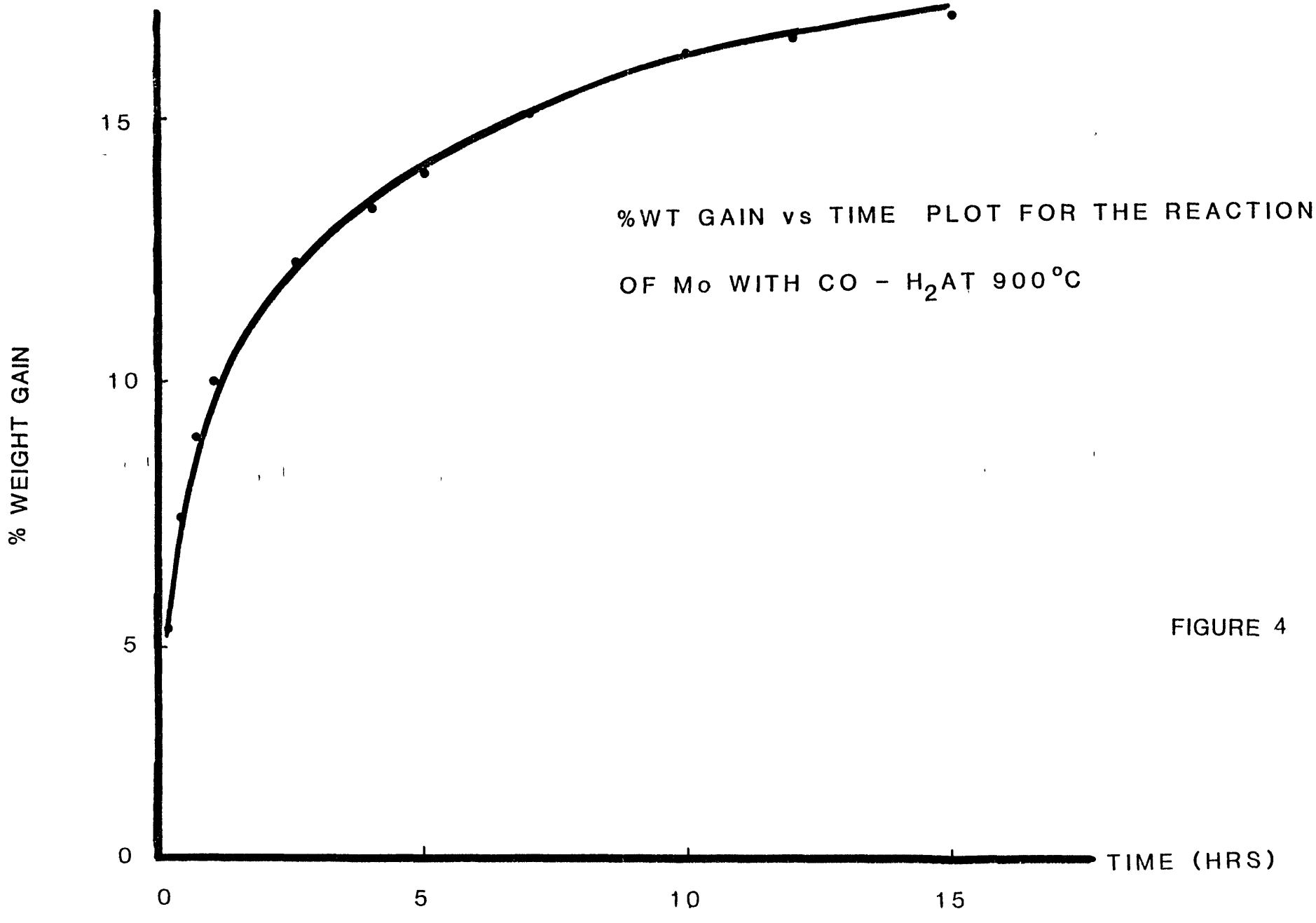
%WT GAIN vs TIME PLOT FOR THE REACTION
OF Mo WITH CO - H_2 AT 900°C
% WEIGHT GAIN
0
5
10
15
TIME (HRS)
0
5
10
15

FIGURE 4

the reaction. However, the rate of carbide formation ceased at the same stage of reaction as previously observed. Another idea was to carburise a mixture of MoO_3 - WO_3 powders. MoC (AA) and WC being isomorphous, it was thought that WC might stabilise MoC. Even though MoC (AA) was stabilised at the expense of MoC (ABAB), the reaction still virtually ceased after about 80% conversion of Mo_2C to MoC.

DISCUSSION

During reactions between molybdenum and CO, at temperatures between 660°C and 900°C, the formation of MoC in addition to Mo_2C was observed. Two MoC structures were observed in the present work. These phases were γ- and γ'-MoC, similar to the observations of Kuo and Hagg[14]. No monocarbide was ever observed in carburisation experiments at 1000°C.

In all cases, the first carbide phase to form was Mo_2C. At low temperatures the monocarbide was nucleated before all the metal was converted to Mo_2C. At temperatures near 900°C there is evidence that molybdenum is completely converted to Mo_2C prior to nucleation of a monocarbide phase.

In experiments with carbon monoxide, the first monocarbide phase nucleated on Mo_2C was MoC (AABB).

With CO-H_2 mixtures at 900°C the nucleation of MoC (AA) is observed directly on Mo_2C, indicating that a higher carburisation potential is required for the nucleation of MoC (AA) on Mo_2C than for MoC (AABB) formation. At lower temperatures even CO-H_2 mixtures led to the nucleation of MoC (AABB) on Mo_2C.

At 900°C a gas mixture containing 6% CO_2 in CO (equivalent to a carbon activity of 0.45) produced only Mo_2C in 120 hours. Experiments using graphite (carbon activity of 1) also yielded Mo_2C only. Under these conditions, the monocarbide cannot be nucleated and therefore it seems that carbon activities greater than unity are essential for

nucleation of the monocarbide.

In all experiments with carbon monoxide, MoC (AA) nucleates after the prior formation of MoC (AABB). Mo_2C is then converted to both monocarbides as X-ray diffraction patterns are interpreted in terms of the intensity of both monocarbide modifications increasing at the expense of Mo_2C as carburisation proceeds. However, at the point when the overall weight increase of the carburised specimens reaches about 10% (equivalent to about 60% conversion of Mo_2C to monocarbides) subsequent carburisation occurs with MoC (AA) forming preferentially to MoC (AABB). These observations indicate that MoC (AABB) transforms to MoC (AA) in addition to continued carburisation of the specimen. The results in CO - 1% CO_2 atmospheres also support this observation. Under these conditions the conversion of the monocarbide phases occurs at a point where more Mo_2C phase exists. At 900°C with CO-H_2 gas mixtures, MoC (AA) is nucleated directly on Mo_2C and grows very slowly without the observation of the MoC (AABB) modification. These results suggest that the monocarbide phase MoC (AABB) is metastable with respect to MoC (AA) and Mo_2C.

Carbon deposition was observed to start after about 10% weight gain in all experiments. This corresponds to the critical point where MoC (AABB) starts to transform to MoC (AA). At this stage, the reaction rate dropped considerably. Unfortunately, the monocarbide was never formed pure, even after one week (168 hours). The growth kinetics of MoC (AA) on Mo_2C were considerably slower than the

corresponding growth of MoC (AABB) on Mo_2C.

Line broadening of the X-ray diffraction pattern was observed between the corresponding reflexions of the two monocarbides in the c-dimension such that a virtually continuous reflexion is observed over a wide range practically joining the reflexions. This observation is an indication of the occurrence of stacking faults in the MoC (AABB) structure.

It is interesting to note that the weight gain observed at which MoC (AA) grows preferentially to MoC (AABB) corresponds to the time at which carbon is first observed. It seems reasonable to assume that both these observations are in some way inter-related. One consequence of this mutual occurrence is that the more metastable phase MoC (AABB) may be richer in carbon than MoC (AA). If this concept is true, the prior growth of MoC (AA) on the more metastable MoC (AABB) must be controlled by interfacial and/or strain energy considerations. This idea seems reasonable, since as the respective phases grow to be thicker, both of these considerations will be less important relative to the overall chemical free energy driving force for the reaction.

REFERENCES

1. Sykes W.P., van Horn K.R. and Tucker C.M. Trans. AIME 117, 1935, 173.
2. Nowotny H., Parthé E., Kieffer R. and Benesovsky Mh. Chem. 85, 1954, 255.
3. Rudy E., Windisch S., Stosick A.J. and Hoffman J.R. AFML-TR-65-2 Part I, Vol. XI, 1967.
4. Parthé E. and Sadagopan V. Acta Cryst. 16, 1963, 202.
5. Bowman A.L., Wallace T.C. and Arnold G.P. 8th Int. Crystallogr. Abst. 1969, 226.
6. Rudy E., Windisch A., Stosick A.J. and Hoffman J.R. Trans. AIME 239, 1967, 1247.
7. Storms E.K. "The Refractory Carbides" Academic Press, New York, 1967.
8. Wallace T.C., Guitierrez C.P. and Stone P.L. J. Phys. Chem. 67, 1963, 796.
9. Moissan H. Compt. Rend. 116, 1893, 1225.
10. Moissan H. and Hoffman M.K. Compt. Rend. 138, 1904, 138.
11. Friederich E. and Sittig L Z. Anorg. Allg. Chem. 114, 1925, 169.
12. Hegedus A.J. and Neugebauer J. Z. Anorg. Allg. Chem. 305, 1960, 216.
13. Huttig G. and Fattinger V. Powder Met. Bull. 5, 1950, 30.

14. Kuo K. and Hägg G. Nature, 170, 1952, 245.

15. Clougherty E.V., Lothrop K.H. and Kafalas J.A. Nature, 191, 1961, 1194.

16. Tutiya H. Tokyo Inst. Phys. Chem. Res. Abstr. 5, 1932, 121.

NIOBIUM CARBIDE

THE NIOBIUM-CARBON SYSTEM

Two compounds are formed in the niobium-carbon system; Nb_2C and NbC, both of which are stable over a wide temperature range. Rudy et al[1] have established the Nb-C phase diagram, which is shown in Figure 1, using DTA measurements and X-ray analyses. Several measurements of the eutectic temperature are in excellent agreement; 2353°C was reported by Rudy et al[1], Storms and Krikorian[2] obtained 2335°C (± 20°C), while Nadler and Kempter[3] measured 2328°C (± 17°C).

A peritectic reaction;

$$\text{liquid} + NbC \rightarrow Nb_2C$$

was observed to take place at 3035°C[1]. Other investigations placed the peritectic temperature at a slightly higher temperature. Storms and Krikorian[2], Nadler and Kempter[3] and Kimura and Sasaki[4] all heat-treated a number of alloy compositions and examined them visually for evidence of liquid formation using a calibrated pyrometer. Storms and Krikorian[2] obtained a temperature of 3090°C for the peritectic reaction and Nadler and Kempter[3] and Kimura and Sasaki[4] determined it to be 3080°C. Pochon et al[5] suggested 3265°C, but because the composition of the molten material was not given, it is impossible to resolve this difference.

The liquidus temperature rises to a maximum of about 3613°C as the carbon content increases and then decreases to a eutectic represented by the reaction

$$\text{liquid} \rightarrow NbC + C.$$

This eutectic temperature was placed by Rudy et al[1] at 3305°C and at

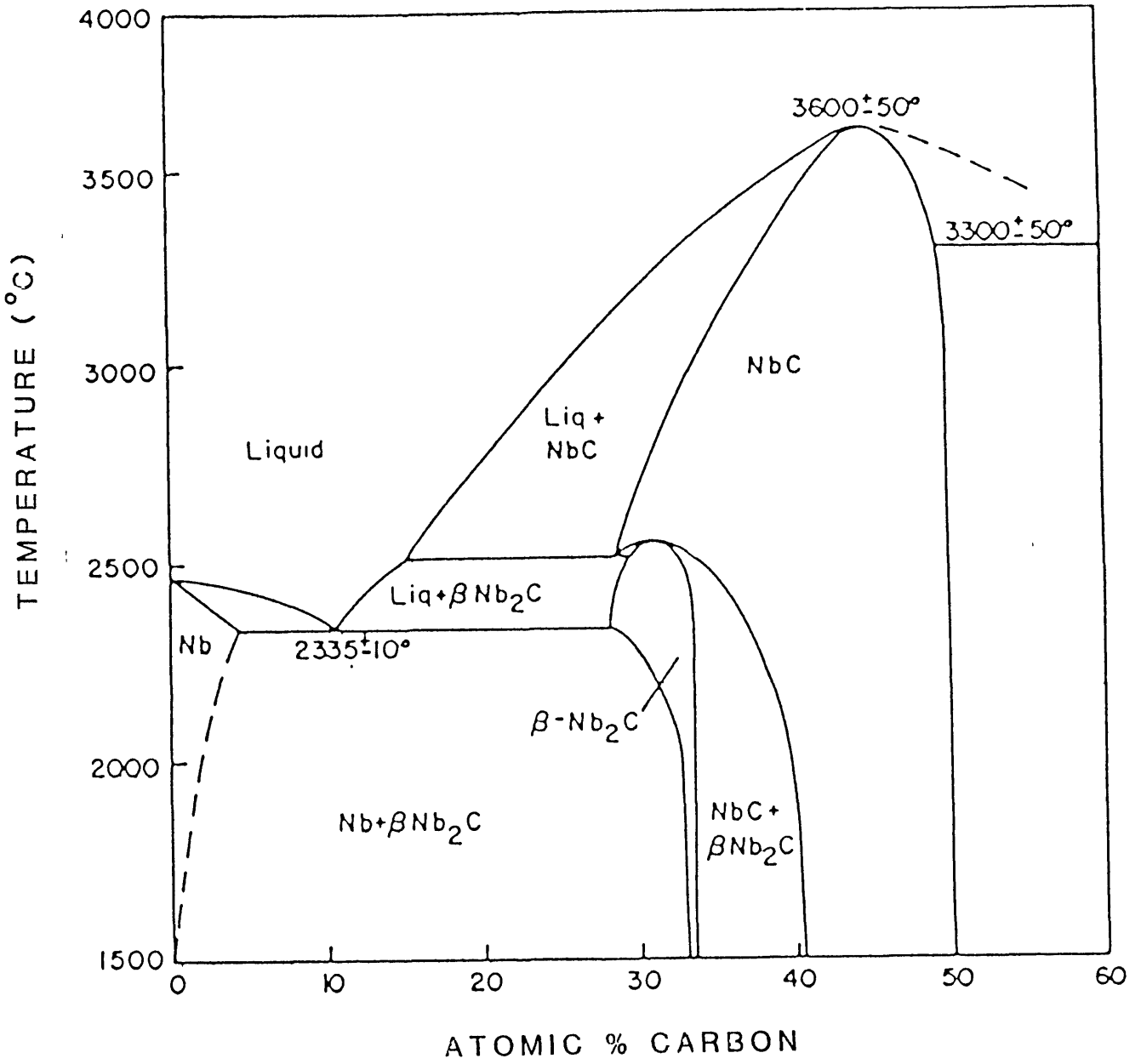

THE Nb-C SYSTEM

FIGURE 1

3300°C by Kimura and Sasaki[4].

A single crystalline modification (close-packed hexagonal) for Nb_2C was reported in the literature, until three modifications were proposed by Rudy and Harmon[6]. The low temperature α- Nb_2C form is orthorhombic with lattice parameters a = 12.36Å, b = 10.89Å and c = 4.96Å. This structure is an orthorhombic distortion of the close packed hexagonal β- Nb_2C, which has dimensions a = 3.126Å and c = 4.972Å, resulting from ordering of the interstitial atoms. The diffraction patterns for α and β- Nb_2C are similar except for the splitting of certain reflexions. The transition between the two phases was reported[6] to take place at about 1200°C. It was also claimed that a high temperature modification γ- Nb_2C exists above 2500°C. The only evidence for the appearance of this phase was obtained from DTA measurements because it was impossible to retain it by quenching to room temperature. Surprisingly it was reported to have a disordered close packed hexagonal structure.

Storms et al[7] determined the Nb-C phase diagram shown in Figure 2 by measuring the vapour pressure of Nb in the monocarbide as a function of composition and temperature using the Knudsen effusion technique in association with a mass spectrometer. They disputed the existence of γ- Nb_2C and reported the decomposition of Nb_2C into NbC and liquid at a lower temperature.

The monocarbide is face-centre cubic with unit cell dimensions; a = 4.4707Å.

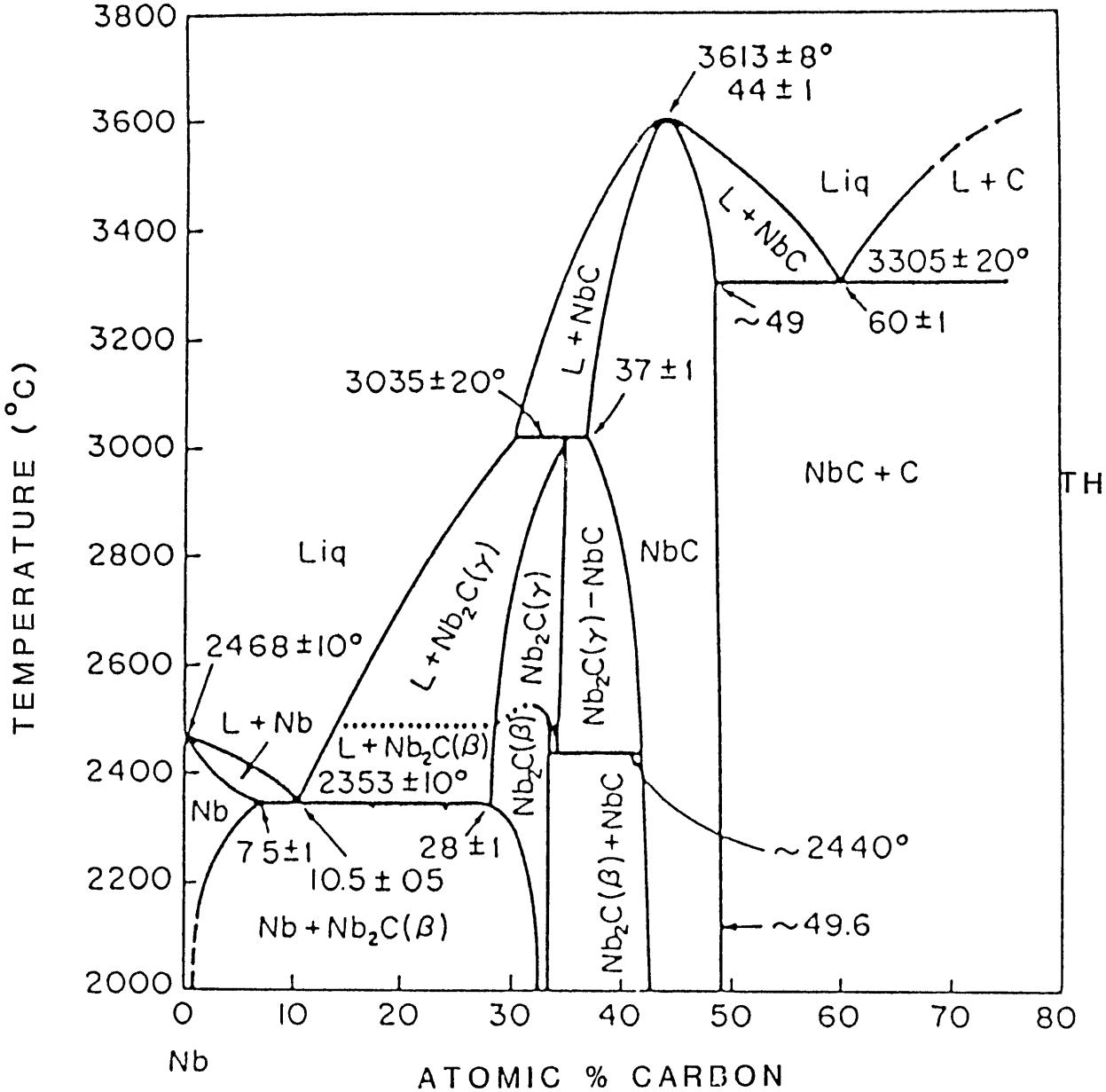

THE Nb-C SYSTEM

FIGURE 2

PREDOMINANCE AREA DIAGRAM

Using the thermodynamic data given by Kubaschewski, Evans and Alcock[8] a predominance area diagram has been constructed for the Nb-C-O system at 1100°C (Figure 3). This diagram shows that NbC and NbO cannot co-exist and that the reduction sequence of Nb_2O under appropriate conditions can be $Nb_2O_5 \rightarrow NbO_2 \rightarrow NbC$. These observations are in essential agreement with the work of Worrell and Chipman[9] who calculated a Pourbaix-Ellingham diagram for the Nb-C-O system.

PREPARATION OF NIOBIUM CARBIDE

A niobium carbide containing 11.37 wt% carbon was first prepared by Joly[10] by reduction of $K_2O.3Nb_2O_5$ with carbon. Brauer et al[11] prepared NbC by reacting NbO_2 or Nb with carbon at 1600°-1700°C. Agte and Moers[12] produced the carbide from niobium metal powder which contained small amounts of tantalum by carburisation with carbon black in a hydrogen atmosphere at about 1700°C. Upon combustion in oxygen, samples gained an average of 26% compared to the theoretical value of 26.5%. Friedrich and Sittig[13] reduced pure Nb_2O_5 with hydrogen to Nb_2O_3 at 1000°C and carburised the latter at 1200°C with carbon in a hydrogen atmosphere. Judging from the weight gain obtained upon combustion the product was claimed to be very pure. However, since their method did not take into account any free carbon, the carbide purity must be considered doubtful. In addition, studies of the Nb-O

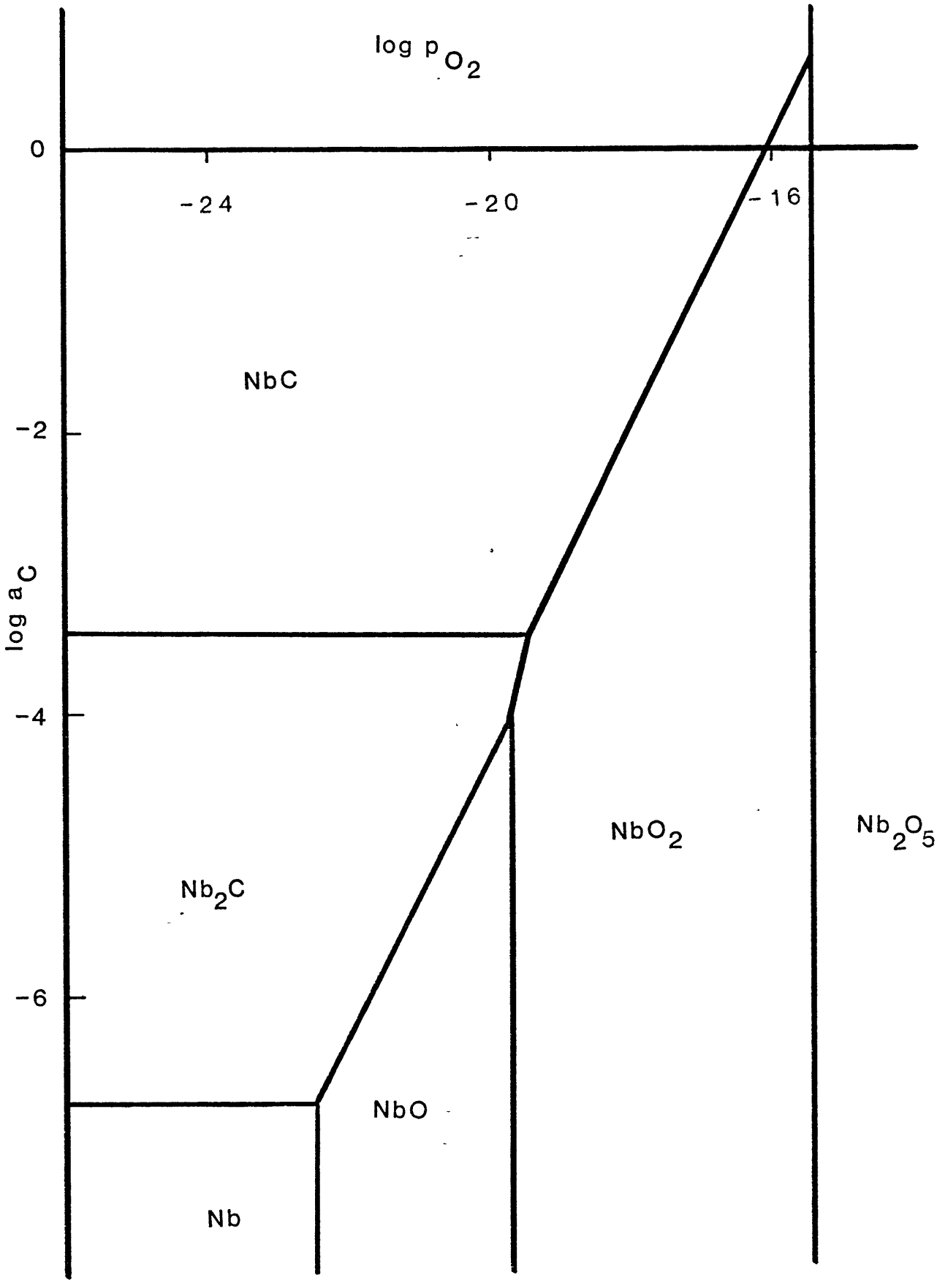

FIGURE 3

Nb-O-C PREDOMINANCE AREA DIAGRAM

system have not confirmed the existence of Nb_2O_3, so presumably the oxide is NbO_2. Moers[14] also studied the direct deposition of NbC from the gas phase onto tungsten by heating a tungsten wire at about 900-1000°C in a gas containing $NbCl_5$, H_2 and hydrocarbons. He found that the deposition of metal was so fast that deposited layers always contained metallic niobium as well as the carbide. By subsequent heating at 1300°C in mixtures of gaseous hydrocarbons and hydrogen, Campbell[15] demonstrated that the deposited product was completely transformed to the carbide.

According to Shveikin[16], during the reaction between Nb_2O_5 and carbon, the products are NbO_2 and NbC which react together to give a solid solution. Alyamouski et al[18] observed the formation of oxycarbides by heating niobium powder in CO between 1300-1700°C at varying pressures. The existence of a cubic oxycarbide Nb(C,O) analogous with NbC and a hexagonal phase $Nb_2(C,O)$ analogous with Nb_2C was claimed.

RESULTS

REDUCTION OF Nb_2O_5 WITH CARBON

The reaction between Nb_2O_5 and spectrographically pure graphite was extremely slow, almost certainly due to the low reactivity of the graphite. After two hours at 1250°C a weight loss of only 1.11% was obtained compared to the theoretical value for complete conversion to carbide of 36.87%.

When Collie coal was used as a source of carbon there was a dramatic change in the kinetics of Nb_2O_5 reduction as shown in Figure 4. X-ray diffraction analyses showed that Nb_2O_5 rapidly reduces to NbO_2 during the initial stages according to the reaction:-

$$Nb_2O_5 + C \rightarrow 2NbO_2 + CO$$

NbO_2 is then directly converted to NbC via the reaction

$$NbO_2 + 3C \rightarrow NbC + 2CO$$

The reaction mechanism was in accordance with the thermodynamic predictions of the predominance diagram and with the observations of Shimada et al[18].

REDUCTION OF Nb_2O_5 WITH CO

The reduction of Nb_2O_5 with CO was studied between 1000°C and 1300°C. The reaction kinetics were extremely slow with the reaction requiring more than two days for completion.

The reaction curves can be divided into two portions. Initially Nb_2O_5 is reduced to NbO_2. The reduction reaction then ceases and carburisation occurs. The experimental results clearly indicate an

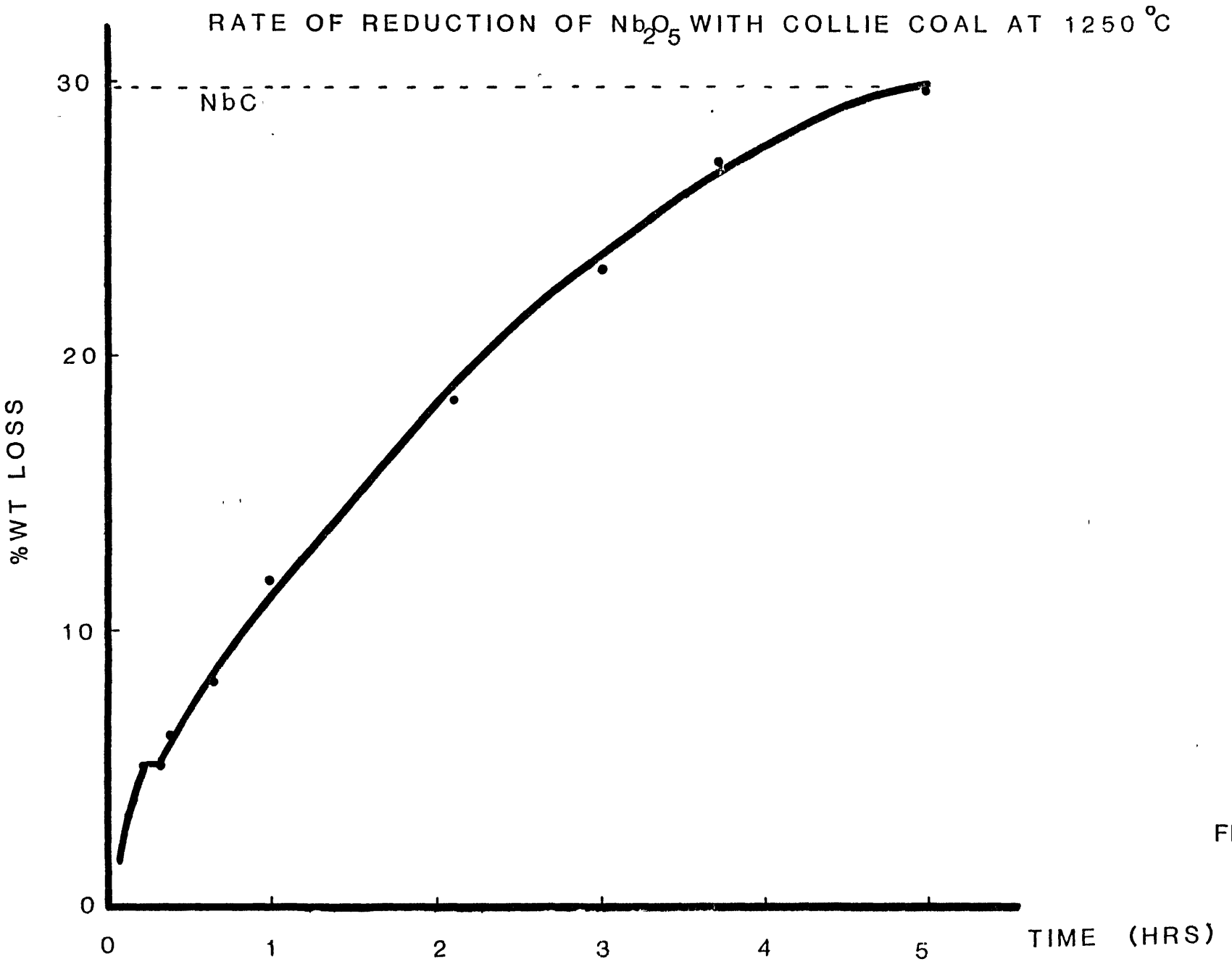
RATE OF REDUCTION OF Nb_2O_5 WITH COLLIE COAL AT 1250 °C
30
NbC
20
10
0
% WT LOSS
0
1
2
3
4
5
TIME (HRS)

FIGURE 4

arrest at weight losses equivalent to the formation of NbO_2. This arrest which exists for a decreasing time with increasing temperature is related to the nucleation of NbC. Plots of weight loss with time are shown in Figures 5, 6 and 7.

REACTION BETWEEN NIOBIUM AND CO

Niobium powder was reacted with CO gas at 1100°C and 1300°C. The expected weight gain for complete carburisation was 12.9%, but surprisingly the metal still gained weight after this change had been achieved. When samples were analysed by X-ray diffraction, Nb, Nb_2C and NbC, NbO and NbO_2 were observed. The reaction was studied at 1100°C by quenching the reaction at appropriate times and analysing the samples using X-ray diffraction techniques. The initial product was Nb_2C followed by NbO. After $1\frac{1}{2}$ minutes (equivalent to a weight increase of 1.3%), NbC was nucleated and soon after evidence of the phase NbO_2 appeared on the diffraction patterns. While NbC and NbO_2 grew with longer reaction times, Nb, Nb_2C and NbO were being depleted. After about 30 minutes (8% weight gain) Nb_2C disappeared completely. The amounts of NbC and NbO_2 continued to increase while the amount of Nb and NbO decreased, until first Nb and then NbO disappeared completely. At this stage, the sample had gained 17.5% which corresponds to 85% NbC and 15% NbO_2 from mass balance calculations. A slow weight loss followed due to the reaction

$$NbO_2 + 4CO \rightarrow NbC + 3CO_2$$

the kinetics being similar to those observed during experiments between Nb_2O_5 and CO. Table 1 shows which phases were present at a particular

% WT LOSS AGAINST TIME PLOT FOR THE CARBURISATION OF Nb_2O_5 WITH CO AT 1000°C

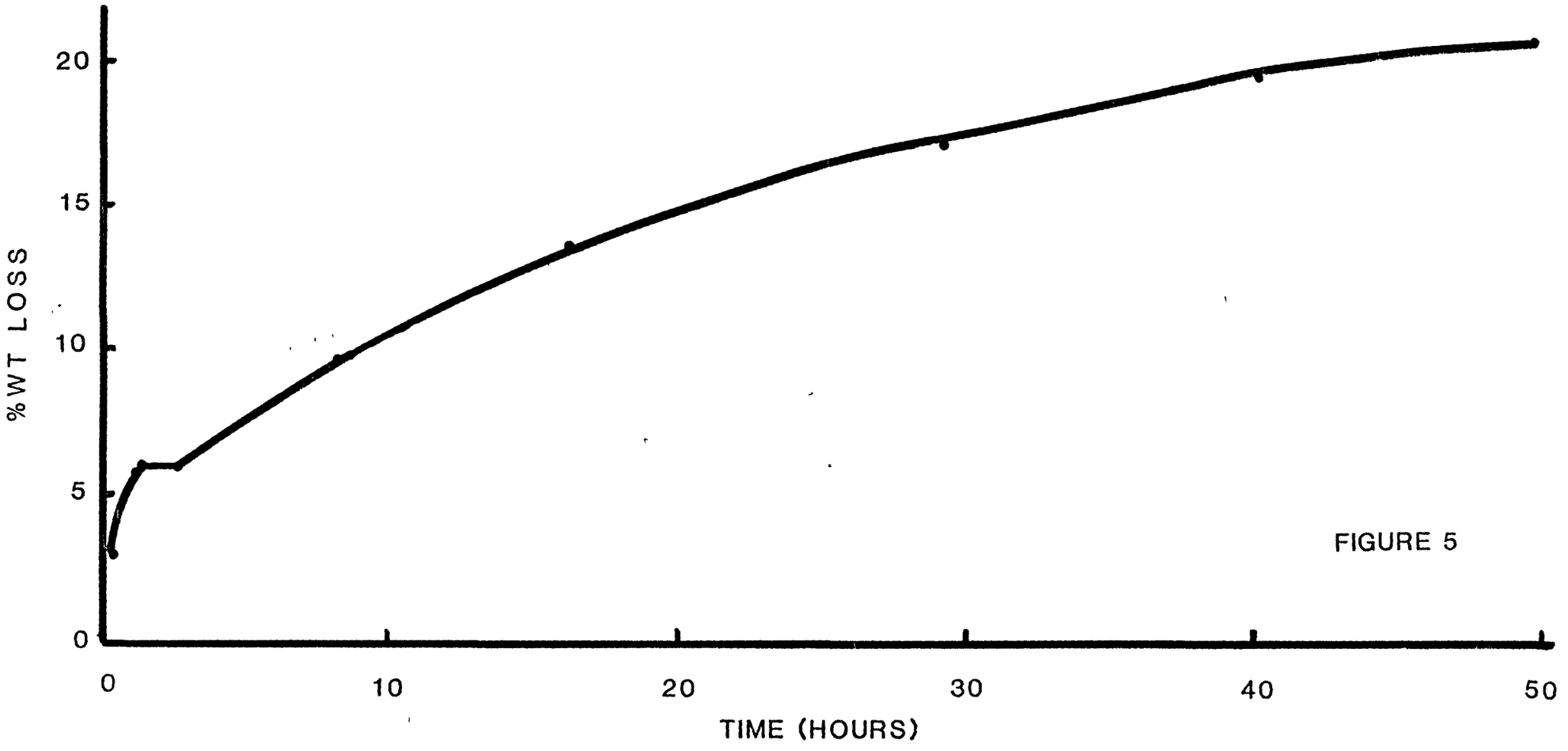

FIGURE 5

RATE OF CARBURISATION OF Nb_2O_5 WITH CO AT 1050°C

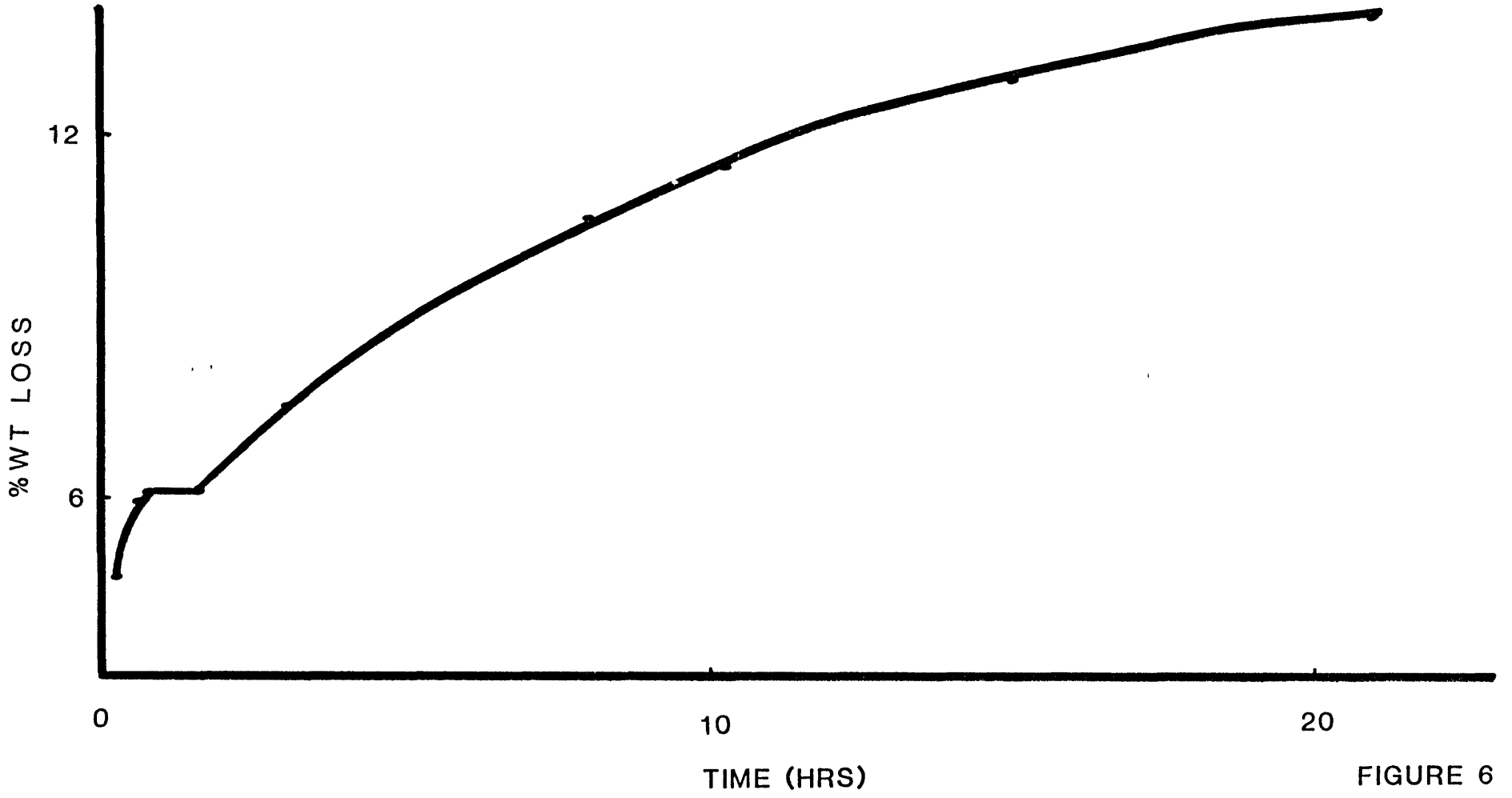

FIGURE 6

RATE OF CARBURISATION OF Nb_2O_5 WITH CO AT 1100°C

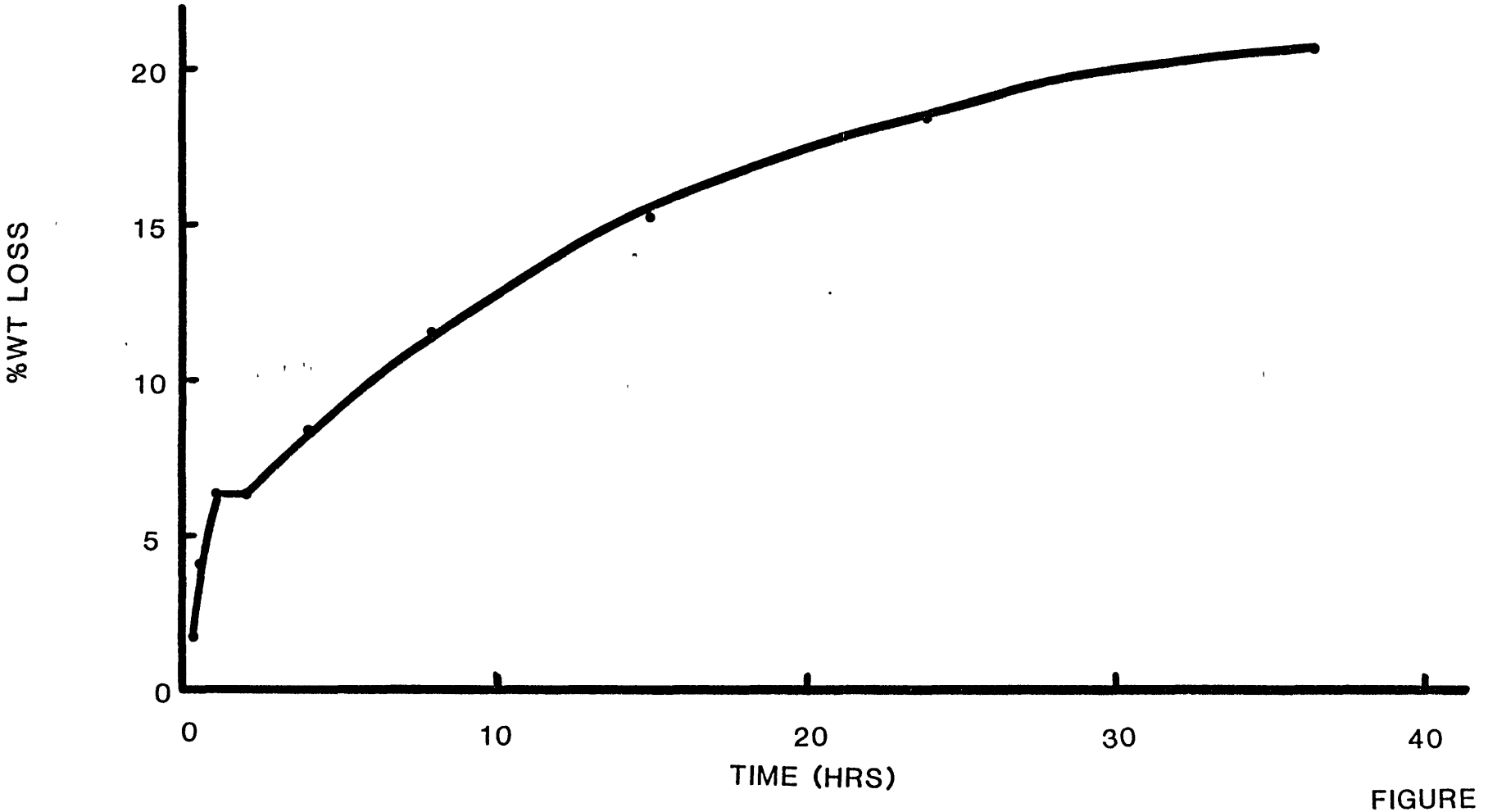

FIGURE 7

time and weight change at 1100°C.

TABLE 1

Time (Minutes)	% Weight Gain	Phases Present
0	0	Nb
1	0.83%	Nb, Nb_2C, NbO
1½	1.3 %	Nb, Nb_2C, NbC, NbO
12	4.5 %	Nb, Nb_2C, NbC, NbO, NbO_2
32	8.5 %	Nb, Nb_2C, NbC, NbO, NbO_2
50	13 %	Nb, NbC, NbO, NbO_2
120	16 %	NbC, NbO, NbO_2
160	17.5 %	NbC, NbO_2
2640	14.84%	NbC, NbO_2

RATE OF CARBURISATION OF Nb WITH CO AT 1100°C

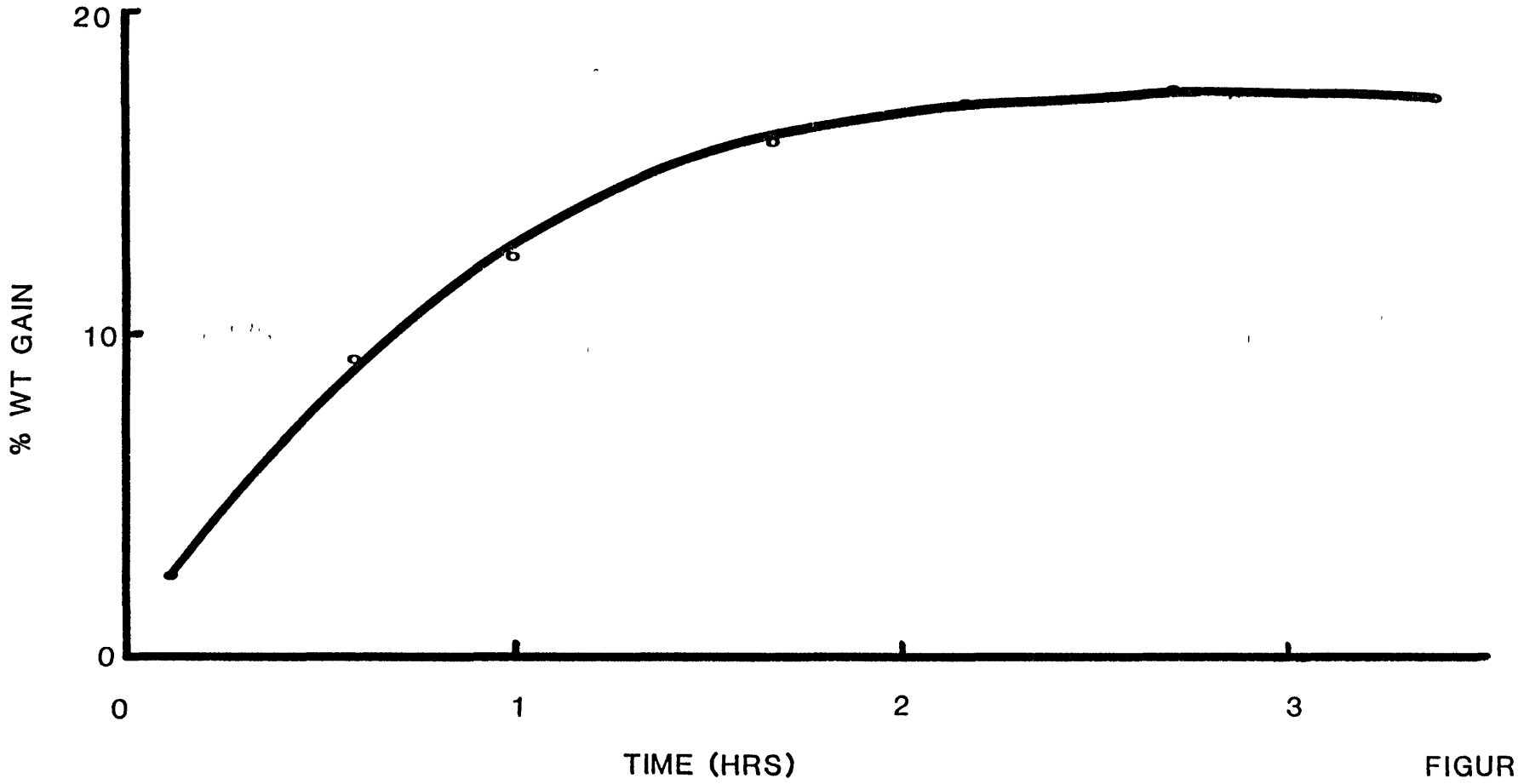

FIGURE 8

DISCUSSION

The simulataneous carburisation and oxidation of niobium powder was most surprising. However, it can be understood from a knowledge of the equilibrium gas compositions for the various reactions taking place, i.e.

1. $2Nb + 2CO \rightarrow Nb_2C + CO_2$ $\quad k = 1.38 \times 10^4$ $\quad p_{CO} = 8.49 \times 10^{-3}$ $\quad p_{CO_2} = 0.992$

2. $Nb_2C + 2CO \rightarrow 2NbC + CO_2$ $\quad k = 6.11$ $\quad p_{CO} = 0.331$ $\quad p_{CO_2} = 0.669$

3. $NbO_2 + 4CO \rightarrow NbC + 3CO_2$ $\quad k = 6.104 \times 10^{-7}$ $\quad p_{CO} = 0.9916$ $\quad p_{CO_2} = 8.4 \times 10^{-3}$

4. $Nb + CO_2 \rightarrow NbO + CO$ $\quad k = 1.059 \times 10^5$ $\quad p_{CO} = 0.9999$ $\quad p_{CO_2} = 10^{-5}$

5. $NbO + CO_2 \rightarrow NbO_2 + CO$ $\quad k = 4.485 \times 10^3$ $\quad p_{CO} = 0.99777$ $\quad p_{CO_2} = 2.23 \times 10^{-4}$

The equilibrium p_{CO_2} for the carburisation reactions 1, 2 and 3 is observed to be high enough for the oxidation reactions 4 and 5 to take place. In other words, enough CO_2 is produced by the carburising reactions to oxidise niobium initially and then to further oxidise NbO. From the X-ray diffraction results it has been established that reaction 1 occurs first, followed by reaction 4, with NbO forming

between niobium and Nb_2C. Later, NbC starts to form around the layer of Nb_2C (reaction 2) with CO_2 diffusing inwards so that reaction 5 commences and NbO_2 begins to form around NbO. Initially NbC grows at the expense of Nb_2C. After all the Nb_2C has been converted, NbC continues to grow on NbO_2 (reaction 3) with CO_2 diffusing inwards to further oxidise niobium and NbO. Niobium then disappears and finally NbO is converted to NbO_2.

At that stage the sample consisted of 85% NbC and 15% NbO_2. The inward diffusion of CO_2 takes place through cracks and pores shown in the micrographs. Eventually, carburisation proceeds via reaction 3 which is very slow. The kinetics of the final stage of carburisation are comparable to those observed during the carburisation of Nb_2O_5 with CO. The reasons for the tardiness of this reaction were investigated.

Gas-solid reactions can be divided into a number of intermediate steps[19].

1. Gaseous diffusion of reactants and products from the bulk of the gas phase to the surface of the reacting solid particle.
2. Diffusion of gaseous reactants or gaseous products through a solid reaction product via pores.
3. Adsorption of the gaseous reactants on and desorption of reaction products from the solid surface.
4. The chemical reaction between the adsorbed gas and the solid.

When one step is much slower than the rest, a limiting condition is reached and this step determines the overall reaction rate.

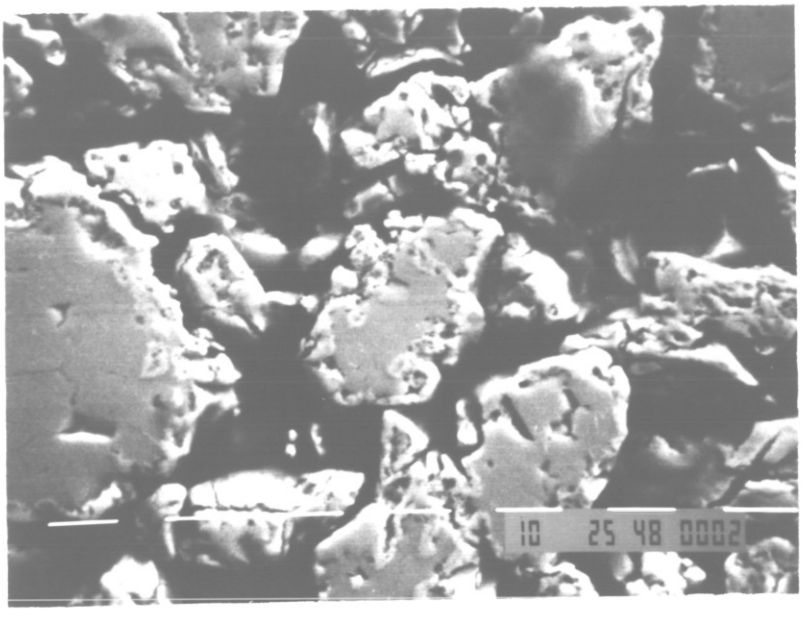

(scanning microscope X500)

PHOTOGRAPH 1

Nb carburised with CO showing the porous nature of the product.

Temperature = 1100°C Time = 50 minutes Wt. gain = 13.01%

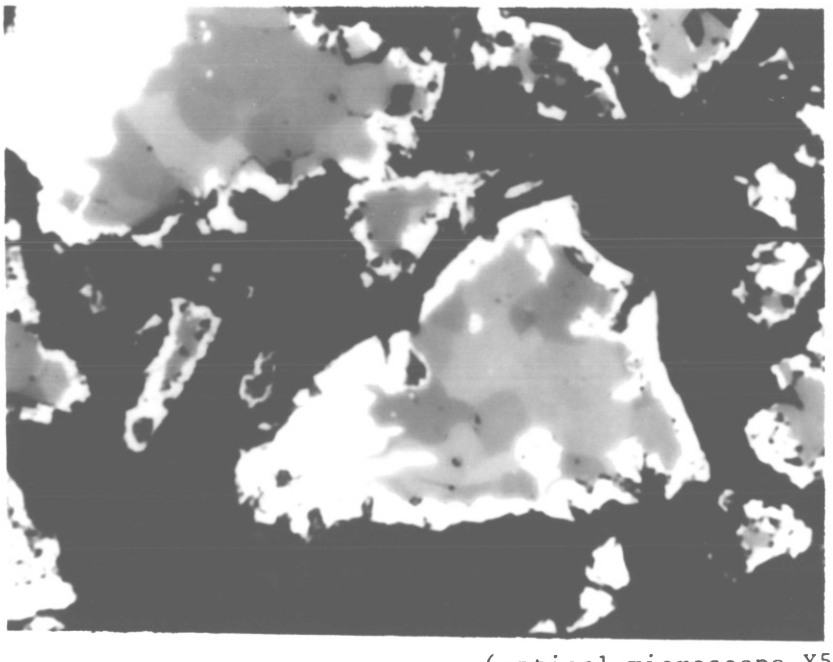

(optical microscope X520)

PHOTOGRAPH 2

Nb carburised with CO at 1100°C for 2 hours.

Weight gain = 16%
Light grey = NbO_2
White = NbC
Dark grey = NbO

Mathematical formulations can be used to assist in determining the rate-controlling step.

When the overall rate is controlled by chemical kinetics, the rate of reaction of a spherical particle is given by the equation

$$1 - (1 - F)^{1/3} = \frac{\nu k}{\rho r} (C_o - C_e)\, t \quad (20)$$

where F = fraction of the reaction completed

k = reaction rate constant in cm/hr

ν = number of moles of reduced solid

ρ = density of product layer in g/cm^3

r = particle radius in cm

C_o = gas concentration in g/cm^3

C_e = equilibrium gas concentration in g/cm^3

t = time in hours

Values of $1-(1-F)^{1/3}$ calculated from the experimental data for the reaction $NbO_2 + 4CO \rightarrow NbC + 3CO_2$ were plotted against time, as shown in Figure 9, at 1000°C, 1050°C and 1100°C. A linear relationship was obtained, the slope being equal to $\frac{\nu k}{\rho r} (C_o - C_e)$. From this, the reaction rate constant, k, was calculated at the three temperatures. This is related to the activation energy by the Arrhenius equation

$$k = A\, e^{-\frac{\Delta H}{RT}}$$

$1-(1-F)^{1/3}$ vs TIME

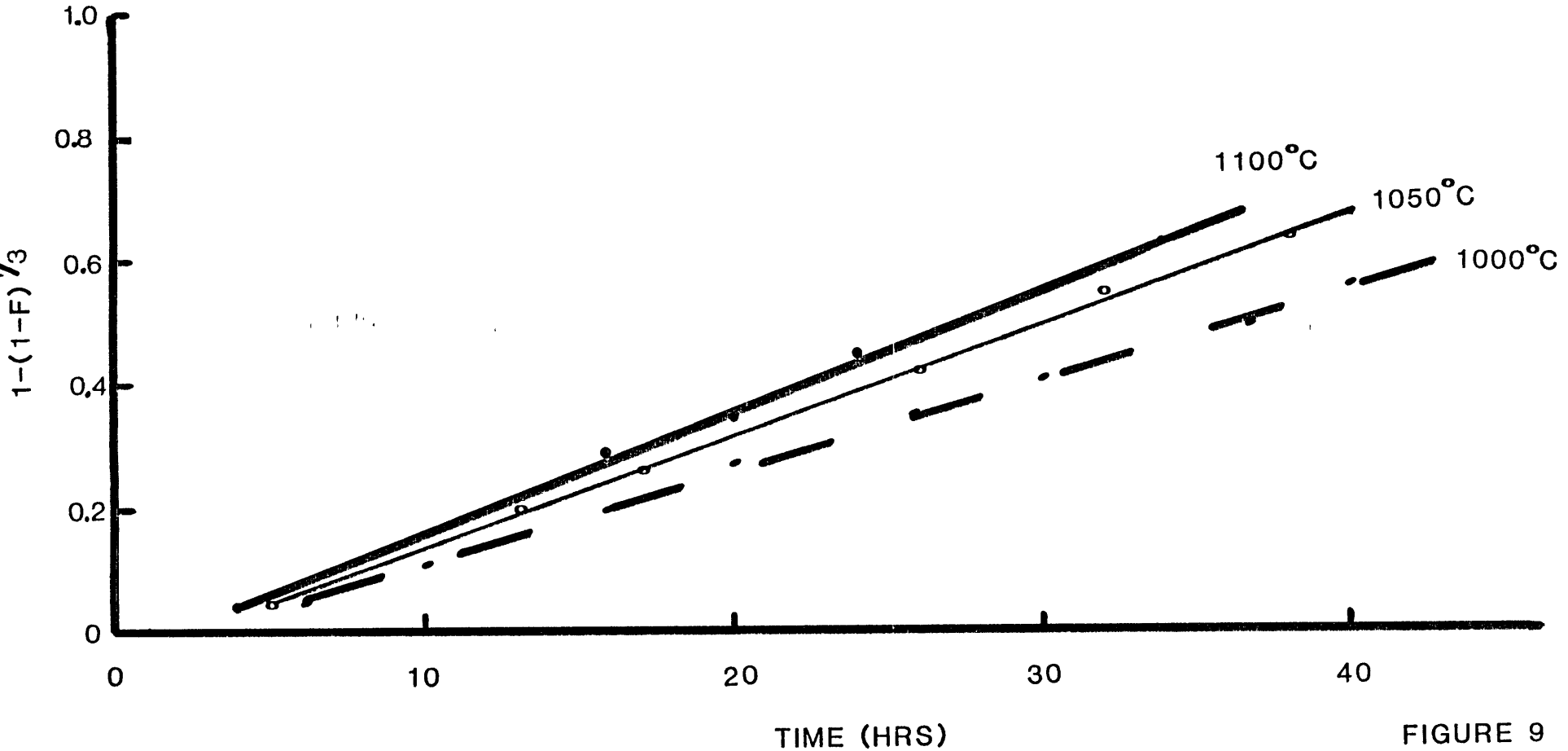

FIGURE 9

where A = constant

ΔH = activation energy for the reaction in cal/mol

R = gas constant in cal/mol K

T = temperature in K

A plot of ln k against $\frac{1}{T}$ was essentially a straight line yielding an activation energy of 24.5 k cal/mol, which is in accordance with a value expected for chemical reaction control.

Gas diffusion control reactions obey the equation

$$1 - \frac{2}{3} F - (1 - F)^{2/3} = \frac{6\nu D}{\rho r^2} (C_o - C_e)\, t \quad (20)$$

where D is the gas diffusivity.

When the experimental data were computed into the above equation, it was found that a linear relationship existed only during the intermediate stages of reaction. Values of the gas diffusivity were obtained which were in the range of 10^{-7} cm^2/sec. However, according to Turkdogan[20], for pore diffusion control for carburising reactions the gas diffusivity must be about 10^{-4} cm^2/sec. This discrepancy indicates that the reaction was more probably controlled by the chemical kinetics than by gas diffusion.

FIGURE 10

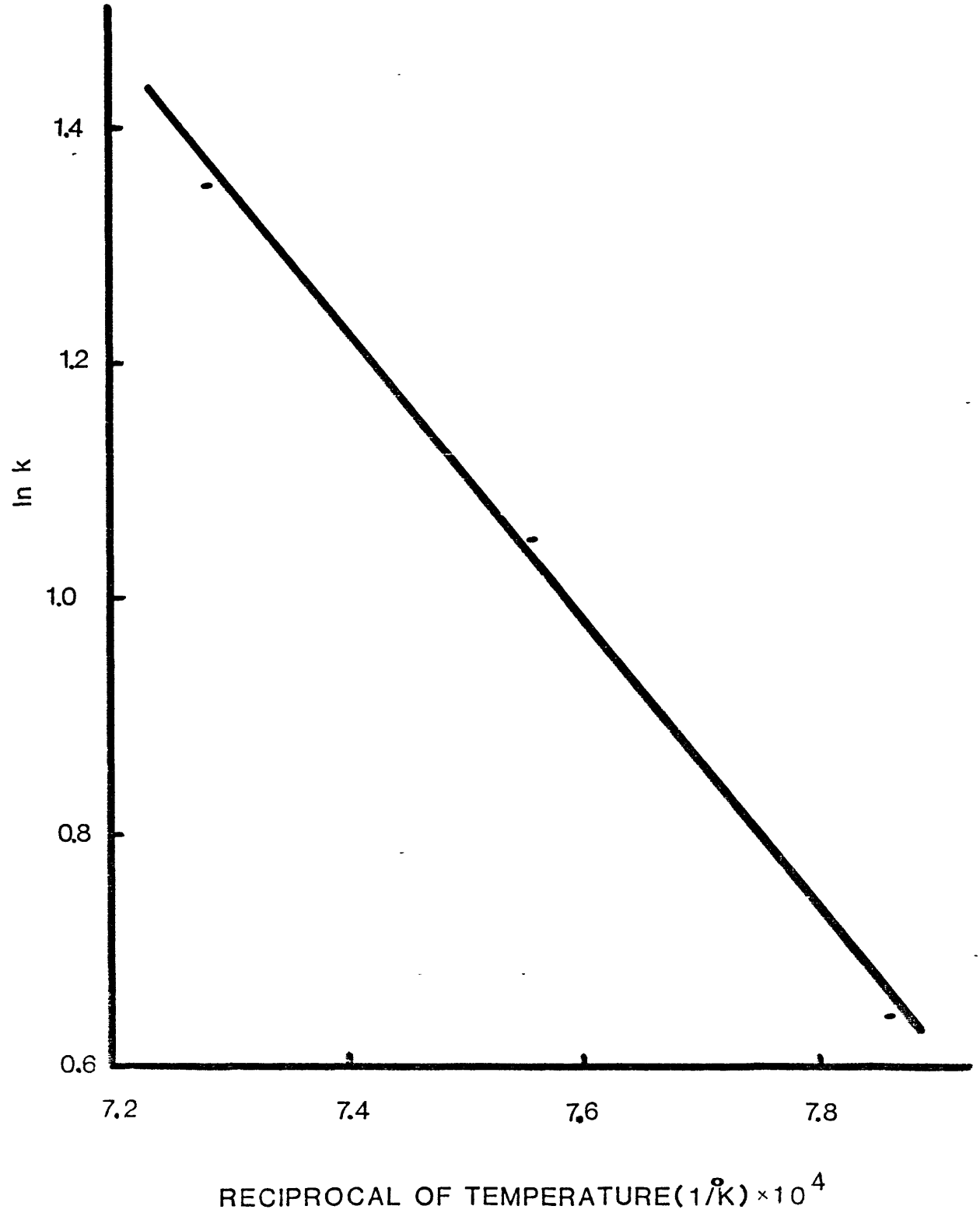

REFERENCES

1. Rudy E., Windisch S. and Brukl Planseeber Pulvermet. 16, 1968, 3.
2. Storms E.K. and Krikorian N.H. J. Phys. Chem. 64, 1960, 1471.
3. Nadler M.R., Kempter C.P. J. Phys. Chem. 64, 1960, 1468.
4. Kimura H. and Sasaki Y. Trans. Japan Inst. Metals 2, 1961, 98.
5. Pochon M.L., McKinsey C.R., Perkins R.A. and Forgeng W.D. Metallurgical Society Conference, Vol. 2: "Reactive Metals" 327, Wiley (Interscience), New York.
6. Rudy E. and Harmon D.P. AFML-TR-65-2, Part I, Volume V, Air Force Materials Laboratory Research and Technology Division, Air Force Systems Command, Wright-Patterson A.F.B. Ohio, 1965.
7. Storms E.K., Chalken B. and Yancha A. J. High Temp. Sci. 1970.
8. Kubaschewski O., Evans E. and Alcock B. "Metallurgical Thermochemistry", Pergamon.
9. Worrell W.L. and Chipman J. Trans. Metal. Soc. AIME 230, 1964, 1682.
10. Joly A. Ann. Sci. Ecole Norm. 6, 1877, 145.
11. Brauer G., Renner H. and Wernet J. Z. Anorg. Allgem. Chem. 277, 1954, 249.
12. Agte C. and Moers K. Z. Anorg. Allgem. Chem. 198, 1931, 233.
13. Friedlich E. and Sittig L. Z. Anorg. Allgem. Chem. 144, 1925, 169.
14. Moers K. Z. Anorg. Allgem. Chem. 198, 1931, 233.

15. Campbell I.E., Powell C.F., Nowicki D.H. and Gonser B.W. J. Electrochem. Soc. 96, 1949, 318.

16. Shveikin G.P. Tr. Inst. Khim. Akad. Nauk. SSSR, Ural'sk. Filial 1958, 51.

17. Alyamovski S.I., Gel'd P.V. and Shveikin G.P. IZU. Akad. Nauk. SSSR, Met. i Gorn. Delo 6, 1963, 139.

18. Shimada S., Koyama T., Kodaira K. and Mastushita T. J. Mat. Sci. 18, 1983, 1291.

19. Szekely J. and Themelis N.J. "Rate Phenomena in Process Metallurgy" 1971, John Wiley and Sons Inc.

20. Turkdogan E.T. "Physical Chemistry of High Temperature Technology" 1980, Academic Press.

CALCIUM CARBIDE

THE POLYMORPHY OF CaC_2

There is great controversy concerning both the structure and the number of CaC_2 polymorphs which exist.

Four types have been reported by Bredig[1] designated I, II, III and IV. CaC_2(I) is stable up to 450°C[1,2] and has a body-centred tetragonal modification with a = 3.89Å and c = 6.38Å. This was later confirmed by Atoji and Medrud[3] using neutron diffraction. According to Barchert and Roder[2] CaC_2(II) is tetragonal with a = 23.4Å and c = 22.31Å. The same authors also reported CaC_2(III) as tetragonal with a = 23.4Å and c = 22.87Å. Because of the similarity of these structures, both of which are close distortions from a cubic structure and essentially the same cell size, it is possible that their occurrence is due to the presence of impurities. The observation[2] that pure CaC_2(IV) at 435°C transforms to CaC_2(III), but in the presence of impurities (such as sulphur and cyanamide) to CaC_2(II) and CaC_2(I), seems to substantiate this observation. Furthermore, CaC_2(II) and CaC_2(III) were both believed to be metastable above 0°C. Vannerberg[4] reported a triclinic structure for CaC_2(II) with a = 8.42Å, b = 11.84Å, c = 3.94Å, α = 93.4°, β = 92.5° and γ = 89.9°, and a monoclinic cell for CaC_2(III) with a = 8.36Å, b = 4.2Å, c = 11.25Å and β = 96.3°. CaC_2(IV) is only stable above 450°C and displays a face-centred cubic modification with a = 5.93Å.

Nast and Pfab[5] reported the occurrence of what they thought was a fifth polymorph of CaC_2. However, their claims have been discounted by Bredig[6] who showed that an erroneous pattern (which was that of a mixture of CaC_2(I), CaC_2(II) and CaO) had been presented.

PREPARATION OF CaC_2

CaC_2 is industrially produced by the reduction of lime with carbon in an arc furnace at around 1900°C to 2000°C. Lime is directly converted to CaC_2[7,8] as shown by the reaction

$$CaO_{(s)} + 3C \rightarrow CaC_{2(s)} + CO_{(g)} \quad (1)$$

The charge descends continuously to the reaction site with CO moving counter-current towards the top of the furnace exchanging heat with the solids. The product is a molten solution of CaO and CaC_2 containing 80% of the latter. It is also thought that calcium gas plays an important role as an intermediate product where CaC_2 can be formed by a two-step mechanism[9,10,11], i.e.

$$CaO_{(s)} + C_{(s)} \rightarrow Ca_{(g)} + CO_{(g)} \quad (2)$$

$$Ca_{(g)} + 2C_{(s)} \rightarrow CaC_{2(s)} \quad (3)$$

These authors also reported the presence of calcium vapour as a product of a reaction between CaO and CaC_2 in the event of the furnace becoming overheated, via the reaction

$$2CaO + CaC_2 \rightarrow 3Ca_{(g)} + 2CO_{(g)} \quad (4)$$

Flusin and Aall[12] and Bredig[13] prepared CaC_2 in arc furnaces, but provided no details of the techniques and conditions used. The starting materials were CaO with petroleum coke and pure $CaCO_3$ with sugar charcoal respectively. Flusin and Aall[12] obtained CaC_2 with up to 1.5% impurities. However, no analysis was supplied by Bredig[13].

The reaction between lime and lampblack to form CaC_2 was studied by Brookes et al[10] at a CO pressure of 50 mm Hg (0.066 atm.) between

1650°C and 1720°C. Fractional conversion to CaC_2 of about 60% was achieved in 10 minutes at 1720°C and in 20 minutes at 1650°C with little weight loss occurring thereafter. Calcium vapour was observed to be evolved and this was thought to be due to the decomposition of CaC_2. A similar observation was reported by Tagawa and Sugawara[14] and by Shanahan and Cooke[15].

The reaction of Ca vapour and carbon was studied by Wilk et al[16] between 1357°C and 1500°C. The rate of CaC_2 conversion was found to be dependent on the reactivity of the type of carbon used.

During a kinetic investigation of the reaction between $CaO-Al_2O_3-SiO_2$ melts with graphite, Edmunds and Taylor[17] observed the formation of CaC_2 at temperatures lower than those consistent with the available thermodynamic data. The thermodynamics for the reaction

$$CaO_{(s)} + 3C_{(s)} \rightarrow CaC_{2(s)} + CO_{(g)}$$

were investigated by measuring the CO pressure in equilibrium with CaO, CaC_2 and C and reported a discrepancy of about 18 Kcal with the accepted thermodynamic data reported by Elliott and Gleiser[18]. A discrepancy with the same accepted thermodynamic data has also been reported by Swisher[19] who observed the formation of CaC_2 from CaO at lower temperatures than those predicted. It was shown that the reaction under atmospheric pressure of CO takes place at 1710°C which is equivalent to a discrepancy of 7.6 Kcal in the established free energy for this reaction.

The standard free energy change for the reaction

$$CaO_{(s)} + 3C_{(s)} \rightarrow CaC_{2(s)} + CO_{(g)}$$

derived from the thermodynamic data of Elliott and Gleiser[18] was

$$\Delta G^\circ = 109,560 - 51.66\ T \text{ cal/mol}$$

As this value was obtained by extrapolating measurements of individual free energies of the reactants and products from low to high temperatures, it was thought that more appropriate data for the above reaction should be found. Kubaschewski et al[20] have compiled values obtained above 1500°C giving a ΔG° for the above reaction

$$\Delta G^\circ = 111,550 - 54.82\ T \text{ cal/mol}$$

This value at 1500°C to 1700°C is about 4 Kcal more negative than the data of Elliott and Gleiser[18]. This new value predicted that reaction between lime and carbon would start at about 1760°C and therefore did not account for the reported discrepancies[17,19].

RESULTS

The reaction of lime with carbon was carried out under controlled atmospheres of CO or argon at 1600°C and 1700°C. Figures 1 and 2 show the fractional conversion to CaC_2, (F), against time, where

$$F = \frac{V_t}{V_e}$$

V_t = volume of gas given off after a particular time

V_e = expected volume of gas to be given off for full conversion to CaC_2

In some experiments, CO was replaced by argon in order to increase the driving force for the reaction. As a result, the reaction rate increased. Lowering the total pressure also had a similar effect.

Gas evolution stopped after about 65% to 75% conversion to CaC_2. The product was predominantly a mixture of CaO and CaC_2 which was molten at 1700°C. Analysis by X-ray diffraction revealed that the carbide was mainly CaC_2(IV). Traces of CaC_2(I) and (II) types were also detected which probably formed by transformation of CaC_2(IV) as it cooled to room temperature.

Some CaC_2 was found deposited on the inside of the reaction tube and around the top of the reaction crucible. This gave no diffraction pattern, probably because the particle size was extremely small, but on addition of water it gave the characteristic smell of acetylene.

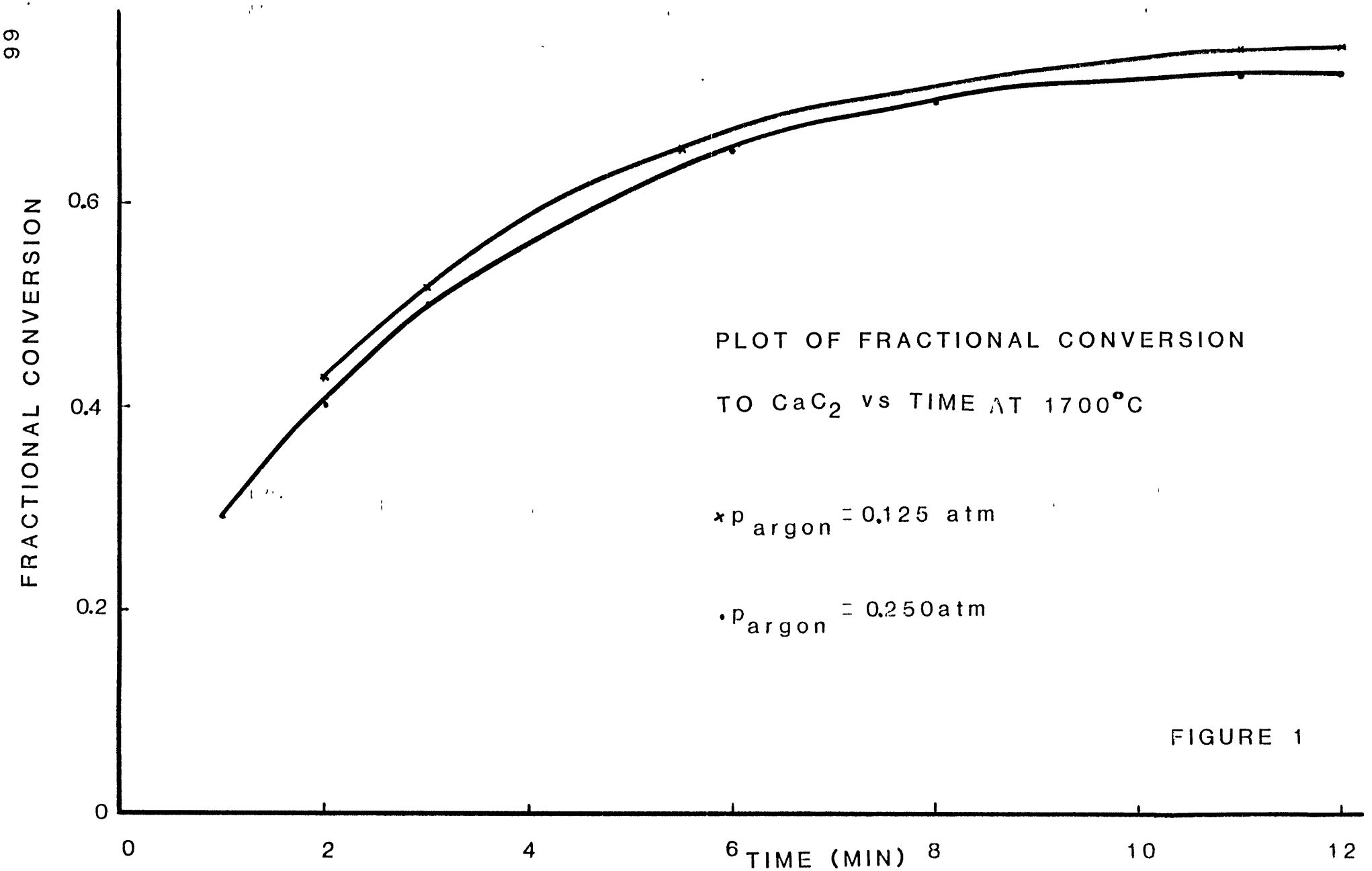
FRACTIONAL CONVERSION
0.6
0.4
0.2
0
0
2
4
6
8
10
12
TIME (MIN)
PLOT OF FRACTIONAL CONVERSION
TO CaC_2 vs TIME AT 1700°C
* p_{argon} = 0.125 atm
• p_{argon} = 0.250atm

FIGURE 1

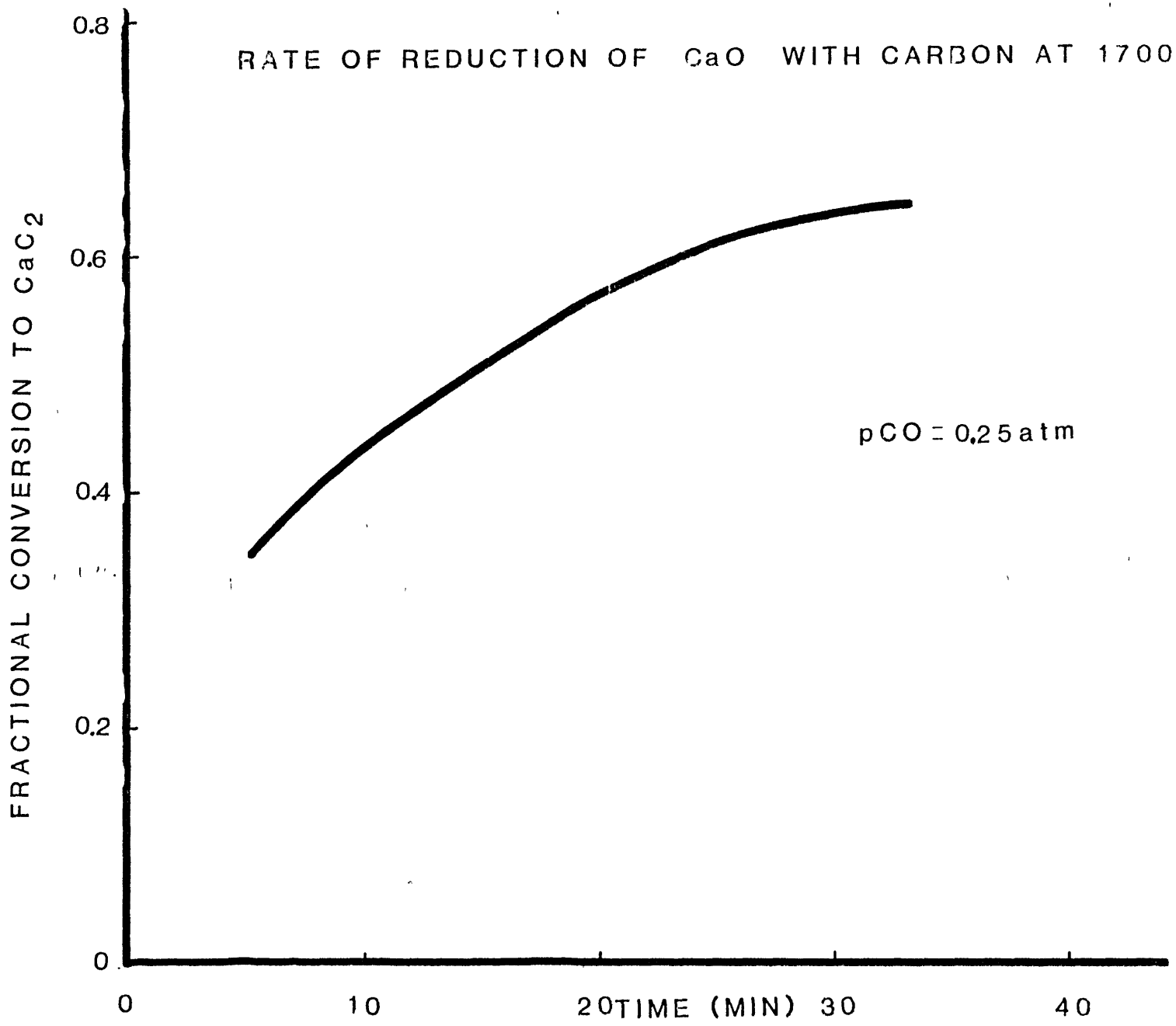
RATE OF REDUCTION OF CaO WITH CARBON AT 1700°C
FRACTIONAL CONVERSION TO CaC_2
0.8
0.6
0.4
0.2
0
pCO = 0.25 atm
0
10
20
TIME (MIN)
30
40

FIGURE 2

DISCUSSION

The reaction steps can be explained by refering to the $CaO-CaC_2$ phase diagram presented in Figure 3. After some initial reaction, the phases present are solid CaO and a liquid solution of CaC_2 and CaO. As the reaction proceeds the amount of liquid increases and it becomes richer in CaC_2. At between 64% to 74% conversion the product is completely molten. The $CaO-CaC_2$ solution is assumed to behave ideally[7] and therefore the ratio of the activity of CaC_2 to that of CaO is about 2 to 3, that is $\frac{a_{CaC_2}}{a_{CaO}} = \sim 2$ to 3. Since the equilibrium constant for the reaction is

$$K = \frac{p_{CO}\ a_{CaC_2}}{a^3_C\ a_{CaO}}$$

and the activity of carbon, a_c, is equal to 1, the equilibrium pressure of CO, p_{CO}, has to decrease to between one-third to one-half of the original p_{CO} in order to maintain a constant value of k. Therefore, the p_{CO} value is lowered such that the reaction is no longer thermodynamically possible. At this stage, the CO pressure in the reaction tube is greater than the equilibrium p_{CO} for the reaction which reverses. While CO reacts with CaC_2 the system experiences a decrease in pressure and as the reference pressure is greater than this experimental value, the movement of mercury in the manometer reverses.

By similar reference to the diagram at 2000°C, it is easily explained why the commercial product is a solution of $CaO-CaC_2$ containing 80% of the latter.

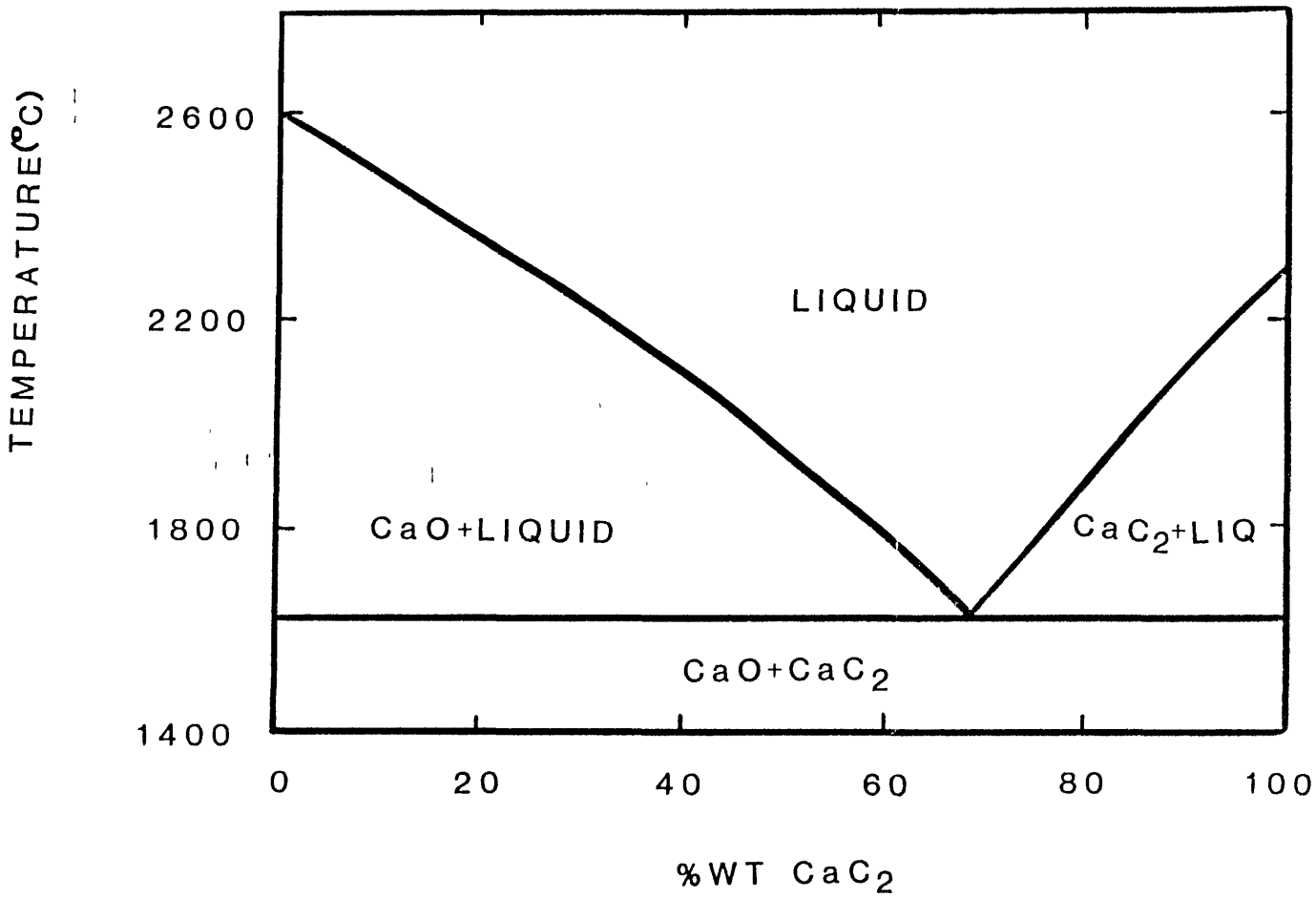

THE SYSTEM $CaO-CaC_2$ FIGURE 3

The equilibrium vapour pressure of Ca in equilibrium with CaC_2 and C at 1700°C is of the order of 10^{-2} atm. This value is high enough for Ca vapour to be evolved after the reaction has started. Thus, CaC_2 can form by reaction of calcium vapour with CO and the graphite crucible and depositing on the inside of the reaction tube and around the top of the reaction crucible is understood.

As with the work of Edmunds and Taylor[17] and Swisher[19] the thermodynamic data for the reaction

$$CaO + 3C \rightarrow CaC_2 + CO$$

have been found to be in error. Table 1 shows the equilibrium p_{CO} values predicted by the thermodynamic data and the p_{CO} values where reaction was observed at various temperatures during the present work.

TABLE 1

TEMPERATURE	EQUILIBRIUM p_{CO} PREDICTED BY DATA[20]	p_{CO} WHERE REACTION WAS OBSERVED
1580°C	0.07 atm.	0.2 atm.
1600°C	0.09 atm.	0.25 atm.
1640°C	0.17 atm.	0.4 atm.
1680°C	0.31 atm.	0.75 atm.

Edmunds and Taylor[17] who measured the p_{CO} for the reaction

$$CaO_{(s)} + 3C \rightarrow CaC_{2(s)} + CO_{(g)}$$

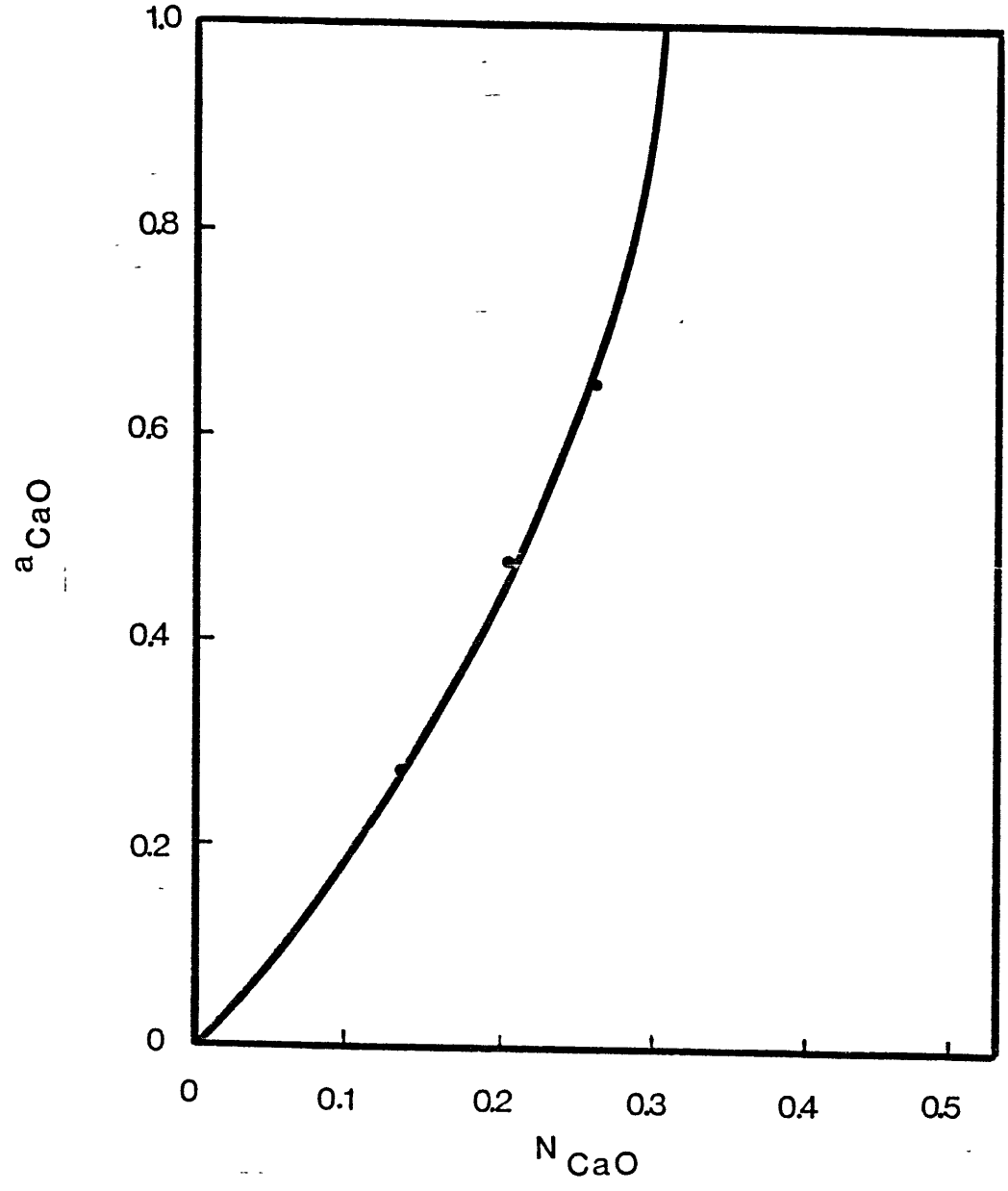

ACTIVITY OF CaO IN $CaO-CaF_2$ AT 1500°C

FIGURE 4

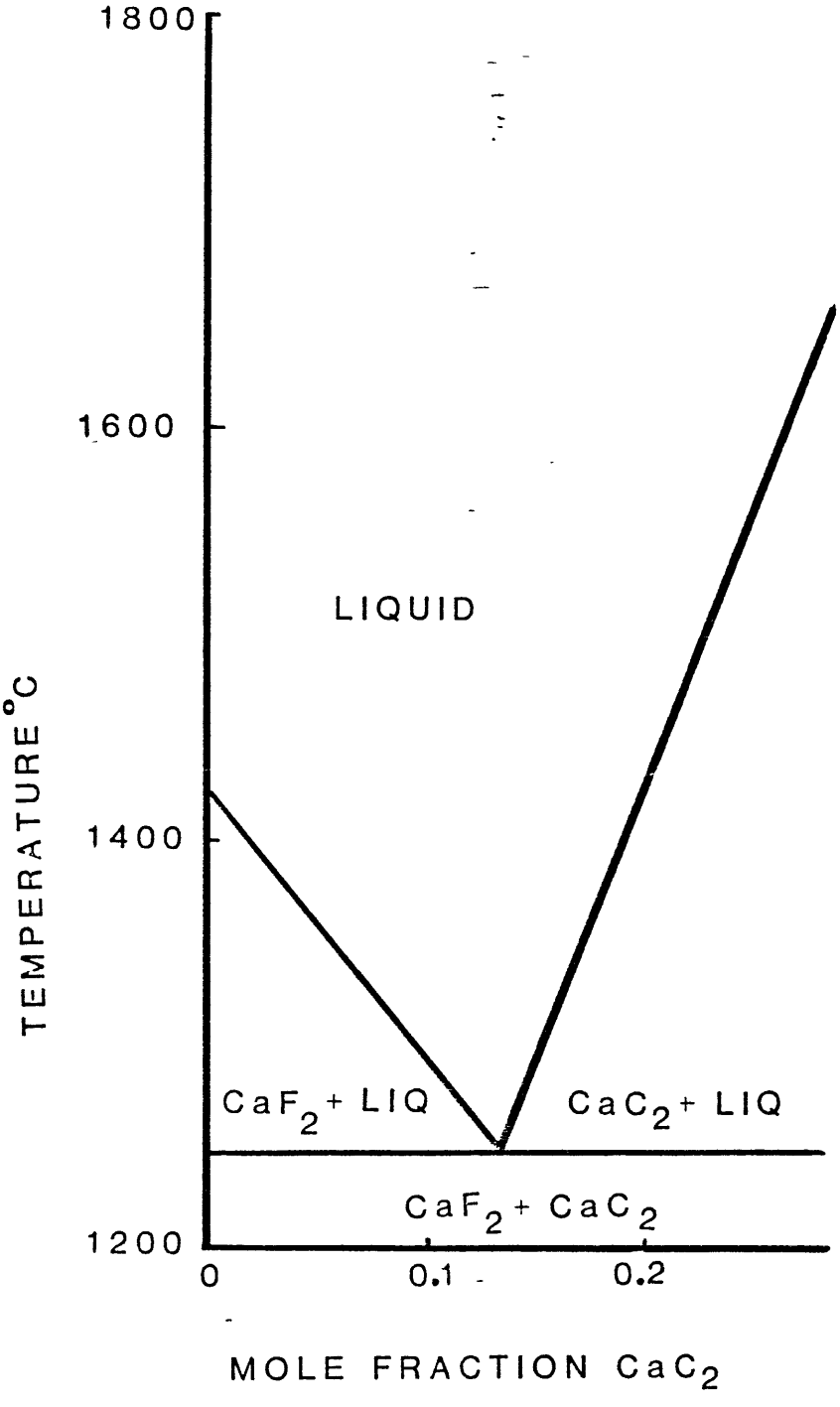

FIGURE 5 THE SYSTEM CaF_2-CaC_2

between 1420°C and 1550°C reported that the rate of the reaction at these temperatures was slow as were the pressure changes observed which made it difficult to decide whether equilibrium had been established. By adding CaF_2 to the starting materials of CaO and carbon to give saturated solutions of CaO and CaF_2 (see Figure 4)[17] the reaction rate was increased to give reliable results. During heating of the charged crucible the reaction tube was evacuated continuously until the equilibrium temperature was reached. At this stage, some CO was introduced into the tube. Since the starting materials were held in vacuo some CaC_2 was formed prior to reaching the established temperature. Since the amount of CaC_2 was very small, a liquid solution was formed between CaC_2 and CaF_2 as expected from the phase diagram shown in Figure 5[21]. The activity of CaC_2 in the CaC_2-CaF_2 system for low CaC_2 mole fractions is small and well below unity as shown in Figure 6[21]. The equilibrium constant k for the reaction is given by the equation:

$$k = \frac{a_{CaC_2}\ P_{CO}}{a^3_C\ a_{CaO}}$$

Under equilibrium conditions for reaction of pure components, C, CaC_2 and CaO have their activities equal to one. However, in this case, the a_{CaC_2} is below unity and therefore the p_{CO} must rise above the equilibrium value for unit activity to maintain k as a constant. Therefore, it is expected that their measured carbon monoxide pressure values were higher than the equilibrium values. This error in neglecting liquid phase formation results in the suggested discrepancy

COMPOSITION DEPENDENCE OF RAOULTIAN ACTIVITY OF CaC_2 IN $CaO-CaC_2$ AT 1500°C

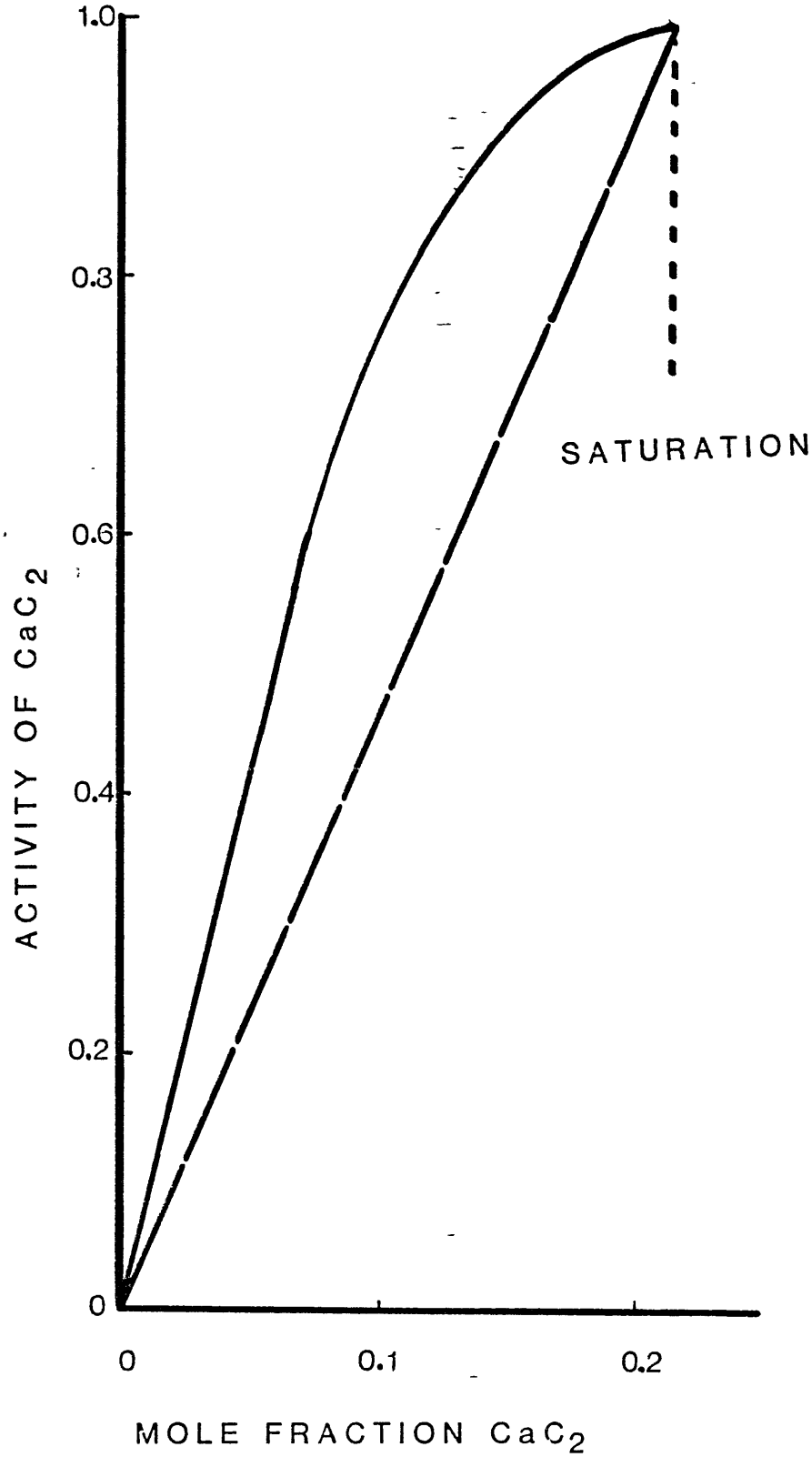

FIGURE 6

with the accepted thermodynamic data being greater than the real discrepancy.

The error in the thermodynamic data is more likely to lie in the ΔH° value rather than the entropy, ΔS°, because the former is more difficult to measure and assess accurately. Using similar reasoning, Edmunds and Taylor[17] plotted the measured p_{CO} against the reciprocal of temperature by drawing a straight line in accordance with the predicted ΔS° value presented in the thermodynamic data even though the presented line did not pass through any of the experimental points obtained at the lower temperatures. If the experimental data are presented to include all the experimental points and extrapolated to lower temperatures the equilibrium p_{CO} at 1250°C can be obtained. This particular temperature is chosen because the CaF_2-CaC_2 phase diagram exhibits a eutectic at 1250°C below which the activities of CaC_2, CaF_2 and CaO will all be unity. By combining this value with the results presented by Swisher[19] and those of the present work a graph of the logarithm of p_{CO} against the reciprocal of temperature was obtained and is shown in Figure 7. From this graph it is deduced that the error in the thermodynamic data does indeed lie in the heat of reaction term. The discrepancy with the data of Elliott and Gleiser[18] corresponds to 8 Kcal or 4 Kcal with the values presented by Kubaschewski et al[20].

PLOT OF ln pCO FOR THE REACTION $CaO + 3C = CaC_2 + CO$ vs THE RECIPROCAL OF TEMPERATURE

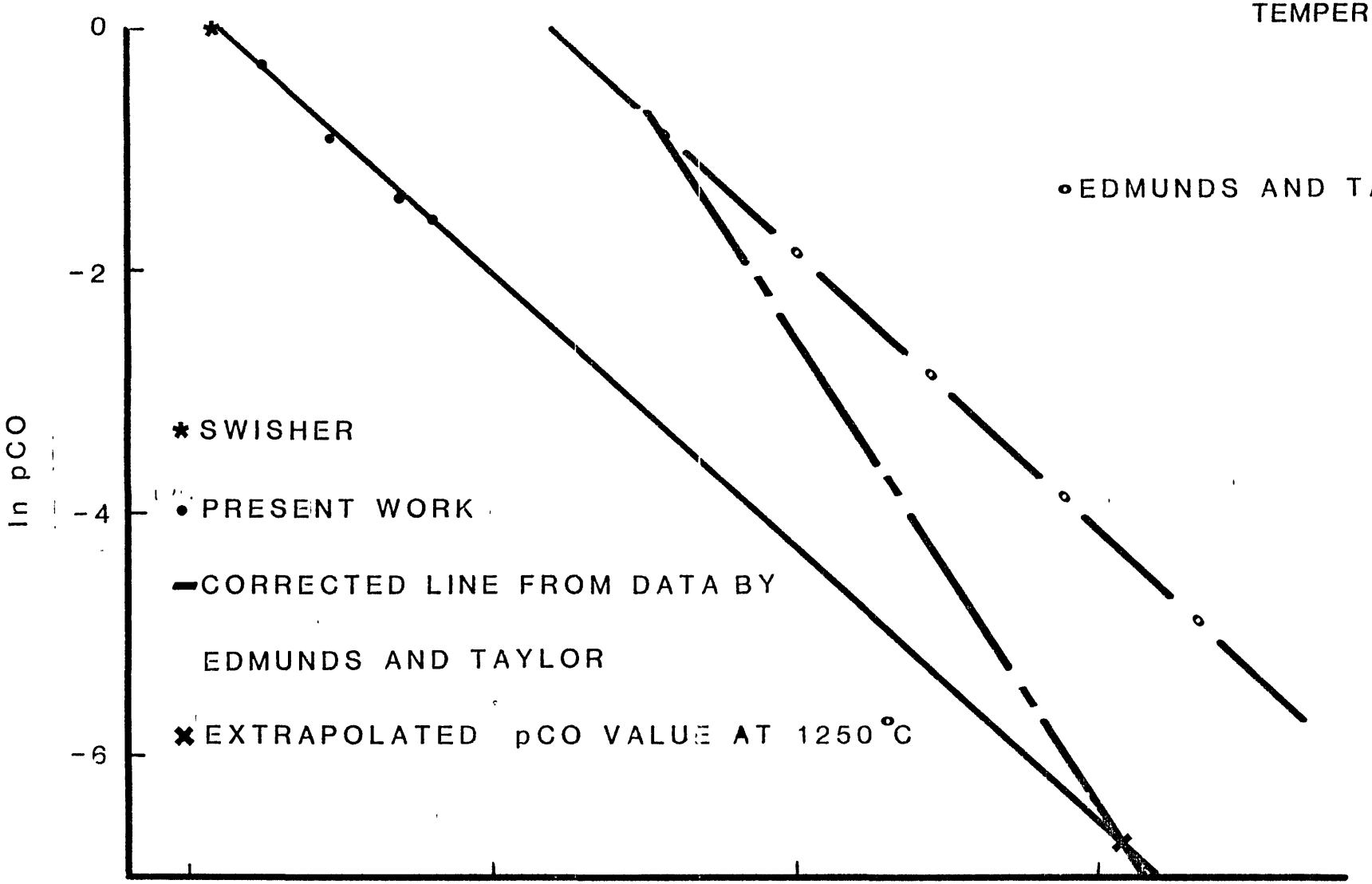

FIGURE 7

REFERENCES

1. Bredig M.A. J. Phys. Chem. 46, 1942, 801.
2. Borchert W. and Roder M. Z. Anorg. Allgem. Chem., 302, 1959, 253.
3. Atoji M. and Medrud R.C. J. Phys. Chem. 31, 1959, 332.
4. Vannerberg N. Acta Chem. Scand. 15, 1961, 769.
5. Nast R. and Pfab W. Z. Anorg. Allgem. Chem. 292, 1957, 287.
6. Bredig M.A. Z. Anorg. Allgem. Chem. 298, 1959, 255.
7. Healy G.W. J. of Metals 18, 1966, 643.
8. Thoburn W.J. and Pidgeon L.M. Can. Met. Q. 1965, 4.
9. Torikai N., Nagaishis T., Saito S. and Miyamoto G. Bull. Fac. Eng. Yokohama Nat. Univ. 16, 1967, 21.
10. Brookes C., Gall C.E. and Hudgins R.R. Can. J. Chem. Eng. 53, 1975, 527.
11. Emons H.H., Hellmold P., Geilhufe C. and Stendte H.J. Chem. Techn. 28. 1976, 19-21, 92-94, 160-163.
12. Flusin G. and Aall C. C.R. Acad. Sci., Paris, 201, 1935, 451.
13. Bredig M.A. J. Phys. Chem. 46, 1942, 801.
14. Tagawa H. and Sugarawa H. Bull. Chem. Soc. Jap. 35, 1962, 1276.
15. Shanahan C.E.A. and Cooke F. J. Appl. Chem. 4, 1954, 602.
16. Wilk K., Raaness O. and Olsen S.E. Scand. J. Metallurgy.
17. Edmunds D.M. and Taylor J. J. Iron and Steel Inst. 1972, 210, 280.
18. Elliott J.F. and Gleiser M. "Thermochemistry of Steel Making" 1963, Pergamon, Oxford.
19. Swisher J.H. Trans. AIME, 242, 1968, 2033.
20. Kubaschewski O., Evans E. and Alcock C.B. "Metallurgical

Thermochemistry", Pergamon, Oxford, 1967.

21. Mitchell A. Trans. AIME, 242, 1968, 2507.

GENERAL CONCLUSIONS

1. The reduction/carburisation sequence for the reaction of WO_3 with graphite or Collie coal is

$$WO_3 \rightarrow W_{20}O_{58} \rightarrow W_{18}O_{49} \rightarrow WO_2 \rightarrow W_2C \rightarrow WC$$

Carbide formation starts when all oxygen is removed.

2. A similar reduction/carburisation sequence takes place for the reaction of WO_3 with CO above 900°C. Below 900°C WC is formed directly from WO_2 without the formation of metallic tungsten. The reaction is completed in two hours.

3. W_2C is formed below the eutectoid temperature as a metastable phase. Its presence is related to the difficulty of nucleation of WC on a tungsten surface.

4. Below 1100°C the orthorhombic modification of W_2C is formed. This structure is related to the ideal stoichiometry W_2C. The composition of W_2C obtained by carburising with CO lies between 33.3 to 35 atom%. Above 1100°C the composition varies from 31 to 32 atom% with carbon monoxide, and the ordered structure was only observed with carbon monoxide-hydrogen mixtures.

5. During the carburisation of tungsten, W_2C is formed initially and grows until about a third of the metal is converted. At that stage WC

converts on the surface of W_2C and continues to grow until all the W_2C is consumed, whereupon WC continues to grow on the remaining tungsten metal until reaction is complete.

6. In reactions with graphite above 800°C, MoO_3 is reduced to the dioxide by way of intermediate Magneli-type phases and then Mo_2C is produced directly from the oxide without any observation of the production of molybdenum metal.

7. In reactions with Collie coal, MoO_3 is reduced to molybdenum. This is due to the greater reactivity of coal compared to graphite.

8. The formation of metastable molybdenum carbides takes place between 660°C and 900°C in the presence of carbon monoxide or carbon monoxide-hydrogen mixtures, indicating the necessity for high carburisation potentials.

9. In all experiments with carbon monoxide, MoC (AA) nucleates after the prior formation of MoC (AABB) on Mo_2C.

10. At 900°C with CO/H_2 mixtures MoC (AA) is nucleated directly on Mo_2C, indicating that MoC (AABB) is metastable with respect to MoC (AA) and Mo_2C.

11. A highly reactive form of carbon such as Collie coal is necessary to reduce Nb_2O_5. The reaction sequence is

$$Nb_2O_5 + C \rightarrow 2NbO_2 + CO$$

followed by

$$NbO_2 + 3C \rightarrow NbC + 2CO$$

12. During reaction with carbon monoxide, niobium carburises and oxidises simultaneously. This takes place because during the carburising reactions enough CO_2 is produced to oxidise niobium.

13. The rate for the reaction

$$NbO_2 + 4CO \rightarrow NbC + 3CO_2$$

are extremely slow. The overall reaction rate is controlled by chemical kinetics. The activation energy for the reaction is 24.5 Kcal/mol.

14. At temperatures above 1630°C the reaction

$$CaO_{(s)} + 3C_{(s)} \rightarrow CaC_{2(s)} + CO_{(g)}$$

ceases after approximately 70% conversion to CaC_2.

15. The available thermodynamic data for the reaction

$$CaO_{(s)} + 3C \rightarrow CaC_{2(s)} + CO_{(g)}$$

were found to be in error. A more accurate free energy equation for the reaction is

$$\Delta G^\circ = 101,600 - 51.66T$$

16. A more accurate equation for the free energy of formation of CaO

$$\Delta G^\circ = -179{,}190 + 46.62T$$

is proposed.

APPENDIX - X-RAY DIFFRACTION PATTERNS

The interpretation of the important factors occurring in the carburisation reactions to form tungsten, molybdenum and niobium carbides are in part based on the identification of phases by X-ray diffraction techniques under a variety of experimental conditions. Whereas, these observations have been reported in the main body of the thesis, this appendix illustrates several of the typical X-ray diffraction patterns obtained in the study.

X-Ray 1 :

This photograph represents the diffraction pattern of W and W_2C which was formed by carburisation of W with CO at 1050°C for 30 minutes. The structure of W_2C is orthorhombic.

X-Ray 2 :

In this case, 'W_2C' was formed at 1120°C under the same conditions and time as sample 1 and exhibits a hexagonal close-packed structure.

X-Rays 3, 4, 5 and 6 :

This series of patterns are taken from samples carburised with CO at 1050°C and show that, after nucleation of WC on W_2C, the structure and lattice parameters of W_2C vary as dictated by the carbon activity at the W_2C/WC interface. The lattice parameters decrease and the ordered orthorhombic structure starts to disorder. After W_2C has been consumed, WC continues to grow on W.

X-Rays 7, 8, 9 and 10 :

This series of patterns show how the W_2C lattice parameters depend on the activity of carbon in the gas phase, which was varied using CO/CO_2 mixtures. At the higher carbon activity (X-ray 7) the W_2C is ordered and as the carbon activity in the gas phase decreases, the unit cell dimensions and carbon contents decrease.

X-Rays 11, 12

This series of patterns is taken from molybdenum samples carburised with CO at 820°C. Photograph 11 shows the appearance of MoC (AABB) and (AAAA) after the disappearance of Mo. MoC (AA) then nucleates with further carburisation and eventually MoC (AABB) transforms to MoC (AA) under these conditions.

X-Rays 13, 14, 15, 16, 17, 18, 19

This series of patterns represents the increasing oxidation/carburisation of niobium with CO at 1100°C. Nb_2C and NbO are the first phases to form, as shown in photograph 13. The next to nucleate is NbC, followed by NbO_2 are being depleted until Nb_2C disappears completely (photograph 17), followed by Nb (photograph 18) and NbO (photograph 19). NbC then continues to grow on NbO_2 until reaction is complete.

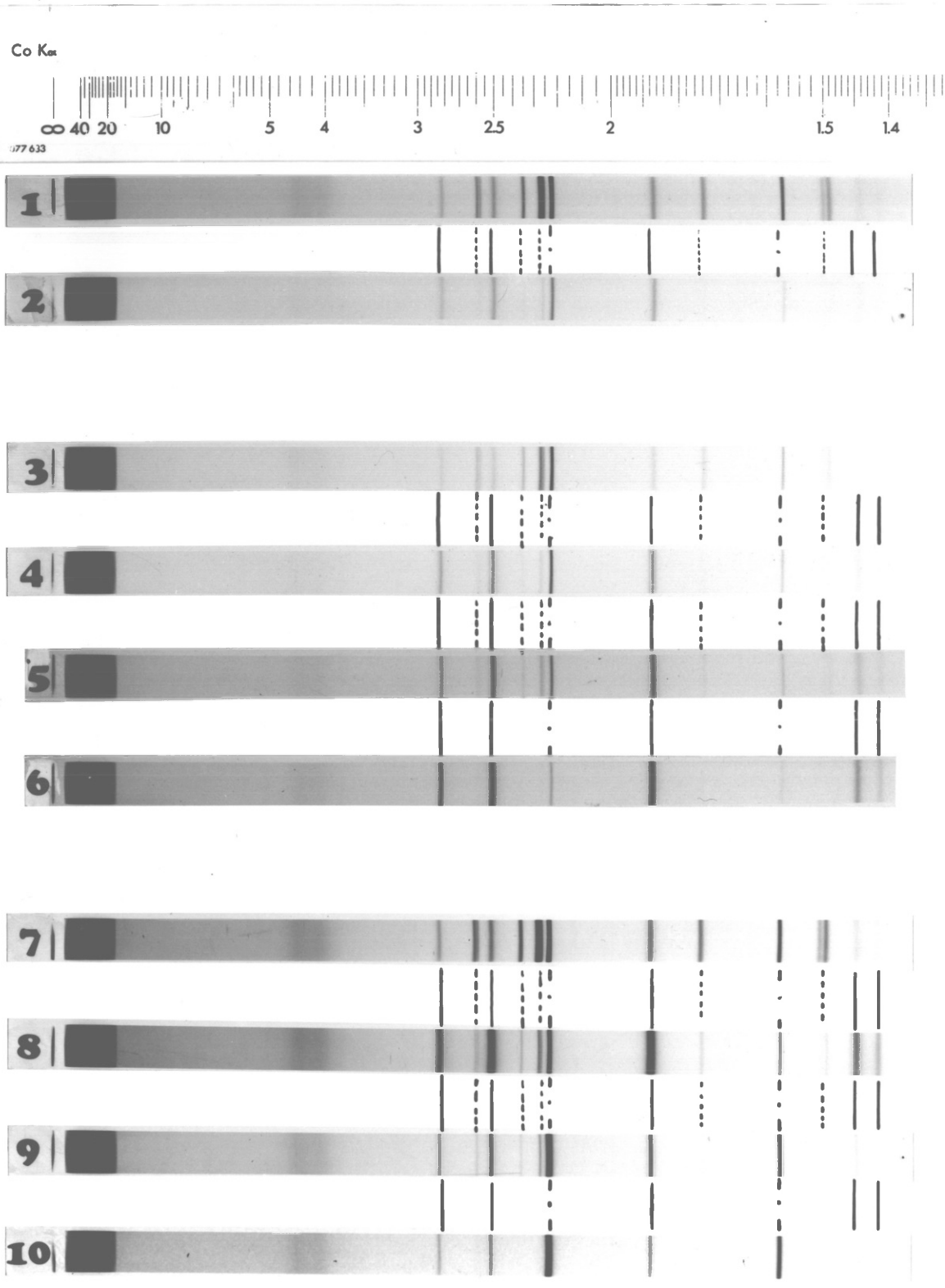

W – · –

W_2C - - - - -

WC ——

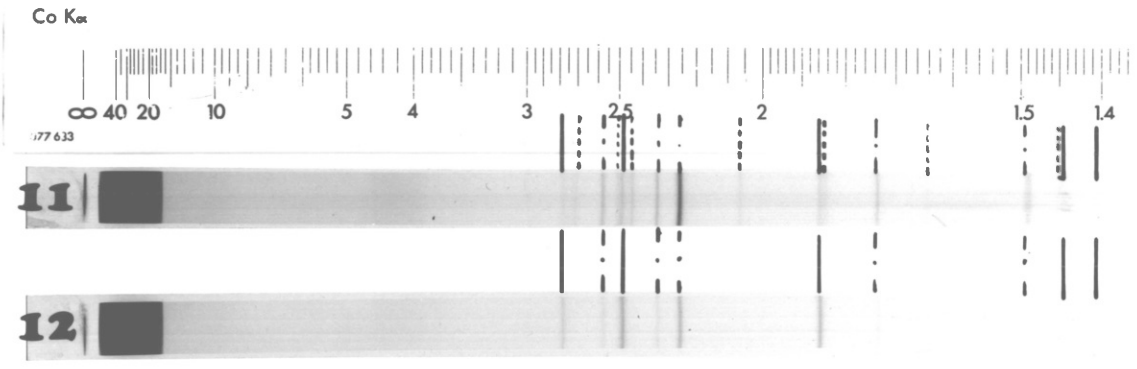

Mo_2C - · -

MoC(AABB) ·····

MoC(AAAA) ——

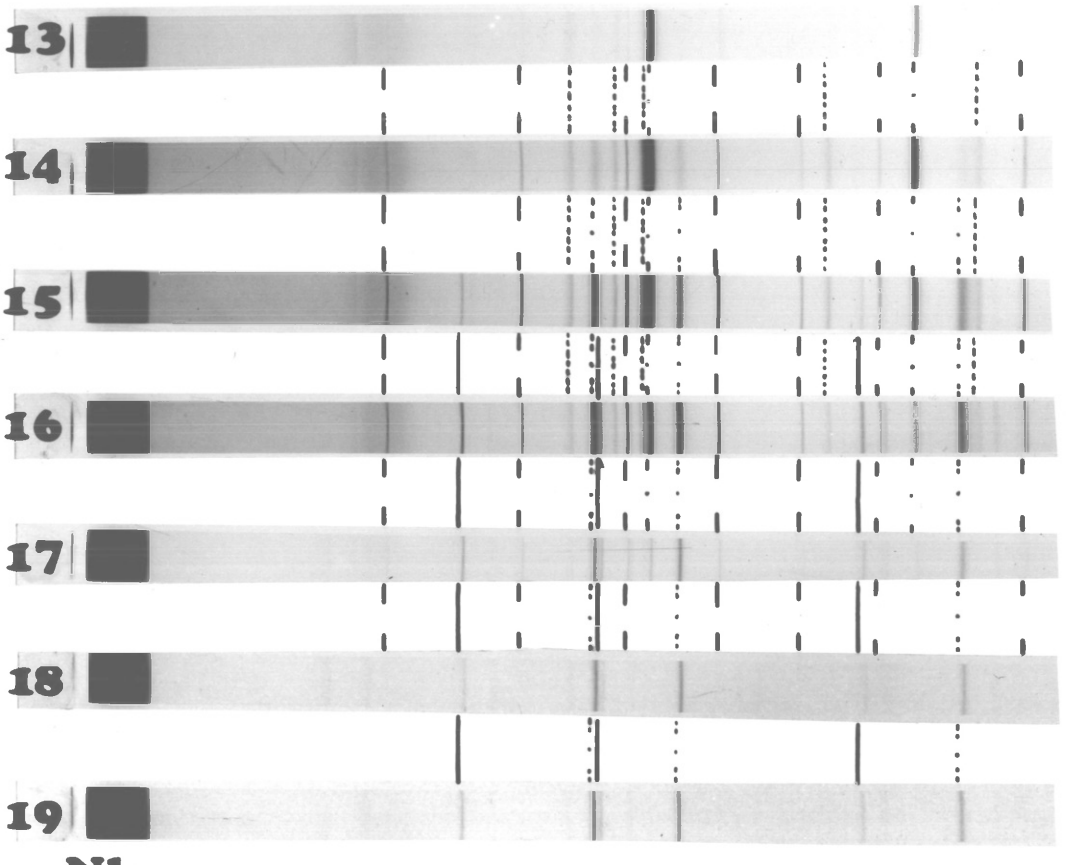

Nb - · -

NbO — —

NbO_2 ——

Nb_2C .....

NbC .. . ..

ACKNOWLEDGEMENTS

I wish to express my gratitude to Professor P. Grieveson for his constructive supervision, constant encouragement and support throughout the course of this work. Thanks are also due to Professor J.H.E. Jeffes for his encouragement and interest in this investigation.

I would like to acknowledge Mr J. Wright, Mr A. Willis, Mr L.E. Leake, Mr A.J. Tipple, Mr J. Rossdale and Miss P. Martins for their technical assistance.

I am grateful to the BTG for their financial support and also to Dr K. Hills for his faith in the project.

I wish to thank Miss S. Hoskins for the excellent typing of this work.

Finally, I wish to thank the members of the group for their continual friendship and companionship.